Canine and Feline Differences in the Cytochrome P450 Transcriptome and Drug Metabolism

by

Marike Visser, DVM

A dissertation submitted to the Graduate Faculty of
Auburn University
in partial fulfillment of the
requirements for the Degree of
Doctor of Philosophy

Auburn, Alabama
May 5, 2018

Key Words: Cytochrome P450, RNA-seq, Microsome,
Recombinant cytochrome, Canine, Feline

Approved by

Dawn M. Boothe, Chair, Professor of Anatomy, Physiology, and Pharmacology
Dawn A. Merritt, Research Director of VMRD Lab Sciences
Robert Judd, Professor of Anatomy, Physiology and Pharmacology
Satyanarayana Pondugula, Associate Professor of Anatomy, Physiology and Pharmacology
Ellen Behrend, Joezy Griffin Professor of Clinical Sciences
Douglas Goodwin, Associate Professor of Chemistry and Biochemistry

Abstract

Cytochrome P450 (CYP) is an important enzyme superfamily, estimated to metabolize 70-90% of pharmaceuticals. Use of pharmaceuticals with at least 30% metabolism by CYP in humans require phenotyping to determine the CYP isoforms involved and the impact common polymorphisms may have. These same drugs are used off-label in canine and feline patients, yet knowledge regarding the CYP isoforms present in the liver and their enzymatic efficacy is unknown. Using human probes and substrates, differences in feline and canine CYP metabolism have been reported, and reflected in the limited pharmacokinetic (PK) studies of both species. The aim of this dissertation was to characterize canine and feline CYP transcriptome in canine and feline, compare and contrast the predicted hepatic clearance (CL_{hep}) between the two species, and carry out reaction phenotyping of selected pharmaceuticals in canine recombinant CYP (rCYP). The first study determined the physiologic expression of CYP mRNA transcripts in whole blood, kidney, duodenum, liver and lung in healthy, adult male (n=4) and female (n=4) beagles via RNA-sequencing (RNA-seq). A total of 45 canine CYPs were identified, with liver, duodenum and lung expressing a high number of xenobiotic metabolizing CYPs, and expressing prominent endogenous metabolizing CYPs expression present in blood and kidney. In the second study, transcriptomes from the 99 Lives Cat Genome Sequencing Initiative databank combined with experimentally acquired whole transcriptome sequencing of healthy, adult male (n=2) and female (n=2) domestic felines was used to characterize CYP expression across a wide variety of tissues. A total of 20 tissues were analyzed and 47 CYP isoforms identified. Depending on the tissue, 9 to 33 CYP isoform transcripts were expressed. This study was the first to describe feline

CYP transcriptome across a wide variety of tissues. Based on the differences in the transcriptome between the two species, the third study compared canine and feline CYP metabolism via *in vitro* liver microsomes. In canine liver microsomes, 3/30 substrates did not have quantifiable intrinsic clearance (CL_{int}), while midazolam and amitriptyline CL_{int} was too rapid for accurate determination. A predicted hepatic clearance (CL_{hep}) was calculated for 29/30 substrates in feline microsomes. Overall, canine CL_{hep} was faster compared to the feline, with fold differences ranging from 2 to 20 fold. A comparison between the well-stirred ($CL_{hep,ws}$) and parallel tube model ($CL_{hep,pt}$) indicates that the $CL_{hep,pt}$ model reports a slightly higher CL_{hep} in both species. With evidence of the variation between the species, reaction phenotyping was applied to identify the CYP isoform pattern for targeted substrates. While the recombinant CYP (rCYP) isoforms are routinely used to screen novel human pharmaceuticals prior to approval, whether the canine isoforms metabolize these drugs in the same pattern is unknown. Utilizing an rCYP metabolic stability assay, 22 drugs used in veterinary medicine were phenotyped using canine rCYP1A1, 1A2, 2B6, 2C21, 2C41, 2D15, 3A12, and 3A26. Four of the 22 substrates required a two or four-fold rCYP dilution in order to achieve the three time points necessary to calculate the CL_{rCYP}. The tricyclic antidepressants, amitriptyline and clomipramine, required a two or four-fold dilution of both rCYP2C41 and rCYP2D15. An isoform reported in only 11% of tested beagles, rCYP2C41, was involved in the metabolism of 9/22 substrates. The contribution of rCYP2B11 in canine drug metabolism altered the rCYP metabolism pattern for 8/22 substrates compared to the CYP metabolism pattern reported for humans. This body of research identified differences in the CYP transcriptome and CYP substrate depletion profile between the two species that suggests the need for species-specific pharmacokinetic studies as a basis for design of dosing regimens. In

addition, canine CYP2B11 metabolism does not follow the reported human profile, highlighting the need for canine- and feline-specific reaction phenotyping.

Acknowledgments

It takes a village to raise a PhD student, particularly this student. I would like to thank my family, who has supported me through 12 years of higher education and encouraged me to always dream of more. None of this would be possible if my parents had not taken a leap into the unknown and immigrated to the USA, almost exactly 20 years ago. Both made great sacrifices, serving as examples for determination and grit to get through the tough times and achieve my dreams. Mom, you are my rock and Dad, I wish you were here to see the conclusion of my perpetual student chapter. Thank you to all my mentors through the years, who guided me to open windows, and encouraged me to walk through doors and to explore opportunities I never knew existed. A special thanks to Dr. Dawn Boothe, Dr. Jamie Bellah, and Dr. Dawn Merritt, who listened to my ideas and helped my dreams become a reality. My dear friends Kristen Grimes, Seth Oster and Cheryl Lawson, who listened to all my concerns and complaints and were always there for wine, sushi and board games. A special thanks to everyone at the Clinical Pharmacology Laboratory and Zoetis, who patiently trained me on a variety of techniques needed to complete the side research projects as well as my doctoral research.

Table of Contents

List of Tables

List of Figures

List of Equations

Supplemental Data

List of Abbreviations

A	Adenine
BLAST	basic local alignment search tool
bp	base pair
BROD	7-benzyloxyresorufin O-dealkylation
C	Cytosine
cDNA	copied DNA
Chr	Chromosome
CL_{hep}	predicted hepatic clearance
$CL_{hep,pt}$	predicted hepatic clearance- parallel tube model
$CL_{hep,ws}$	predicted hepatic clearance- well-stirred model
CL_{int}	intrinsic clearance
CL_{rCYP}	rCYP clearance
CYP	Cytochrome P450
Cys	Cysteine
DDI	drug-drug interaction
EFC	7-ethoxy- 4-(trifluoromethyl) coumarin
EM	extensive metabolizer
EROD	7-ethoxyresorufin
F_b	fraction bound
FDA	Food and Drug Administration
FMO	falvin-containing monoxygenase

F_u	fraction unbound
$F_{u,mic}$	microsomal binding
$F_{u,pl}$	plasma protein binding
G	Guanine
HTS	High throughput sequencing
HTS	High throughput sequencing
IACUC	Institutional Animal Care and Use Committee
IM	intermediate metabolizer
IS	Internal Standard
k	rate constant
LC	Liquid chromatography
M	million
M1	O-Desmethyltramadol
M2	N-Desmethyltramadol
MRM	multiple reaction monitoring
mRNA	messenger RNA
MROD	7-methoxyresorufin
MS	Mass spectroscopy
MW	molecular weight
$NADP^+$	nicotinamide adenine nucleotide phosphate
NGS	Next generation sequencing
PBPK	physiologically-based pharmacokinetic modeling
PK	Pharmacokinetic

PM	poor metabolizer
Q_h	hepatic blood flow
qPCR	quantitative polymerase chain reaction
Rb_e	response of buffer following dialysis
rCYP	recombinant CYP
RMSE	root mean square error
RNA-Seq	RNA-sequencing
Rp_e	response of plasma following dialysis
Rp_i	response of plasma before dialysis
RS	Reference single nucleotide polymorphism
SD	standard deviation
SNP	single nucleotide polymorphism
SNV	single nucleotide variant
SSRI	selective serotonin reuptake inhibitor
T	Thymine
$t_{1/2}$	half-life
TPM	transcript per million
w	weak inhibitor

Chapter 1: Literature Review

Cytochrome P450 Overview

Metabolism and excretion of xenobiotic substances are vital for an organism to survive. Xenobiotics encompass all chemical compounds (e.g. drug, pesticide, toxins, etc.) that are foreign to an organism. For mammals, the liver is the primary organ responsible for metabolism of these compounds, promoting excretion as polar compounds via the kidneys or bile. Other functions of the liver include the biotransformation of prodrugs to active or inactive toxic metabolites and intermediates. Biotransformation of exogenous compounds by the liver is broadly divided into two categories, phase I and phase II reactions. Phase I reactions, primarily oxidation, reduction or hydrolysis, produce polar compounds by either adding a polar functional group or unmasking one already present. Cytochrome P450 (CYP) is a major enzyme superfamily involved in phase I reactions[2]. Other enzyme families involved in phase I metabolism include flavin-containing monoxygenases (FMO) and alcohol dehydrogenase. A superfamily consists of proteins with a common structural fold, a conserved amino acid sequence and catalytic activity. An individual enzyme present within a superfamily is known as an isoform. A single superfamily can catalyze the transformation of a wide variety of substrates. This is particularly so with CYP which has been reported to catalyze oxidation of broad range of xenobiotics, sterols, fatty acids, vitamins and eicosanoids[3,4]. CYP is one of the most ancient xenobiotic metabolizing families, with the enzymes found in bacteria, fungi, and all eukaryotic species. Due to the plasticity of CYP genes, no two species have the same number of CYP isoforms[5]. With the use of genome sequencing, CYP evolutionary relationships continue to be examined and a CYP nomenclature committee has established the naming of CYP isoforms, and the constant discovery of new polymorphisms continues to necessitate modifications in CYP nomenclature[6]. Knowledge regarding CYP continues to generate interest due to the significant impact this superfamily of enzymes has on drug metabolism and the risk of drug-drug interactions (DDI)[7].

CYPs metabolize an estimated 70-90% of all pharmaceuticals on the market in addition to a large variety of exogenous and endogenous compounds. Due to the competition for drug metabolism, there is an increased risk of DDI and adverse drug events, leading the Food and Drug Administration (FDA) to develop *in vitro* and *in vivo* substrate and inhibitor markers of

CYP activity to be used during the human drug approval process[8]. A DDI occurs when two drugs given concomitantly alter the pharmacokinetic (PK) parameters of one substrate (victim) due to competition with another substrate (perpetrator/inhibitor) at the active site. Changes in PK parameters can be due to DDI at sites of absorption, distribution, metabolism, or elimination[9]. Further, DDI can be either beneficial or harmful. For example, ketoconazole is used clinically to prolong the clearance of cyclosporine A, resulting in an increase in the dosing interval[10,11] and zonisamide clearance increases with the addition of phenobarbital, an inducer of CYP3A in canines, which may lead to therapeutic failure[12].

The name of an individual CYP is based on amino acid sequence, which can be derived via genotyping *in silico*. Families with greater than 40% amino acid similarity are classified by an Arabic number (ex: 1, 2, 3). If the subfamily has more than 55% amino acid similarity, they are classified by a letter (2B, 2C, 2D) and then the individual isoforms receive an Arabic number (ex: CYP1A2)[13,14]. The same nomenclature is used by all species, and in humans, the CYP nomenclature committee verifies new sequences and maintains a CYP bank with individual isoform names[15].

Cytochrome P450 Structure

Of the 57 CYP enzymes in humans, 50 are bound to the endoplasmic reticulum, and 7 are in the mitochondrial membrane. The major CYP families involved in the metabolism of pharmaceuticals include CYP1A, CYP2B, CYP2C, CYP2D, and CYP3A[14]. CYP was initially described by C.A Mac Munn in 1886, where he described "a new colouring matter which I had discovered in muscle using a spectroscope"[16]. This was further expounded upon in the 1920's when David Keilin observed that a heme enzyme absorbed light at 450nm and named this group cytochromes[17]. Then, in the 1950's, several rapid discoveries were made regarding the impact of this enzyme system on xenobiotic metabolism, the detection of the CO binding pigment in liver, and the heme component with an absorption at 450nm[18-20]. All CYP contain a signature motif of 10 amino acids: Phe-XX-Gly-X_bXX-Cys-X-Gly, where X_b is a basic residue playing a key role with the reductase co-enzyme and mediating the interaction between oxygenase and iron-sulfur proteins. The cysteine (Cys) residue present at the axial ligand gives the spectroscopic 450nm band[4,21] in the difference spectrum.

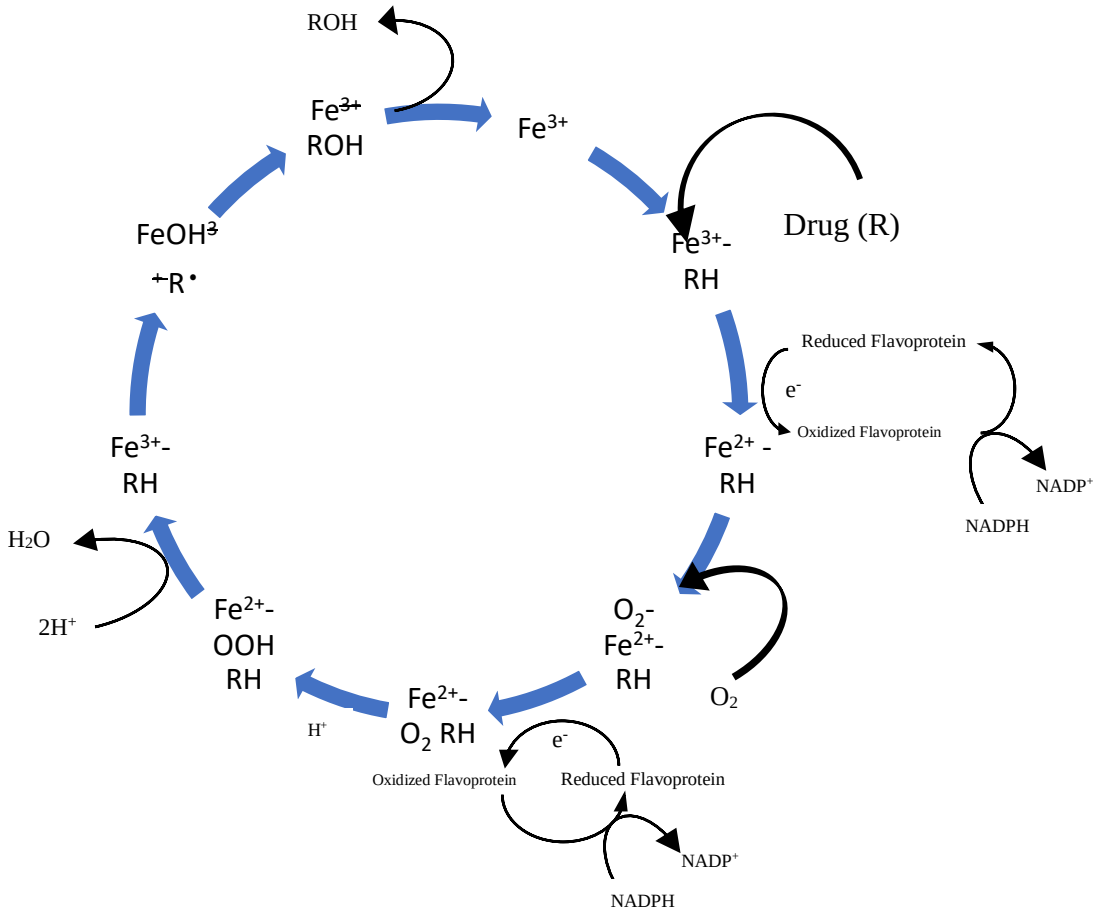

Figure 1: The basic oxidation-reduction cycle to reduce a drug molecule to its more polar form

Figure 1 provides an overview of the basic catalytic reaction that occurs between a drug and an individual CYP. The natural resting state for the enzyme is a reduced state, and when a compound is introduced, with the ferryl acts as ‘nature's blowtorch,' so-called due to its oxidative power and ability to catalyze a great variety of different reactions[4]. The size and shape of the active site can vary significantly from an L-shaped cavity in CYP2C8 to a more open cavity in CYP3A4, resulting in the wide array of substrate specificity. For an in-depth structural analysis, atomic resolution is required; these being produced by x-ray crystallography, NMR, or cryo-electron microscopy. Currently, there are no structures solved for any canine or feline CYP, but only *in-silico* model based on structures from other species..

Cytochrome genomics

Each genome carries two copies of a CYP gene on a chromosome. Alleles are genetic variations between the two copies. This variation could be due to random mutation of that particular gene, or the variation could be a haplotype, which is a group of genes inherited from a parent. If the haplotype evolved from a common ancestor, then the clade is defined as a haplogroup.

The influence of pharmacogenetics on CYP metabolism has been extensively studied in human medicine[22,23]. Changes in one or both alleles of a CYP result in phenotypic changes, including an ultrarapid metabolizer (UM) if there are more than 2 actives genes, an extensive metabolizer (EM) with 2 functional genes, or a poor metabolizer (PM) lacking a functional CYP. An intermediate metabolizer (IM) phenotype can carry one functional allele and one defective allele. These factors further complicate predictions of DDI and the risk of adverse drug events. These variations are known as polymorphisms and can occur from a single nucleotide change, or known as single nucleotide variant (SNV), in addition to gene deletion, duplication, insertion or deletion. A SNV CYP that is present in at least 1% of the population is defined as a single nucleotide polymorphism (SNP), and is denoted by an * (ex: CYP3A12*2)[5].

The impact of polymorphisms in ethnicities have been extensively studied and classified due to the potential for adverse drug events or therapeutic failure[24]. For example, an UM may have no or a poor response to a drug, an EM a standard response and an IM or particularly a PM, an adverse event due to drug accumulation. A CYP SNP meta-analysis identified 176 CYP haplotypes across European, African, East Asian, South Asian and American populations[25]. A survey of FDA drug labels for pharmacogenetic information found that 51% of FDA labels contained specific pharmacogenetic subheadings, and 25% of those labels contained information regarding dose modifications based on metabolic phenotypes[26].

The impact of CYP polymorphisms in small animal pharmacology is not as well understood. Accordingly, dosing modifications based on such polymorphisms are not described. In dogs, some polymorphisms have been found serendipitously during pharmacokinetic studies and further examined after the initial discovery[13,27]. Other polymorphisms have been detected during genetic sequencing, and the use of whole-genome sequencing has produced an extensive databank of SNVs, but without a phenotypic description. The use of metadata collections and the improved ability to predict genetic variants, has enabled databases such as Ensembl to collect

SNV in canine (Supplemental Table 1) and feline (Supplemental Table 2) SNV data[13]. Whether these SNV have a clinical effect requires additional *in vitr*o and *in vivo* testing.

Epigenetic factors reported to influence CYP expression and function include environmental pollutant-induced CYP1A and 3A expression in fish, eagles and rats[28-30]. In addition to the effect of SNP and epigenetics, additional reported sites of variation influencing CYP function include the gene promotor, upstream regulators, introns, 3'-untranslated regions, or regions which may affect splicing of the mRNA transcript[14]. CYP gene expression can be induced by both promoters and regulators. Prior to studying epigenetics, the gene itself must be characterized and CYP protein phenotyped.

Identification of CYP

Multiple techniques for identification and characterization of CYP have been reported, depending on the aim of the research and the questions to be answered.

Gene Expression

Initially, genomic identification of CYP involved developing primers targeted for an individual CYP mRNA transcript of interest, followed by sequencing. This method has identified multiple canine and feline CYP, particularly isoforms important in drug metabolism[31-36]. With the development of whole-genome sequencing, large databases have been created for genomic, transcriptomic and protein data. Two of the most substantial databases are GenBank, maintained by the National Center for Biotechnology (Bethesda, MD), and Ensembl, maintained by the EMBL European Bioinformatics Institute (Cambridgeshire, United Kingdom)[37].

The GenBank database contains Reference Sequences (RefSeq), a collection of annotated genetic sequences, transcripts and proteins for a species[38]. This database has expanded from 6 annotated organisms in 2004 to 416 annotated organisms in 2017, now encompassing prokaryotes and eukaryotes[39]. An annotation describes the location of both coding and non-coding genes in a particular chromosome. Using the publically available genomes of an extensively annotated organism such as human or mouse, automated pipelines have been developed to annotate genomes of less well characterized species[40]. Once an initial annotation is developed, manual curation by researchers focusing on that particular genome or transcriptome can improve the boundaries of the annotations. The Ensembl database, also uses publically available genomes to develop annotations, predict variant structure, and compare orthologs

between species[41]. Orthologs are genes in different species that evolved from a common ancestor and typically retain similar function (e.g. CYP-like oxidation). Due to the accurate and in-depth annotations available in the human and mouse genomes, these two can be used to identify orthologs in other species. A gene is considered a paralog if it is a duplicate evolved within the same species[42,43].

High throughput sequencing (HTS), also known as next-generation sequencing (NGS), combines the ability to identify genes without the need for the development of individual primer sequences[44-46]. This provides a global overview of gene expression, making pattern recognition and pathway examination feasible. Several commercial platforms have been designed and improved upon over the past 10 years, aiming to decrease the error rate during sequencing while producing vast quantities of accurate data. When sequencing, coverage refers to the number of reads that align to a reference base. The better the coverage, the more confident the researcher can be in the detection of SNV within an individual genome, or the detection of low transcript expression. The coverage produced depends on the sequencing platforms utilized, the purpose of the study and the quality of the sample preparation[47].

The vast quantity of data produced by HTS requires different analysis techniques, depending on the purpose of the study. Transcript analysis, including detection of differential expression, is completed via RNA-seq, while studies focusing on translation, including control of protein production, can be completed via Ribo-seq[47,48]. Both commercial and free software have been developed, and new techniques continue to be described in the literature, improving the ability to identify differences in genomes and transcriptomes. Analysis of these data requires vast computational power in addition to a large sample size to detect small differences. This has led to the development of consortiums, targeting specific diseases or goals, to provide samples and analytical power[47]. While this technology can help identify genes, map pathways of disease and determine factors that influence protein production, other techniques are necessary to identify and quantity the protein itself.

Protein Quantification

To develop and advance models capable of predicting DDI, identify pathological changes due to disease states, and identify targets for drug therapy, protein identification and quantification are required. Western blotting remains the most common method of protein identification and quantification. This immunoblotting technique requires antibodies that are

specific for a given enzyme with minimal cross-reactivity to non-target proteins. Currently, there are no canine and feline CYP-specific antibodies available; therefore, cross-reactivity with different isoforms makes exact identification and relative quantification a challenge. The technique is frequently used to correlate mRNA expression with protein quantity, and has been used to verify the presence of multiple canine and feline CYP proteins[31-33,35,36,49]. The development of liquid chromatography from separation coupled to mass spectroscopy (LC-MS) provides an accurate quantification technique, capable of discerning between CYP isoforms without the labor-intensive development of specific antibodies. However, isoform-specific amino acid sequences must be designed for a targeted isoform, requiring proteomic expertise.

Proteomics provides a global overview of an organism's proteome. Instead of focusing on targeted proteins, proteomics addresses all proteins expressed by the organism in order to identify pathways and examine differential tissue protein expression. Studies of the canine proteome includes characterization of normal serum[50]and urine[51], diseased mitral valves[52], and mammary carcinoma[53]. A single study of the domestic cat proteome reports differences in the urine of healthy cats compared with that of cats with chronic kidney disease[54], highlighting the need for further studies of both the healthy feline proteome and disease states.

Phenotyping CYP Function

Several different *in vitro* techniques have been developed to characterize CYP function. Characterizing, or phenotyping, enzyme function includes determination of enzyme kinetics (rate and extent of metabolism) and the influence of the cellular environment on the enzyme. Once phenotyped, the influence of SNP and epigenetics on drug disposition can be further studied. Each technique has its own advantages and disadvantages, moving from a global overview of the role of the CYP in organ function down to the individual CYP via recombinant CYP (rCYP). Two frequently used techniques are microsomes and rCYP.

Microsomes

Early in drug discovery, liver microsomes and rCYP are frequently used to predict the intrinsic clearance (CL_{int}) of a drug in a target species to determine the risk of toxicity and determine a targeted dosing interval. Microsomes are subcellular fractions prepared by homogenization and differential centrifugation of a whole organ of interest[55]. This subcellular fraction consists of endoplasmic reticulum, containing phase I metabolism enzymes such as

CYP, acetylases, N-acetyl, and glucuronosyl transferases. Activation of a CYP metabolic pathway is initiated by the addition of the cofactor nicotinamide adenine dinucleotide phosphate-oxidase (NADPH)[56]. Several commercially available preparations of liver, duodenum, and lung microsomes are available for a variety of species[55]. Overall, these microsomes are very stable and can be frozen for many years with minimal loss of activity and reproducibility.

Liver microsomes can be utilized to determine the CL_{int} via a substrate depletion assay, also known as a drug stability assay. A known amount of a microsomal preparation (standardized by protein concentration) is exposed to the drug of interest under conditions supporting metabolic activity. By taking aliquots over a specified period (ex: 0, 5, 10, 20, 30 and 60 minutes) and quantifying the amount of substrate still present, a half-life ($t_{1/2}$) can be determined and used to calculate the CL_{int} [55]. Non-linear regression fitting to an exponential function produces the rate constant (k) for the parent compound (Eqn 1).

Equation 1

$$\%\ substrate\ remaining = Ax \times e^{-kt}$$

$$t_{1/2} = -\frac{\ln(2)}{k}$$

Where *Ax* represents the back extrapolated substrate concentration in the incubation media. CL_{int} can be estimated by using the rate of parent loss (Eqn 2)[57].

Equation 2

$$CL_{\text{int}} = \frac{0.693}{t_{1/2}} \times \frac{ml\ incubation}{mg\ microsomal\ protein} \times \frac{mg\ microsomal\ protein}{g\ liver\ weight} \times \frac{g\ liver\ weight}{kg\ bodyweight}$$

Microsomal stability assays are a great tool for the initial screening of compounds and determining metabolic pathways for their processing (e.g., CYP vs UGT). However, provided-to-provider and batch-to-batch variation between microsome preparations present considerable challenges. This is due to individual variation in CYP quantity and function due to SNV, and differences in preparation and storage techniques[56,58]. In addition, microsomes do not pinpoint which CYP is involved in metabolism unless known CYP inhibitors or antibodies are used[55].

Recombinant Cytochrome P450

Recombinant CYP can be utilized in a variety of techniques to study the enzyme kinetics of individual isoforms and determine the impact of various site mutations. These *in vitro* systems are designed by first sequencing the copied DNA (cDNA), then expressing the cDNA along with the NADP reductase sequence to produce a recombinant enzyme. In canines two types of rCYP have been described, an rCYP with a human reductase expressed in an insect cell line, producing a baculovirus[59] and an rCYP with a canine reductase expressed in an *Escherichia coli* vector [60]. Recently, recombinant expression of domestic feline CYP1A2, CYP2A13, CYP2E2 and CYP3A131 have been reported and these provide the first isoform phenotyping data for this species[61].

Methods for phenotyping include the substrate depletion assay (see equation 1 above) and inhibitory studies. Inhibition studies utilize substrates that are metabolized by a specific CYP and determine changes in the enzyme kinetics, specifically K_M, when a second substrate (inhibitor) is added. This strategy has been used to characterize isoform kinetics and identify substrate affinity in liver microsomes. To study enzyme kinetics and determine the rate of metabolite formation, a more complex assay measuring the rate of metabolite formation combined with substrate depletion is required. A combination of methods has been utilized to describe differences between humans, dogs, cats and other species[60-63].

In vitro species differences

The dog serves as a model for human safety and toxicity studies, and several studies have been used to identify differences through the use of "CYP cocktails." These cocktails contain multiple CYP substrates that target selected human CYP isoforms and can be used in inhibitory studies, *in vivo* SNP detection, and DDI studies both *in vitro* and *in vivo*. For example, the Inje cocktail[64] consisting of caffeine, losartan, omeprazole, dextromethorphan and midazolam reports that canine microsomal clearance is within three-fold of the human clearance[65]. A screening of 43 substrates in human, canine and rat microsomes report that CL_{int} in dogs is within 10-fold of human microsomes[66]. These similarities have led to the use of the canine as a model for safety and toxicity study in humans.

There are limited data comparing feline CL_{int} to human or canine values, but studies have reported that overall feline CYP activity is lower compared to these two species. Commonly used human CYP probe substrates report limited CYP2C activity and gender differences in

felines, with the rate of CYP2D6 metabolism greater in females than males, and an inverse relationship reported in CYP3A[67]. A comparison between human, equine, canine and feline CYP probe substrates found a statistically significant higher clearance of coumarin in humans compared to felines and higher tolbutamide, dextromethorphan O-demethylase, and chlorzoxazone 6-hydroxylase clearance in human and equine compared to cat [68]. While these cocktails offer a rapid method for characterization and comparison, the underlying assumption regarding similar substrate affinity can lead to incorrect conclusions. One example of this false assumption is the use of fluorescent probe cocktail assay comparing liver CYP activity between cat, dog, and human. This report found lower activity of feline CYP1A, CYP2C, CYP2D, CYP2E and CYP3A compared to canine, but higher feline CYP2B activity[69]. However, feline CYP2B6 was recently characterized, and mRNA transcripts were found in the lung and small intestine but not in the liver[31]. This raises the question of the validity of inferences that can be made using probe cocktails between species without knowledge regarding the specific isoform(s) present and affinity for a specific substrate.

Current Knowledge of Canine and Feline Metabolizing Cytochromes

Probes and inhibitor studies phenotyping CYP isoforms have been described in the canine; in comparison, a limited number of substrates have been reported in the feline (Table 1). Most of these studies utilize microsomes and probe cocktails combined with inhibitory substrates or polyclonal antibodies, with limited use of rCYP for phenotyping. Cytochrome P450 expression in tissues has also been described and quantified through the use of quantitative polymerase chain reaction (qPCR), western blotting, and LC/MS[13,70,71].

Table 1: Reported Substrates and Inhibitors in Canine and Feline

Human	Canine			Feline		
Isoform[#]	Isoform	Substrate	Inhibitor	Isoform	Substrate	Inhibitor
1A1/2	1A1/2	Ethoxyresorufin O-de-ethylation; theophylline[72]; phenacetin, caffeine[27]	Fluoroquinolones[73]; ondansetron, omeprazole, fluvoxamine, furafylline[27]; ketoconazole, miconazole[63]	1A1/2	Phenacetin, theophylline, 7-ethoxyresorufin, benzo[*a*]pyrene [74]	Fluvoxamine, tryptamine, clopidogrel, dexamethasone[61]
2B6	2B11	Propofol, diazepam, temazepam, midazolam, ketamine, atipamezole, S-medetomidine, R-medetomidine, methadone, pentobarbital, warfarin, phenytoin[27]; atipamezole, ketamine, diclofenac, medetomidine, midazolam, temazepam [13], tramadol(M2)[75]	Chloramphenicol, S-medetomidine, atipamezole, ketoconazole, miconazole, propofol[27]; ondansetron, loperamide, griseofulvin, ketoconazole, diazepam, fluoxetine, deracoxib, piroxicam[63], clompramine[76]	2B6	EFC, Coumarin, 7-Ethoxycoumarin[31]	EROD, MROD, sertraline, medetomidine, atipamezole, clopidogrel[31], ticlopidine[61]
2C8/9/19	2C21/41	Diclofenac, midazolam[13,27] tramadol(M2)[75]	ketoconazole[27], ketoconazole, miconazole, vincristine,	2C*	N/A	N/A

			praziquantel, piroxicam [63]			
2D6	2D15	Bufaralol, bunitrolol, celecoxib, despiramine, dextromethorphan, imipramine, metoprolol, proporanolol, maropitant[13,27], tramadol (M1)[75]	Clomipramine, fluoxetine, ketoconazole, loperamide, quinidine[27], metoclopramide, ondansetron, loperamide, ketoconazole, miconazole, ivermectin, buspirone, fluoxetine, omeprazole[63]	2D6	tramadol[75]	N/A
3A4/5/7	3A12/26	Diazepam, midazolam, eplerenone, diclofenac[63], tramadol(M2)[75]	Ketoconazole, loperamide[63]	3A131/132	N/A	Ketoconazole, clotrimazole, miconazole, sertraline, quinidine, erythromycin[(w)] , dexamethasone[(w)61]

Weak inhibitor(w)

[#] Human isoform may not have the same substrate profile as reported in cat and dog

[*]CYP2C isoforms have not been identified in the feline

CYP1A

In the canine, two CYP isoforms, CYP1A1 and CYP1A2, have been identified and, together, they are estimated to constitute about 4% of liver CYP protein expression[27]. Amino acid sequence identity between humans and canines report that the CYP1A family is the highest conserved family. CYP1A2 is polymorphic, with a substitution of Cytosine (C) for Thymine (T) at position 1117 (C1117C>T), resulting in a premature stop codon. This SNP was reported in more than 10% of the study population, and a homozygous CC allele frequency of 37% in dogs has been reported. Genotyping has revealed a statistically significant different frequency of the CYP1A2 CC wildtype genotype between boxers and purebred dogs[77,78]. The polymorphism was initially identified when a difference in a PK study using beagle dogs was identified. This polymorphism resulted in differentiating dogs into EM or PM. Canines with a homozygous TT allele frequency are likely to have prolonged clearance due to a nonfunctional CYP1A2. Prevalence of the SNP indicates that the Irish wolfhound has the highest TT allele frequency at 42%. Breeds with a TT allele frequency greater than 25% include Japanese beagle and Berger Blanc Suisse[13]. Other breeds noted to have the SNP include Australian Shepherd, Bearded Collie, Collie, Dalmatian, Border Collie, Deerhound, German Shepherd, Greyhound, Jack Russell Terrier, Shetland Sheepdog, and Whippet[79]. Screening of wildtype and CYP1A2-deficient reports differences in the metabolism of phenacetin o-deethylase, ethoxyresorufin o-deethylase, and tacrine 1-hydroxylase[80]. The clinical relevancy of this SNP has not been described. To screen a population for this SNP, tizanidine has been suggested as a marker to identify canine patients with the polymorphism and study the impact on drug efficacy[81].

Clinically important CYP1A inhibitors include the fluoroquinolone family, with chronic concomitant administration of ofloxacin, enrofloxacin, or marbofloxacin in conjuction with theoplhylline resulting in decreased theophylline clearance[72,82,83]. High theophylline plasma drug concentrations can result in mild signs such as vomiting or severe adverse events including cardiac arrhythmias and central nervous stimulation resulting in agitation, nervousness and seizures[84]. While no studies comparing pharmacokinetics of theophylline in dogs with the TT SNP have been reported, the clearance of theophylline along with other CYP1A substrates are likely to be prolonged and may require altered dosing.

The feline has two CYP1A isoforms, with CYP1A1 having an 87.4% amino acid homology compared to the canine isoform, and CYP1A2 having 82.4% homology compared to

the canine orthologue. CYP1A1 mRNA transcript expression has been found in the liver, lung, stomach, small intestine and pancreas of cats. CYP1A2 mRNA transcripts were only detected in the liver. Enzyme kinetic studies using theophylline reveal a demethylation as well as an oxidation pathway, with the rate of demethylation much higher than oxidation, an inverse from rat CYP1A. Compared to rat CYP1A2, the demethylation and reduction were much slower. The catalysis of phenacetin by feline CYP1A2 is also much slower compared to rats, perhaps explaining the increased risk of drug toxicity in cats compared to other species[74]. Neither phenotyping nor inhibitory studies have been completed for these two feline isoforms, limiting the ability to predict DDI.

CYP2B

Canine CYP2B11 is estimated to constitute 10% of total hepatic CYP expression[27] and a lesser, more variable quantity has been reported in small intestine microsomes[85]. This enzyme has been implicated in the metabolism of multiple anesthetics. Differences in the PK between greyhounds and mixed breed dogs have been reported, and whether these differences are due to CYP2B11 polymorphisms or lean muscle content continues to be an area of research[62,86,87]. The differences in the rate of metabolite formation between humans and canines have also been highlighted via a comparison of tramadol metabolite formation. This common opioid analgesic produces two metabolites: O-Desmethyltramadol (M1) and N-Desmethyltramadol (M2). M1 is produced by CYP2D15, while the M2 metabolite is the result of CYP2B11 and CYP3A12 catalysis. These isoforms exhibit sterioselectivity, complicating the ability to predict the rate of metabolite formation. Compared to human and cat microsomes, the ratio of M1/M2 in canine microsomes is significantly different, with canine microsomes favoring the production of M2, while cat microsomes favor M1 production[88]. The analgesic property of tramadol is due to the plasma drug concentration of the M1 metabolite, which has been found to be subtherapeutic in dogs, correlating with *in vitro* experimental findings.

The common anticonvulsant phenobarbital has also been shown to induce canine *CYP2B11* mRNA transcript expression after hepatocytes were treated *in vitro* for 48 hours, resulting in a 2-fold change in the rate of 7-benzyloxyresorufin O-dealkylation (BROD) catalysis[89]. Induction of CYP2B11 via phenobarbital has also been reported to increase the rate of tramadol M2 metabolite formation in dogs [75]. Whether this induction results in differences in the pharmacokinetic profile of CYP2B11 substrates remains unclear.

Feline CYP2B6 was recently described and found to have 81.8% amino acid identity with canine CYP2B11 followed by equine, pig, primate and human with 73.9-77.7% amino acid similarity. The highest mRNA transcript quantity was found in the lung, followed by the small intestine, colon, and rectum. CYP2B6 transcripts were lacking in the liver, which was confirmed via western blotting using an anti-human CYP2B6 polyclonal antibody[31]. CYP2B6 substrate affinity appears to vary between humans and cats. Two CYP2B human probe substrates, PROD and BROD, were not significantly metabolized by feline rCYP2B6, but the human CYP1A1 and CY1A2 probe substrates 7-ethoxyresorufin (EROD) and 7-methoxyresorufin (MROD) were metabolized by feline rCYP2B6[61]. The lack of CYP2B6 in the feline liver may also contribute to the hepatic toxicity of selected drugs reported in felines. In dogs, diazepam is metabolized into two active metabolites, nordiazepam via CYP2B11 and temazepam via CYP3A12. Temazepam can be further metabolized by CYP2B11 into oxazepam or glucoronidated, a phase II enzyme lacking in the feline liver in addition to CYP2B6. This results in intrahepatic accumulation of diazepam and may contribute to the hepatic necrosis observed with chronic dosing[90].

CYP2C

Two CYP2C canine isoforms (CYP2C21 and CYP2C41) are estimated to constitute 33% of total hepatic CYP protein content[27]. The two isoforms are reported to have 70% nucleotide and amino acid similarity. However, while *CYP2C21* was found to be expressed in all animals tested, only 11% of tested dogs expressed *CYP2C41*[91]. This finding was further confirmed in a study using Beagles, where 6/11 dogs had *CYP2C41* mRNA transcripts[13]. While there are only two isoforms reported in canines, 4 isoforms are reported in humans. This makes prediction of substrate affinity more challenging, since only CYP2C21 is present in all dogs and few dogs also express CYP2C41. CYP2C21 has been implicated in the metabolism of the active tramadol M1 metabolite into the inactive M5 metabolite, with a greater than 70-fold difference in the rate of M5 metabolite formation between individual dog liver microsomes. This highly variable rate of drug metabolism may account for the varied analgesic response reported in canine patients and the rapid clearance of M1[75].

There are no reports of CYP2C transcript expression or protein quantification studies in felines. *In vitro* feline microsome studies report decreased catalysis of human CYP2C probes in

felines and differences in the clearance between male and female felines[67-69]. However, as discussed previously, this relies on the assumption of similar isoform substrate affinity between the species, and results should be interpreted with caution.

CYP2D

A single canine isoform, CYP2D15 is estimated to make up 20% of total hepatic CYP protein content[27]. *CYP2D15* mRNA transcripts were highest in the liver, and transcripts were also observed in bladder, spleen, brain, kidney, and lung, with no gender differences reported[33]. rCYP2D15 had high catalytic activity but appeared to have unique substrate specificity, with reported low catalytic activity for debrisoquine compared to other species[92]. This isoform is the sole isoform responsible for the tramadol M1 metabolite, and is reported to have a higher affinity for the (+) stereoisomer compared to the (-) tramadol steroisomer[75]. In humans, the (+)M1 metabolite for tramadol has been suggested as a probe substrate to identify PM in population pharmacokinetic studies[93].

A single *CYP2D6* isoform transcript has been detected in feline liver and testis. This isoform shares 86% nucleotide and 80% amino acid similarity with the dog[94]. An *in vitro* microsome assay found oxidation of 3-[2-(N, N-diethyl-N-methylamino)ethyl]-7-methoxy-4-methylcoumarin was significantly higher in male cats than females[69]. No further characterization nor phenotyping of feline CYP2D6 exists in the literature, to our knowledge.

In humans, CYP2D6 is an important isoform due to the wide variety of substrates metabolized by this enzyme, and is estimated to metabolize up to 20% of all pharmaceuticals. This isoform has a high degree of interindividual variability due to the extensive SNP, with over 80 alleles described. Up to 10% of Caucasians are reported to have the null allele, resulting in no functional CYP2D6 protein[95]. Unlike humans, no polymorphisms for this isoform have been reported in dogs or cats.

CYP3A

The two canine CYP3A isoforms, CYP3A12 and CYP3A26, are estimated to constitute 14% of total hepatic CYP protein content[27]. CYP3A12 protein is also present in lower quantities in small intestinal microsomes, decreasing as one progresses down the gastrointestinal tract[85].

Comparison of mRNA transcripts expression in liver versus duodenum indicates a higher amount of *CYP3A26* in the liver compared to the *CYP3A12*, with an inversion of this relationship in the duodenum. The two isoforms are 96% identical, with a difference of 22 out of 503 amino acids, but located in highly conserved areas, altering the hydrophobicity and charge of the enzyme, and, therefore, the rate of metabolism[96]. For example, steroid hydroxylation by CYP3A26 was found to be only 22% compared to CYP3A12 hydroxylation[97]. CYP3A is considered to be an important drug metabolizing isoform in both humans and dogs, encompassing a wide variety of substrates from antifungals to immunosuppressants. Due to the wide variety of substrates metabolized by this enzyme, co-administration of drugs can result in DDI, especially if there is competition for the same site. For example, coadministration of ketoconazole, an inhibitor of CYP3A12, and cyclosporine, a CYP3A12 substrate, in dogs can result in a 75% reduction in the cyclosporine dose required to achieve therapeutic plasma drug concentrations[11].

Two CYP3A isoforms have also been identified in the feline, CYP3A131 and CYP3A132. The two isoforms share 94.9% open reading frame similarity and 90.9% amino acid similarity. CYP3A131 shares 74.8-91.1% coding and 65.3-88.3% amino acid similarity with other mammalian CYP3A isoforms, and CYP3A132 shares 74-90.7% coding and 64.5-88.7% amino acid similarity. Both isoforms share the highest homology with canine CYP3A12. *CYP3A131* transcript expression appears to be predominant in the liver and small intestine with some expression in the brain and lung. Only a small amount of *CYP3A132* expression is present in the liver[34]. Based upon inhibitory studies using rCYP3A131, the antifungals clotrimazole, ketoconazole and miconazole were found to be strong inhibitors, similar to CYP3A12 activity. The selective serotonin reuptake inhibitor (SSRI) sertraline was also an rCYP3A131 inhibitor, while fluvoxamine, a member of the SSRI family, was an inhibitor of rCYP1A2. No protein quantification studies have been completed for the CYP3A isoforms in felines, a necessity to determine the overall impact of this enzyme family.

In summary, the differences in amino acid homology combined with the variation in CYP mRNA expression in the liver and differences in CYP protein content are expected to result in differences in the rate of substrate metabolism. CYP substrate affinity and rates of clearance should not be assumed based on other species.

Aim

The aims of these studies were to 1) using RNA-sequencing, characterize the whole CYP transcriptome across multiple tissues in both the canine (Chapter 2) and feline (Chapter 3) using RNA-sequencing, 2) using liver microsomes and depletion studies of selected marker substrates, relate differences in the canine and feline transcriptome to differences in intrinsic clearance using liver microsomes and depletion studies of selected markers substrates (Chapter 4), 3), determine whether inferences regarding drug phenotypes between human and canine CYP are justified (Chapter 5).

Supplemental Table 1: Canine Single Nucleotide Variants

	Variant ID	Chr: bp	Alleles	Conseq. Type
CYP1A1	rs23665075	30:37789718	T/C	downstream gene variant
	rs23665076	30:37789756	C/T	downstream gene variant
	rs23665077	30:37789759	G/A	downstream gene variant
	rs23665078	30:37789782	C/T	downstream gene variant
	rs23665079	30:37789865	C/T	downstream gene variant
	rs23665093	30:37790115	T/C	downstream gene variant
	rs23627268	30:37797327	T/C	intron variant
	rs23627269	30:37797398	C/T	intron variant
	rs23627271	30:37798238	G/C	intron variant
	rs23659027	30:37799374	G/C	intron variant
	rs8953578	30:37801236	C/T	upstream gene variant
	rs23645261	30:37801241	G/A	upstream gene variant
	rs23645262	30:37801378	T/C	upstream gene variant
	rs23635321	30:37802109	T/A	upstream gene variant
	rs23635323	30:37802967	G/C	upstream gene variant
	rs23620416	30:37803281	T/C	upstream gene variant
	rs23620414	30:37803928	G/A	upstream gene variant
	rs23635324	30:37804140	A/T	upstream gene variant
	rs23658298	30:37804307	G/A	upstream gene variant
	rs23635326	30:37804309	G/A	upstream gene variant
	rs23635327	30:37804643	A/C	upstream gene variant
	rs23635337	30:37805036	T/C	upstream gene variant
CYP1A2	rs23653070	30:37813758	G/A	upstream gene variant
	rs23653075	30:37815004	T/C	upstream gene variant
	rs23653081	30:37815006	G/A	upstream gene variant
	rs23636696	30:37815323	A/G	upstream gene variant
	rs23653084	30:37815514	C/A	upstream gene variant
	rs23653086	30:37816897	C/T	upstream gene variant
	rs23653099	30:37817263	G/C	upstream gene variant
	rs8897992	30:37817279	T/C	upstream gene variant

	Variant ID	Chr: bp	Alleles	Conseq. Type
	rs8897991	30:37817311	T/C	upstream gene variant
	rs8897990	30:37817377	T/C	upstream gene variant
	rs23629094	30:37817424	C/G	upstream gene variant
	rs8897988	30:37817478	C/T	upstream gene variant
	rs23653101	30:37817711	T/C	upstream gene variant
	rs8897983	30:37818061	G/T	upstream gene variant
	rs23629093	30:37818074	C/G	upstream gene variant
	rs23629092	30:37818387	T/C	upstream gene variant
	rs8897981	30:37818505	A/G	splice region variant;intron variant
	rs23653109	30:37819341	C/A	splice region variant;intron variant
	rs23653112	30:37819412	G/A	missense variant
	rs23653115	30:37819431	C/T	missense variant
	rs23653141	30:37819709	C/A	missense variant
	rs23653143	30:37819712	A/T	missense variant
	rs23655378	30:37819854	C/T	missense variant
	rs8897972	30:37819922	C/A	missense variant
	rs23630848	30:37820036	A/T	missense variant
	rs23630846	30:37820037	A/C	missense variant
	rs8897971	30:37820048	G/T	missense variant
	rs23643750	30:37820118	C/T	missense variant
	rs23643751	30:37820180	C/T	splice region variant;intron variant
	rs23653202	30:37823782	C/G	missense variant;splice region variant
	rs23653204	30:37823842	G/A	missense variant
	rs23653206	30:37823990	G/A	missense variant
	rs23653212	30:37824228	C/G	downstream gene variant
	rs23652078	30:37824317	A/G	downstream gene variant
	rs23652080	30:37824512	A/G	downstream gene variant
	rs8616932	30:37824647	A/G	downstream gene variant
	rs23653214	30:37824673	T/A	downstream gene variant
	rs23653215	30:37824709	C/T	downstream gene variant
	rs23653219	30:37824742	T/C	downstream gene variant

	Variant ID	Chr: bp	Alleles	Conseq. Type
	rs23653221	30:37824860	A/G	downstream gene variant
	rs23653225	30:37825033	A/G	downstream gene variant
	rs23653227	30:37825193	C/G	downstream gene variant
	rs23653231	30:37825288	T/G	downstream gene variant
	rs23653269	30:37826502	T/C	downstream gene variant
	rs23653275	30:37826694	C/G	downstream gene variant
	rs23653277	30:37826720	G/C	downstream gene variant
	rs23653278	30:37826721	C/T	downstream gene variant
	rs8616936	30:37826801	C/T	downstream gene variant
	rs23653295	30:37826816	T/C	downstream gene variant
	rs23653301	30:37827067	C/T	downstream gene variant
	rs23653303	30:37827141	T/C	downstream gene variant
	rs23653308	30:37827505	A/T	downstream gene variant
	rs23653312	30:37827657	T/C	downstream gene variant
	rs23653315	30:37827773	C/G	downstream gene variant
	rs23639939	30:37828490	A/C	downstream gene variant
	rs23639941	30:37828538	T/C	downstream gene variant
	rs23639942	30:37828605	C/T	downstream gene variant
	rs23639944	30:37828881	C/T	downstream gene variant
	rs8841443	30:37829200	T/G	downstream gene variant
CYP2B11	rs21979577	1:112812702	T/C	upstream gene variant
	rs21979572	1:112813023	C/T	upstream gene variant
	rs21894687	1:112828499	G/A	splice region variant;synonymous variant
	rs21964373	1:112835194	C/T	downstream gene variant
	rs21964372	1:112837109	A/G	downstream gene variant
CYP2C21	rs23459991	28:8751640	G/A	upstream gene variant
	rs23459992	28:8752256	T/A	upstream gene variant
	rs23459993	28:8753349	T/C	upstream gene variant
	rs23459994	28:8753525	T/C	upstream gene variant
CYP3A12	rs24331991	6:9833925	A/C	downstream gene variant
	rs24333657	6:9834982	A/G	downstream gene variant

	Variant ID	Chr: bp	Alleles	Conseq. Type
	rs24333639	6:9835023	G/A	downstream gene variant
	rs24333637	6:9835219	G/A	downstream gene variant
	rs24333636	6:9835233	A/C	downstream gene variant
	rs24333635	6:9835380	G/A	downstream gene variant
	rs24333634	6:9835774	G/C	downstream gene variant
	rs24333631	6:9836010	C/T	downstream gene variant
	rs24333630	6:9836076	T/C	downstream gene variant
	rs24333629	6:9836116	G/A	downstream gene variant
	rs24334216	6:9838331	A/G	missense variant
	rs24334217	6:9838417	G/C	missense variant
	rs24334218	6:9838424	C/T	missense variant
	rs24334219	6:9838437	C/T	splice region variant;intron variant
	rs24360201	6:9847300	G/A	splice region variant;intron variant
	rs24356444	6:9861384	T/C	missense variant
	rs24310976	6:9869704	T/A	upstream gene variant
	rs24310978	6:9869770	G/A	upstream gene variant
	rs24310995	6:9870184	A/G	upstream gene variant
	rs24310997	6:9870192	A/G	upstream gene variant
	rs24322803	6:9870630	G/T	upstream gene variant
	rs24322821	6:9870700	C/T	upstream gene variant
	rs24322819	6:9870894	G/A	upstream gene variant
	rs24308842	6:9872030	A/G	upstream gene variant
	rs24308845	6:9872217	C/T	upstream gene variant
	rs24308848	6:9872397	G/T	upstream gene variant
	rs24338370	6:9872637	G/T	upstream gene variant
	rs24338369	6:9872663	T/A	upstream gene variant
	rs24338367	6:9872781	G/A	upstream gene variant
	rs24338366	6:9872792	A/C	upstream gene variant
	rs24322908	6:9873690	T/C	upstream gene variant
	rs24322910	6:9873810	G/A	upstream gene variant
	rs24322912	6:9874196	C/T	upstream gene variant

	Variant ID	Chr: bp	Alleles	Conseq. Type
CYP3A26	rs24307050	6:9773693	T/C	downstream gene variant
	rs24309413	6:9774895	G/A	downstream gene variant
	rs24306505	6:9776734	C/A	downstream gene variant
	rs24323373	6:9795907	G/T	missense variant
	rs24323375	6:9796052	G/C	splice region variant;intron variant
	rs24322803	6:9816608	G/T	upstream gene variant
	rs24322821	6:9816678	C/T	upstream gene variant
	rs24334169	6:9816811	C/T	upstream gene variant
	rs9034343	6:9816879	C/T	upstream gene variant
	rs24334170	6:9817385	T/C	upstream gene variant
	rs24334172	6:9817460	G/T	upstream gene variant
	rs24334173	6:9819548	C/G	upstream gene variant
	rs24334191	6:9820169	G/A	upstream gene variant
	rs24331056	6:9820191	C/A	upstream gene variant
	rs24331054	6:9820244	C/G	upstream gene variant
	rs24331052	6:9820300	G/A	upstream gene variant
	rs24331051	6:9820309	G/A	upstream gene variant

Reference single nucleotide polymorphism (rs); Alleles: Alternative nucleotide compared to the published genome. Chromosome (Chr); base pair (bp); Guanine (G); Adenine (A); Cytosine (C); Thymine (T). [1]

[1] http://useast.ensembl.org/index.html. Accessed 01 Feb 2018; Canine SNP variant

Supplemental Table 2: Feline Single Nucleotide Variants

	Variant ID	Chr: bp	Alleles	Conseq. Type
CYP1A2	rs43832285	B3:33515572	G/T	missense variant
	rs43832287	B3:33518219	A/G	upstream gene variant
	rs43832290	B3:33520374	G/T	upstream gene variant
	rs43832291	B3:33520997	G/A	upstream gene variant
	rs43832292	B3:33521159	A/G	upstream gene variant

Reference single nucleotide polymorphism (rs); Alleles: Alternative nucleotide compared to the published genome. Chromosome (Chr); base pair (bp); Guanine (G); Adenine (A); Cytosine (C); Thymine (T).[2]

[2] http://useast.ensembl.org/index.html. Accessed 03 Feb 2018; Feline SNP variant

Chapter 2: Use of RNA-seq to determine variation in canine cytochrome P450 mRNA expression between blood, liver, lung, kidney and duodenum in healthy beagles.[3]

Abstract

RNA-sequencing (RNA-seq) is a powerful tool for the evaluation and quantification of transcriptomes and expression patterns in animals, tissues or pathological conditions. The purpose of this study was to determine the physiologic expression of cytochrome P450 (CYP) mRNA transcripts in whole blood, kidney, duodenum, liver and lung in healthy, adult male (n=4) and female (n=4) beagles via RNA-seq. Data quality assessment included sequencing depth, and reads per million. mRNA expression was above background (transcripts per million) for 45 canine CYPs, with liver, duodenum and lung expressing a high number of xenobiotic-metabolizing CYPs, while prominent endogenous-metabolizing CYP expression was present in blood and kidney. The relative expression pattern of *CYP2A13*, *2B11*, *2C21*, *2D15*, *2E1*, *3A12* and *27A1* in liver, lung and duodenum was verified through qPCR. This is the first global profiling of physiologic CYP mRNA expression in multiple canine tissues, providing a platform for further studies characterizing canine CYPs and changes in gene expression in disease states.

Keywords: cytochrome P450, beagle, single nucleotide polymorphism, RNA-seq, qPCR

Introduction

Cytochrome P450 (CYP) constitutes the major enzyme family catalyzing oxidative metabolism of drugs and lipophilic xenobiotics. This family also serves an important role in endogenous synthesis and metabolism of steroid hormones, prostaglandins, bile acids and

---

[3] Visser, M., Weber, K., Rincon, G., & Merritt, D. (2017). Use of RNA-seq to determine variation in canine cytochrome P450 mRNA expression between blood, liver, lung, kidney and duodenum in healthy beagles. *Journal of Veterinary Pharmacology and Therapeutics*, *40*(6), 583-590.

eicosanoids. In humans, there are 57 functional genes and 58 pseudogenes, clustered into 18 families and 44 subfamilies based on their amino acid sequence homologies[98]. Important CYP families involved in drug metabolism include CYP1A, CYP2B, CYP2C, CYP2D, CYP2E, and CYP3A. These CYPs have been implicated in drug-drug interactions (DDI), where drugs/xenobiotic acting as a substrates, inhibitors or inducers to alter the pharmacokinetics of important drugs. Over- and under-expression among CYPs can lead to sub-therapeutic doses or toxicities[99]. An additional complication is single nucleotide polymorphisms (SNP), which can result in amino acid changes, altering CYP expression and/or function in affected populations. These can produce potentially life threatening adverse drug reactions or sub-therapeutic dosing[98,99]. Advancement in the understanding of human CYP expression and metabolism have led to the development of genetic screening to identify individuals or populations who may be at greater risk for DDI. This level of pharmacogenetic understanding is lacking in veterinary patients, with limited information available regarding CYP expression profiles. Current knowledge of canine CYP includes: 1) sequences corresponding to 4 CYP families[100,101], 2) the identification of SNPs that lead to functional changes in CYP1A2, CYP2C41 and CYP2D15 metabolism, and 3) protein quantification of 7 CYPs in the liver and 2 CYPs in the intestine[13].

RNA-sequencing (RNA-Seq) allows for the evaluation of the entire transcriptome of a tissue and has become a powerful tool for quantifying gene expression and transcripts, discovering alternative splicing sites, detecting gene fusions, mapping transcription pathways, and detecting SNP[102,103]. Short paired reads are aligned to a published genome, with alignment based upon selected conditions including mismatch frequency, indel and exon junction call. Once mapped, transcript data can be quantified as unique counts and normalized via transcript per million (TPM), which takes into account the variation of transcript length as well as sequencing depth. By normalizing for these sources of variation, expression of different genes across tissues can be compared, giving an overview of the variation between disease states, tissues or individual animals[104]. RNA-seq has been used in physiological studies to characterize the equine transcriptome[105] and alterations in the transcriptome of Holstein milk over a 250-day period[106]. Pathological conditions such as alterations in the immune response of sheep to *Fasciola hepatica*[107] and pathway analysis of canine lymphoma[108] highlight the use of RNA-seq in monitoring alterations in the transcriptome in response to disease states. Armed with the canine genome, drug-induced toxicities caused by drug transporter mutations in P-glycoprotein

have been characterized, allowing for the development of genetic screening to identify at-risk dogs[27]. CYP SNP have been implicated in alterations in metabolism of non-steroidal anti-inflammatory drugs, causing altered pharmacokinetics in celecoxib[109].

The published canine genome consists of annotations, which describe the location and function of each gene.[110] Annotations are based upon curation by researchers targeting specific genes as well as automated programs such as Ensembl, which predicts annotations based upon a combination of gene sequences placed in public databases, gene orthologs from other species and protein homology.[111] Annotations are constantly evolving, with manual curations improving gene boundaries and next generation sequences providing large quantities of data from individual animals allowing for the identification of SNP.

The purpose of this study was to quantify and compare CYP mRNA expression in the liver, kidney, lung, duodenum and blood via RNA-seq, providing a global overview of the CYP transcriptome in the healthy canine. These sites were selected for evaluation due to their importance in determining pharmacokinetic parameters such as absorption, metabolism, distribution and excretion in the canine.

Methods:

Subjects acted as a control group for a separate study. All protocols were approved by the Institutional Animal Care and Use Committee (IACUC) at Zoetis.

Sample collection:

Male (n=4) and female (n=4) healthy 18 month-old purpose-bred beagles (Marshall Farms) were euthanized via injection of sodium pentobarbital. One tissue sample per animal for blood (n=8), and sections of liver (n=8), kidney (n=7), lung (n=8), duodenum (n=8), were collected. One kidney sample (F) was accidentally not collected. Blood (PAXgene Blood RNA Tube, PreAnalytiX, Hombrechtikon Switzerland) and tissues (RNA*later*®, Qiagen, Valencia, CA, USA) were kept frozen at -80˚C until processing. Liver and kidney total RNA was isolated using the RNA Mini protocol (Qiagen®, Valencia, CA, USA), lung and duodenum isolated using the Fibrous RNA protocol (Qiagen®, Valencia, CA, USA) and blood using PAXgene Blood RNA Kit, PreAnalytiX (Qiagen®, Valencia, CA, USA). RNA integrity number (Bioanalyzer 2100, Agilent Technologies, Santa Clara, CA, USA) and cDNA quality (NanoDrop 8000, ThermoScientific, Wilmington, DE, USA) were evaluated prior to individual tissue cDNA library preparation (Schroeder et al., 2006). cDNA library preparation was completed utilizing

the TruSeq® Stranded mRNA sample preparation protocol (Illumina ®, San Diego, CA, USA). Libraries were quantified (Quanti-IT® High-Sensitivity DNA Assay Kit, ThermoScientific, Grand Island, NY, USA), pooled into 4 lanes and submitted for sequencing (Eureka Genomics®, Hercules, CA, USA).

RNA-seq Analysis and Statistics:

RNA sequence analysis was performed using CLC Genomics Workbench 8.0 (Qiagen ®, Valencia, CA, USA). Quality checks of RNA sequencing reads included statistics on the number of reads per tissue sample, base quality score, read length, GC content, and most frequent 15-mers. Reads were mapped to the most recent canine annotated reference genome (CanFam 3.1, Ensembl release 81), a publicly available boxer genome (Lindblad-Toh et al., 2005). In order to maximize the likelihood of detecting all CYPs in the genome, orthologs of human CYP annotations were identified via Ensembl Biomart, a data mining tool allowing for comparison between the annotated genome of two organisms. An extensive literature search was also done to ensure that all known canine CYP were accounted for (Table 2). Canine *CYP2D15* was not present in ENSEMBL annotations but was available via the National Center for Biotechnology Information (NCBI, www.ncbi.nlm.nih.gov). The lack of annotations meant this sample was treated as a "novel" gene; therefore, the NCBI gene sequence was used in the basic local alignment search tool (BLAST) to detect and quantify *CYP2D15*. Annotations which do not have an individual canine nomenclature were named based upon the human orthologue, denoted by * (ex: CYP3A7*). Data were normalized using transcript per million (TPM), correcting for transcript length and allowing comparison between tissues[112]. Only uniquely mapped reads were included in the data analysis in order. The mean CYP expression and standard deviation (SD) for each organ were determined and presented in figure form.

Primer design and quantitative real-time PCR

Quantitative real-time PCR (qPCR) was performed to verify RNA-seq expression pattern of *CYP2A13*, *CYP2B11*, *CYP2C21*, *CYP2E1*, *CYP3A43*(*designated as human CYP3 based on RNA-seq analysis*), CYP3A12*, *CYP27A1* and *CYP2D15*. The genes selected were the top two or three genes expressed in liver, lung and duodenum. Specific primer pairs (IDT®, Coralville, IO, USA) were selected for the eight individual CYPs and two housekeeping genes (*HRPT*, *ACT-β*)

(Table 3). Reverse transcription (Invitrogen iScript, BioRad, Hercules, CA, USA) was performed at the three sites of xenobiotic absorption and metabolism, liver (n=8), duodenum (n=8) and lung (n=8). Quantification of cDNA (NanoDrop 8000, ThermoScientific, Wilmington, DE, USA) was done prior to qPCR (CFX384 Touch™ Real-Time PCR Detection System, BioRad, Hercules, CA, USA) utilizing SYBR green detection (SsoAdvanced Universal SYBR Green Supermix, BioRad, Hercules, CA, USA). Amplification protocol was: 95˚C for 30 seconds, 40 cycles at 95˚C to denature and 59˚C for 10 seconds to anneal. Melt curve analysis was performed with temperature range from 55-95˚C, with 0.5˚C increment increase every 5 seconds. Samples were run in triplicate. Relative quantification was done utilizing *HPRT* to standardize all the samples. In order to normalize the data, all samples were compared to *ACT-β*. Relative expression of qPCR was compared to the TPM for the selected genes. Pearson correlation coefficient was utilized to determine the strength of the overall expression pattern between qPCR and RNA-seq.

Results

The reads per sample ranged from 28.7-44.7 million, with the total unique reads mapped per sample ranging from 6.5-23 million reads per sample. In total, expression of 40 CYPs was identified and quantified in any of the 5 different tissues (Table 4). No significant difference in CYP expression was found between male and female dogs. *CYP2E1* had the highest mean transcript expression in the liver, followed by transcript levels for *CYP2C21, CYP3A7**, *CYP3A26* and *CYP3A12* (Figure 2). In the duodenum, *CYP3A12* was the highest expressed followed by *CYP27A1* ≥*CYP2B11* (Figure 3). In the lung, *CYP2B11* was the highest expressed, with minimal transcript expression of other metabolizing CYPs (Figure 4). The highest expressed CYPs in kidney (*CYP4A37*) (Figure 5) and blood (*CYP4F**) (Figure 6) are correlated with eicosanoid production, and limited CYP xenobiotic enzyme expression was present at these two sites.

Discussion

CYPs can be categorized by their function. For example, *CYP2F-S, CYP4,* and *CYP20-*51 are classically associated with homeostatic functions. Functions for this subset of CYPs include eicosanoid production, angiogenesis, regulation of inflammation[113], bile production and cholesterol homeostasis[114]. The prevalence of these CYPs in the kidney and blood cells indicates

important functions in homeostasis with perhaps limited drug and xenobiotic metabolism. An estimated 70-80% of drug biotransformation is attributed to CYP1A2, 2B11, 2C21, 2C41, 2D15, 3A12 and 3A26 in the dog[98]. Of note is that *CYP2C41* mRNA was not expressed in any of the sampled tissues, nor could expression of this gene be found through the use of novel transcript detection. This gene has only been reported in 16% of beagles studied, and its prevalence in other breeds have not been reported[13]. The presence of this gene has been suggested as a cause of the rapid metabolism of celecoxib and may also influence the metabolism of other CYP2C-dependent drugs.[109]

Known CYPs in humans that utilize pharmaceuticals as substrates, inhibitors or inducers include 1A1; 1A2; 2B6; 2D; 2C8,919; 2E1; and 3A4,5,7 [115]. The canine orthologs to these genes include 3A12/26 for 3A7, 2C21 for 2C9, 2D15 for 2D6, and 2B11 for 2B6[98]. The majority of CYP expressed in the canine orthologue are mirrored by human transcript expression. The three highest transcript signals observed in the liver were CYP2E1, CYP2C21 and CYP2A13. The pattern of transcript expression conflicts with previous reports in which CYP2D15 had greater transcript expression than CYP3A26 and CYP3A12 based on qPCR rather than RNA-seq[116]. Transcripts for both CYP3A12 and 3A26 were observed in the canine as well as CYP3A7* and CYP3A5*. These two annotations have not been well characterized and may either suggest two additional CYP3A variants or gene duplication. Alignment of the 4 genes indicates areas of conservation, but sequencing and recombinant expression are necessary to determine whether additional CYP3A enzymes are present in the canine. In humans, a gene duplication of CYP2D6 has been implicated in alterations of drug metabolism, and it is possible the CYP3A5* and 3A7* may be gene duplications[117].

Comparison of qPCR and RNA-seq results must be done with caution since the methods of quantification vary significantly. In this case, qPCR is relative quantification compared to housekeeping genes, while RNA-seq quantification is based solely on the number of transcripts without comparison to any housekeeping genes. Therefore, each gene was reported as a percentage of the total expression sum of the seven genes of interest. In the liver, there appears to be the same percent of expression, but there is variation in the duodenum. *CYP3A12* and *CYP3A7* qPCR does not compare to RNA-seq expression. If *CYP3A7* is a gene duplication, it is possible that the primers share a consensus sequence and therefore cannot distinguish between the two genes. All attempts to avoid this were made by blasting primers against both sequences

to limit the risk of this happening, but unlike RNA-seq. Full characterization of *CYP3A7** and *CYP3A5** would not only clarify whether these are gene duplicates, but also allow for more specific primers to be developed.

Whether the level of RNA expression correlates with protein expression requires further evaluation, since protein abundance is subject to post-transcriptional and translational regulation[118]. Previous quantitative protein mass spectroscopy (LC/MS) suggested the presence of very little CYP3A26 protein but a large quantity of CYP3A12, CYP2E1, CYP2D15, CYP2C21 and CYP1A2. However, the mRNA transcript expression was much lower, which could be a reflection of the efficiency of the translation or variation between study populations. Unlike the liver, CYP expression in the duodenum does correlate with LC/MS CYP quantification in the duodenum, with CYP3A12 > CYP2B11[116]. Using a single study population to examine both transcription expression and the presence of protein may help to clarify these discrepancies.

In the lung, *CYP2B11* has the greatest transcript expression, but, to the authors' knowledge, there are no protein quantification studies to determine if there is a correlation between the mRNA expression and protein. This enzyme has been implicated in the metabolism of anesthetic drugs such as propofol[87], ketamine and midazolam while being inhibited by medetomide[62] and ketoconazole[119]. One *CYP2B11* SNP identified causes an amino acid change, suggesting that there may be a breed difference between the beagle and the canine reference genome (boxer) or there may be a highly prevalent SNP within the sample colony (purpose-bred laboratory beagles). Reports have indicated that SNP in CYP important for drug metabolism can alter pharmacokinetic parameters within and between breeds[109]. With the decrease in the cost of whole genome sequencing combined with the ability for cloud-based analysis, examination of differences between various breeds can create individual medicine approaches, decrease the risk of adverse drug reactions and aid in drug development to predict SNP with an increased risk of adverse drug events.

This is the first report regarding global CYP mRNA expression in multiple tissues in the canine using RNA-seq. By utilizing this powerful tool, a selection bias is removed since all expressed genes are reported. However, the power of this analysis is limited if CYP genes are not annotated or incorrectly annotated, as in the case of *CYP2D15*, or individual genes cannot be distinguished, as in the case of *CYP3A5** and *CYP3A7**. An understanding of baseline

expression is vital to understanding drug metabolism in both healthy and disease states. In this work, transcripts for 40 CYP enzymes were identified and quantified in the canine compared to 57 in humans. As anticipated, the liver, duodenum and lung are important sites for drug metabolism. In contrast, the kidney and blood may have greater expression of enzymes important for homeostasis. Additional research to fully characterize the relationship between transcript signal and CYP protein abundance/expression along with an understanding of the impact from altered expression when xenobiotically-induced or in disease states is required to help guide therapeutic management.

Table 2: Identified Canine CYP genes

CYP	Ensembl Canine ID	Chromosome	Gene Start	Gene End
CYP11A1	ENSCAFG00000017888	30	37,475,246	37,487,340
CYP17A1	ENSCAFG00000010279	28	15,292,522	15,299,029
CYP19A1	ENSCAFG00000015338	30	16,957,215	16,988,392
CYP1A1	ENSCAFG00000017937	30	37,793,073	37,800,053
CYP1A2	ENSCAFG00000017941	30	37,818,419	37,824,226
CYP1B1	ENSCAFG00000006164	17	30,269,745	30,278,554
CYP20A1	ENSCAFG00000012765	37	12,086,971	12,140,228
CYP21	ENSCAFG00000000712	12	1,450,677	1,453,734
CYP24A1	ENSCAFG00000011839	24	39,860,978	39,878,155
CYP26A1	ENSCAFG00000007574	28	7,428,543	7,432,724
CYP26B1	ENSCAFG00000009005	17	50,634,286	50,653,930
CYP27A1	ENSCAFG00000014943	37	25,366,035	25,401,253
CYP27B1	ENSCAFG00000000287	10	1,825,193	1,829,911
CYP27C1	ENSCAFG00000004542	19	23,375,348	23,399,773
CYP2A13	ENSCAFG00000032339	1	112,932,246	112,938,257
CYP2A7^	ENSCAFG00000031823	1	112,900,488	112,906,745
CYP2B6	ENSCAFG00000005052	1	112,817,437	112,833,488
CYP2C21	ENSCAFG00000008099	28	8,727,010	8,750,427
CYP2D15^	n/a	10	23,255,259	23,259,380
CYP2E1	ENSCAFG00000013318	28	41,078,615	41,090,460
CYP2F1	ENSCAFG00000023821	1	112,974,519	112,985,841
CYP2J2	ENSCAFG00000018871	5	49,942,193	49,984,322
CYP2R1	ENSCAFG00000008504	21	37,550,262	37,579,759
CYP2S1	ENSCAFG00000005049	1	112,734,986	112,747,565
CYP2U1	ENSCAFG00000011203	32	28,425,473	28,444,361
CYP2W1	ENSCAFG00000011551	6	15,883,508	15,889,186
CYP39A1	ENSCAFG00000002026	12	14,727,773	14,817,905
CYP3A12	ENSCAFG00000014877	6	9,836,676	9,869,352

CYP	Ensembl Canine ID	Chromosome	Gene Start	Gene End
CYP3A26	ENSCAFG00000014942	6	9,777,663	9,815,345
CYP3A*	ENSCAFG00000014939	JH373739.1	21	13,206
CYP3A43*	ENSCAFG00000014990	6	9,722,712	9,743,588
CYP46A1	ENSCAFG00000017838	8	68,072,603	68,097,030
CYP4A37^	ENSCAFG00000023282	15	13,604,130	13,623,797
CYP4A38^*	ENSCAFG00000025004	15	13,638,745	13,657,531
CYP4A11*	ENSCAFG00000023399	15	13,573,988	13,581,711
CYP4A39	ENSCAFG00000004169	15	13,663,448	13,675,044
CYP4B1	ENSCAFG00000004097	15	13,675,916	13,694,493
CYP4F11	ENSCAFG00000023401	20	46,611,481	46,631,393
CYP4F22	ENSCAFG00000023053	20	46,674,180	46,694,052
CYP4V2	ENSCAFG00000007384	16	44,525,644	44,544,809
CYP4X1	ENSCAFG00000023824	15	13,508,318	13,546,829
CYP51A1	ENSCAFG00000001945	14	17,746,739	17,766,635
CYP7A1	ENSCAFG00000007098	29	9,285,140	9,347,795
CYP7B1	ENSCAFG00000007246	29	14,444,860	14,613,129
CYP8B1	ENSCAFG00000005370	23	11,967,341	11,968,846

Canine identified CYP genes. ^ indicates that the specific gene name was identified via ncbi.gov, while * denotes the human name because a canine is not available. One gene remains located on the canine scaffold (JH373739.1). n/a if Ensembl canine ID was unavailable.

Table 3: Primers utilized in qPCR

Gene	Forward	Tm-F	Reverse	Tm-R
2E1	AGAAATCGACAGGGTGATCG	60.07	CATCGTGTCCTGGTTTGCTA	59.72
2C21	CCCTGTATGGTCCAGTCCAA	60.77	GCAGAGAATTATGGCCCTGT	59.15
2A13	GAGATTGATCGGGTGATTGG	60.28	GGAGGAGAAACTCCCGAAAC	60.05
3A43*	CCGAGTGGACTTTCTTCAGC	59.99	TGCAGTTTCTGCTGGACATC	59.99
3A12	TGTTTCTTTACAAGGTTTGAAGGAG	60.08	TACCTGCCTTTTGGAACTGG	60.1
2B11	TTCGAGCTTTTCCACAGCTT	60.13	CAGGTAGGCGTCGATGAAGT	60.28
27A1	CAGAAGGACTTTGCCCACAT	60.11	TTTATGGGGACCACAGGGTA	60.14
2D15	TGGACTTCCAGGAACCAATC	59.9	GGACTGTCCAACCAGCTCTC	59.84
HPRT	CCCTCGAAGTGTTGGCTATAA	59.23	TCAAGGGCATATCCTACAACAA	59.8

Primers utilized for each gene, including housekeeping genes: *HPRT* and ACT-β.

Table 4: Mean canine CYP expression by tissue

	Liver	Duodenum	Lung	Kidney	Blood
CYP11A1	0.0 (0)	0.0(0)	0.1(0.1)	2.6(0.4)	0.3(0.1)
CYP17A1	0.1(0)	0.0(0)	0.1(0)	0.1(0)	0.0(0)
CYP19A1	0.1(0)	0.1(0)	0.2(0.1)	0.1(0.1)	0.0(0)
CYP1A1	11.9(2)	44.9(39.5)	60.3(31.3)	0.8(0.3)	0.0(0)
CYP1A2	135.3(26)	0.0(0)	0.1(0)	0.1(0)	0.0(0)
CYP1B1	2.6 (0.4)	48.8(4.7)	73.8(17.4)	0.0(0)	0.1(0)
CYP20A1	6.4 (0.4)	14.2(2.1)	23.3(2.3)	27.8(1.4)	9.9(1.3)
CYP21	4.3 (0.5)	3.8(1.2)	0.3(0.1)	1.1(0.2)	0.1(0)
CYP24A1	0.0 (0)	0.1(0)	0.0(0)	7.8(3.1)	0.2(0.1)
CYP26A1	11.2 (1.2)	0.1(0)	0.1(0)	0.1(0)	0.0(0)
CYP26B1	3.8 (0.7)	3.8(0.8)	52.7(12.4)	7.3(1.2)	0.4(0)
CYP27A1	307.9 (13.7)	65.5(8.6)	150.1(19.3)	56.9(3.9)	87.8(13.5)
CYP27B1	0.0 (0)	0.0(0)	0.4(02.)	14.1(2.9)	0.0(0)
CYP27C1	0.4 (0.1)	0.6(0.2)	2.5(0.3)	0.8(0.1)	0.6(0.1)
CYP2A13	1146.0 (179.7)	0.1(0.1)	47.3(18.4)	0.9(0.7)	0.0(0)
CYP2A7^	432.0 (33.9)	0.0(0)	0.5(0.1)	0.1(0)	0.0(0)
CYP2B11	644.8(53.4)	107.3(34)	951.7(192.6)	0.3(0.1)	0.1(0)
CYP2C21	2172.8 (82)	0.3(0)	1.2(0.2)	0.7(0.2)	0.2(0.1)
CYP2D15^	888.1(49.9)	0.2(0)	0.8(0.2)	14.1(1.8)	1.5(1.1)
CYP2E1	12668.2(412.3)	0.0(0)	3.1(0.8)	2.0(0.6)	0.0(0)
CYP2F1	6.6(0.6)	0.0(0)	2.6(1.2)	0.0(0)	0.0(0)
CYP2J2	50.2(2)	44.3(9.9)	22.5(4.5)	130.7(5.4)	0.8(0.2)
CYP2R1	10.7(1)	26.3(3.7)	22.1(2.5)	17.3(0.9)	2.5(0.4)
CYP2S1	0.6(0.1)	18.0(5.5)	83.7(9.4)	0.3(0.1)	0.2(0.1)
CYP2U1	56.2(1.6)	7.8(0.8)	18.9(1.6)	14.8(0.9)	4.8(1.1)
CYP2W1	14.8(1.3)	0.4(0.2)	1.9(0.5)	1.3(0.1)	1.2(0.2)
CYP39A1	11.7(1.1)	8.3(0.8)	30.8(3)	15.5(0.8)	3.8(0.6)
CYP3A*	482.5(34.8)	0.0(0)	0.1(0.1)	0.1(0)	0.2(0.1)
CYP3A12	631.2(42.1)	338.7(116.2)	5.6(3.2)	0.3(0.1)	0.9(0.2)
CYP3A26	1145.3(75.4)	54.7(4.6)	78.3(9.6)	45.9(1.5)	53.7(6.9)
CYP3A43*	93.2 (9.9)	20.5(5)	0.4(0.2)	0.1(0)	0.0(0)
CYP46A1	0.2(0.1)	0.6(0.2)	1.8(0.2)	1.1(0.4)	3.8(0.3)
CYP4A11*	0.1(0)	0.0(0)	0.2(0.1)	1.4(0.3)	0.0(0)
CYP4A37^	643.5(29.7)	0.1(0)	1.5(0.4)	2008.2(126.5)	0.4(0.1)
CYP4A38^*	309.1(21.4)	0.1(0)	1.6(0.1)	383.3(13.6)	0.1(0)
CYP4A39	326.9(17.8)	0.0(0)	1.7(0.2)	942.8(125.4)	0.0(0)
CYP4B1	1.8(0.2)	1.6(0.8)	502.0(105.8)	6.7(0.4)	0.2(0.1)
CYP4F11	59.5(4.6)	0.8(0.5)	23.9(2.4)	0.4(0.1)	1835.9(160.5)
CYP4F22	0.2(0)	0.2(0.1)	0.1(0)	0.4(0.1)	0.7(0.1)
CYP4V2	194.2(10.9)	18.8(2.6)	61.0(7)	148.1(17.4)	79.4(11)

	Liver	Duodenum	Lung	Kidney	Blood
CYP4X1	5.4(0.4)	10.8(1.4)	11.5(2.1)	13.3(0.7)	1.9(0.3)
CYP51A1	72.3(7.6)	12.1(1.3)	20.3(2.4)	10.1(0.6)	7.2(0.8)
CYP7A1	246.4(39.2)	3.1(0.3)	4.3(0.7)	3.0(02.)	1.6(0.2)
CYP7B1	133.3(9)	4.0(1.6)	56.8(7)	5.7(0.5)	0.3(0)
CYP8B1	395.8(47.7)	3.3(1.2)	2.2(0.6)	22.5(2.8)	0.0(0)

Mean transcript per million (TPM) plus the standard error (SE). * the human annotation correlates with the presence of an annotated canine CYP which has not received individual isoform identification.

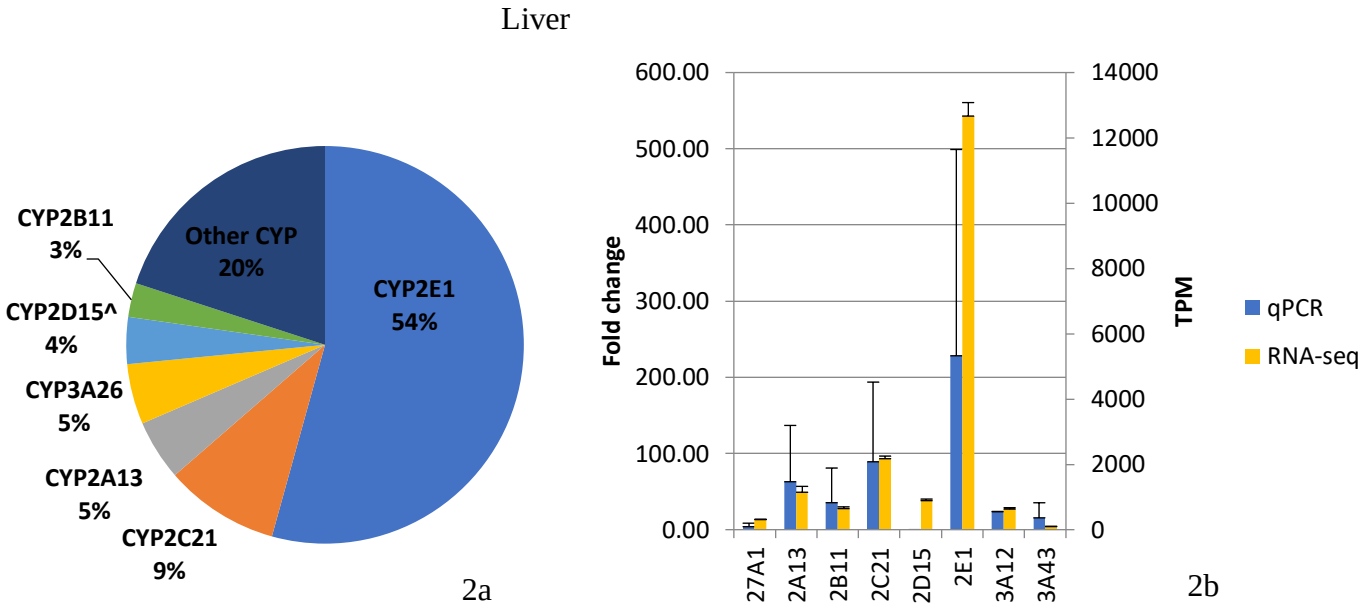

Figure 2: Liver CYP expression profile

Figure 2a: RNA-seq liver CYP transcriptome profile. *denotes human annotation without a properly characterized canine cytochrome. ^ denotes canine CYP information found on ncbi.gov. Other CYP include: *CYP4A37^, 3A12, 3A*,2A7^, 8B1, 4A39, 4A38^, 27A1, 7A1, 4V2, 1A2, 7B1,*

3A438, 51A1, 4F11, 2U1, 2J2, 2W1, 1A1, 39A1, 26A1, 2R1, 2F1, 20A1, 4X1, 21, 26B1, 1B1, 4B1, 2S1, 27C1, 46A1, 4F22, 4A11, 17A1, 19A1*. Figure 2b: Comparison of the relative expression of genes with standard error compared to the RNA-seq quantification.

Duodenum

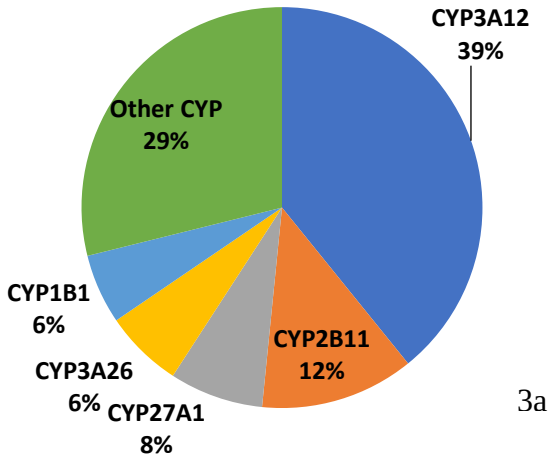

3a

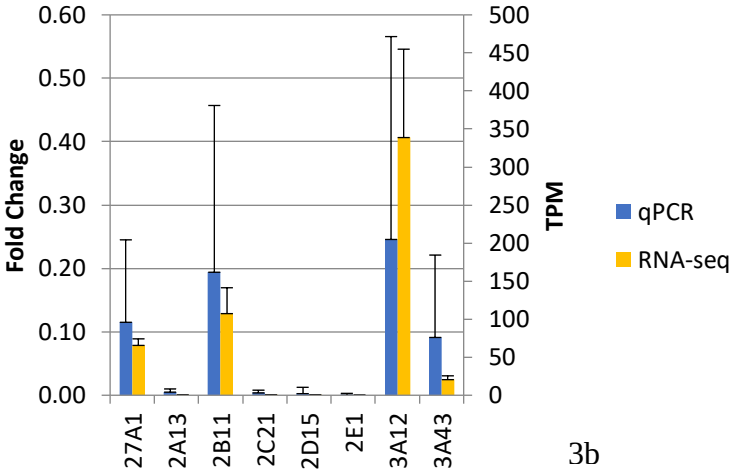

3b

Figure 3a : RNA-seq duodenum CYP transcriptome profile.*denotes human annotation without a properly characterized canine cytochrome. ^ denotes canine CYP information found on ncbi.gov. Other CYP includes: *CYP1A1, 2J2, 2R1, 3A43*, 4V2, 2S1, 20A1, 51A1, 4X1, 39A1, 2U1, 7B1, 26B1, 21, 8B1, 7A1, 4B1, 4F11, 27C1, 46A1, 2W`, 2C21, 4F22, 2D15^, 24A1, 2A13, 4A37^, 4A38^, 26A1, 19A1*. Figure 3b: Comparison of the relative expression of genes with standard error compared to the RNA-seq quantification.

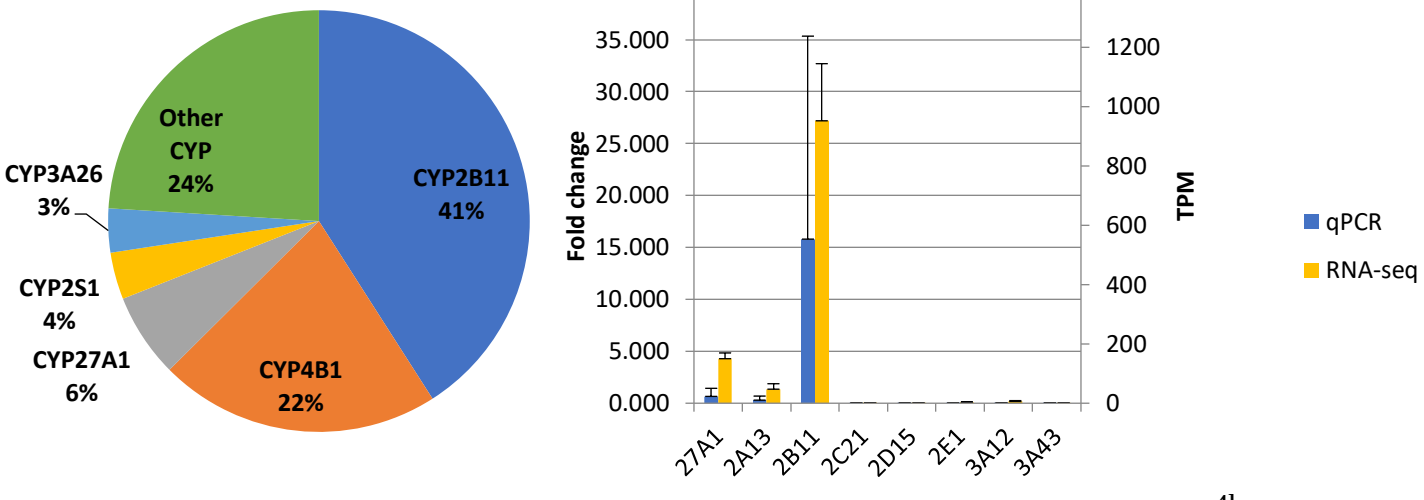

4a

4b

Lung

Figure 4: Mean TPM expression pattern in lung.

Figure 4a: RNA-seq lung CYP transcriptome profile. *denotes human annotation without a properly characterized canine cytochrome. ^ denotes canine CYP information found on ncbi.gov.

Other CYP includes: *CYP1B1, 4V2, 1A1, 7B1, 26B1, 2A13, 39A1, 4F11, 20A1, 2J2, 2R1, 51A1, 2U1, 4X1, 3A12,7A1, 2E1, 2F1, 27C1, 8B1, 2W1, 46A1, 4A39, 4A38^, 4A37^, 2C21, 2D15^, 2A7^, 27B1, 3A43^*, 21, 19A1, 4A11*, 11A1, 1A2, 17A1, 26A1, 3A*, 4F22* . Figure 4b: Comparison of the relative expression of genes with standard error compared to the RNA-seq quantification.

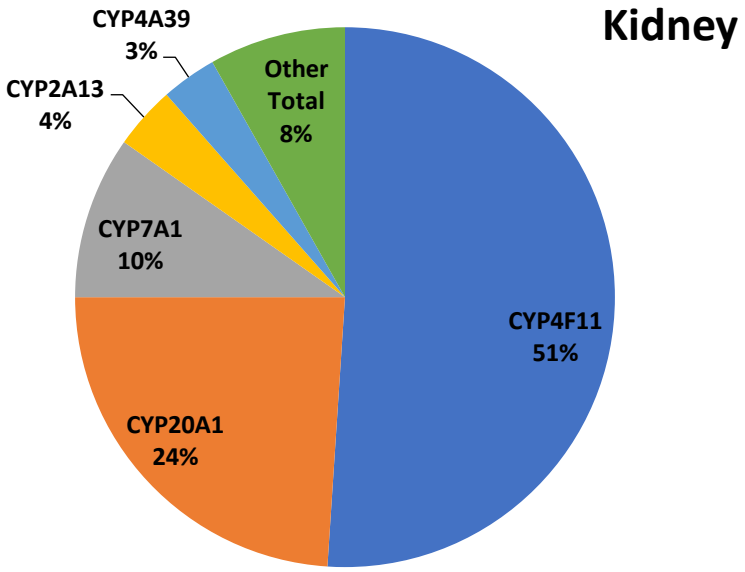

Figure 5: Mean TPM expression pattern in kidney.

*denotes human annotation without a properly characterized canine cytochrome. ^ denotes canine CYP information found on ncbi.gov. Other CYP includes: *CYP3A12, 3A*, 2S1, 27A1, 26B1, 2C21, 1A2, 2F1, 17A1, 11A1, 51A1, 1A1, 2R1, 2D15^, 1B1, 27C1, 27B1, 4A11*. 2U1, 4F22, 2J2, 19A1, 46A1, 8B1, 21, 4A37^, 2B11, 4V2, 4B1, 24A1, 26A1, 2W1, 2A7^, 3A43*, 7B1, 39A1, 4A38^, 3A26, 2E1, 4X1*.

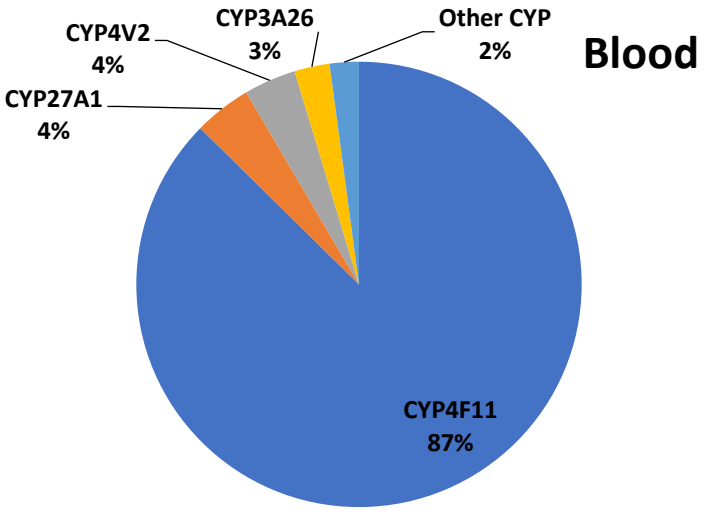

Figure 6: Mean TPM expression pattern in blood.

*denotes human annotation without a properly characterized canine cytochrome. ^ denotes canine CYP information found on ncbi.gov. Other CYP includes:*CYP20A1, 51A1, 2U1, 46A1, 39A1, 2R1, 4X1, 7A1, 2D15^, 2W1, 3A12, 2J2, 27C1, 26B1, 4A37^, 11A1, 7B1, 4B1, 2S1, 2C21, 3A*, 24A1, 4A38^*, 1B1, 21, 2B11*.

Chapter 3: Identification and Quantification of Domestic Feline Cytochrome P450 Transcriptome across Multiple Tissues.[4]

Abstract

Understanding of cytochrome P450 (CYP) isoform distribution and function in the domestic feline is limited. Only a few studies have defined individual CYP isoforms across metabolically relevant tissues, hampering the ability to predict drug metabolism and potential drug-drug interactions. Using RNA-sequencing (RNA-seq), transcriptomes from the 99 Lives Cat Genome Sequencing Initiative databank combined with experimentally acquired whole transcriptome sequencing of healthy, adult male (n=2) and female (n=2) domestic felines, CYP expression was characterized across a wide variety of tissues. A total of 20 tissues were analyzed and 47 CYP isoforms identified. Depending on the tissue, 3-33 CYP isoform transcripts were expressed. qPCR was performed on matching RNA samples and compared to the RNA-seq normalized expression values for *CYP2B6, 3A131, 3A132*, and *2D6*. The correlation was strong in lung (r=0.88) and duodenum (r=0.96). The feline genome annotations did not differentiate *CYP2E1* and *2E2* genes, and *CYP2B6* overlapped an assembly gap, leading to poor annotation of the reference genome. This study is the first to identify and characterize 40 additional CYP isoforms, increasing the number of identified CYP from the previously reported 7 isoforms to a total of 47 across 20 tissues.

Keyword: feline, RNA-seq, cytochrome P450, 99 Lives Cat Genome Sequencing Initiative

---

[4] Visser, M., Weber, K., Rincon, G., Boothe, D., & Merritt, D. Identification and Quantification of Domestic Feline Cytochrome P450 Transcriptome across Multiple Tissues. *Journal of Veterinary Pharmacology and Therapeutics* (Accepted with revisions)

Introduction

Cytochrome P450 (CYP) constitutes the major enzyme family catalyzing oxidative metabolism of drugs and lipophilic xenobiotics. This family also serves an important role in homeostasis, with the synthesis of steroid hormones, prostaglandins, bile acids, and eicosanoids. In humans, there are 57 functional genes and 58 pseudogenes, clustered into 18 families and 44 subfamilies based on their amino acid homologies[98]. This contrasts with the 44 CYP identified in the canine transcriptome[120]. Based on the major substrates utilized, CYP isoforms can broadly be classified into sterols, xenobiotics, fatty acid, eicosanoid, vitamin and unknown[4]. Significant CYP families involved in xenobiotic or drug metabolism include CYP1A, CYP2B, CYP2C, CYP2D, CYP2E, and CYP3A. These CYP have been implicated in drug-drug interactions (DDI), acting as a substrate, inhibitor or inducer to alter the pharmacokinetics of concurrently used drugs[99].

Differences between the canine, feline and human CYP profile include gene expression, *in vitro* microsomal clearance, and enzyme kinetics of probe substrates[61,66,121-123]. Compared to the understanding of the canine CYP genome and function, only a few individual feline CYP isoforms have been described. Reported differences between canine and feline, include feline CYP2B6 expression in lung and duodenum but not in the liver[31] and two isoforms of CYP2E[32]. Additional feline CYP previously described include CYP2A13[35], 3A131, 3A132[124], and 2D6[125]. These differences are reflected in fluorescent substrate studies, with human probe substrates having different inhibitory kinetics in cats compared to humans and dogs[126]. An important xenobiotic metabolism family, CYP2C, has not been described and limited *in vitro* probes suggest limited activity.

Next generation sequencing accurately sequences the entire genome or transcriptome of an organism. A powerful tool for quantifying gene expression and transcripts, discovering alternative splicing sites, detecting gene fusions, mapping transcription pathways, and detecting single nucleotide variations is RNA-sequencing (RNA-Seq)[102,103]. This technology has been used to map cell response to feline immunodeficiency virus[127], identify orthologs to genes in the published genome[128] and determine a missense mutation in *HES7* leading to short tails in Asian domestics cats[129]. Currently, there is a large scale, community research project entitled “99 Lives”, which uses whole genome and transcriptome sequencing to identify genetic variation

between breeds, identify mutations of health concern and provide individual feline sequences to clinicians[130].

Recently, the authors utilized RNA-seq to characterize CYP in canine liver, lung, duodenum, kidney and whole blood[120]. The purpose of this study was to identify and quantify CYP expression in five experimentally collected tissues in the domestic feline and combine the sequenced transcriptome with 99 Lives transcriptomes to characterize CYP isoform expression in multiple tissues.

Methodology

Subjects acted as a control group for a separate study. All protocols were approved by the Institutional Animal Care and Use Committee (IACUC) at Zoetis.

Sample collection:

Male (n=2) and female (n=2) healthy domestic felines were euthanized via injection of sodium pentobarbital; blood (n=4), and sections of liver (n=4), kidney (n=4), lung (n=4), duodenum (n=4), were collected. Blood (PAXgene Blood RNA Tube, PreAnalytiX, Hombrechtikon Switzerland) and tissues (RNA*later*®, Qiagen, Valencia, CA, USA) were kept frozen at -80°C until processing. Liver and kidney total RNA was isolated using the RNA Mini protocol (Qiagen®, Valencia, CA, USA), lung and duodenum isolated using the Fibrous RNA protocol (Qiagen®, Valencia, CA, USA) and blood using PAXgene Blood RNA Kit, PreAnalytiX (Qiagen®, Valencia, CA, USA). RNA integrity number (Bioanalyzer 2100, Agilent Technologies, Santa Clara, CA, USA) and cDNA quality (NanoDrop 8000, ThermoScientific, Wilmington, DE, USA) were evaluated before cDNA library preparation (Schroeder et al., 2006). cDNA library preparation was completed utilizing the TruSeq® Stranded mRNA sample preparation protocol (Illumina ®, San Diego, CA, USA). Libraries were quantified (Quanti-IT® High-Sensitivity DNA Assay Kit, ThermoScientific, Grand Island, NY, USA) and submitted for sequencing (Eureka Genomics®, Hercules, CA, USA).

99Lives Cat Genome Sequencing Initiative:

Samples from a panel of 32 tissues were provided by the Lyons lab, frozen at -80ºC. Samples were derived from 15 cats, collected between 2010 and 2015, suffering from a variety of health conditions including: congenital myasthenic syndrome (occipital brain), hydrocephalus (lung, pancreas, heart, muscle, ear cartilage, spinal cord, and thymus), polycystic kidney disease

(kidney, testes, and cerebellum), progressive retinal atrophy (retina, salivary gland, and bone marrow), seizures (temporal lobe, parietal lobe, hippocampus, cerebellum, and liver), tail abnormality (skin and retina), carrier of LPL deficiency (skin and kidney), carrier of Bengal and Persian progressive retinal atrophy (kidney, spleen, uterus, and ear tip), and fetal tissues from healthy cats. Total RNA was extracted using Qiagen RNeasy Mini protocol, and NGS libraries prepared using the Illumina TruSeq® Stranded mRNA sample preparation protocol. Libraries were sequenced on an Illumina HiSeq 2500 (v4), 2x125 to a read depth of approximately 121M reads/sample at HudsonAlpha Institute for Biotechnology (Huntsville, AL).

RNA-seq Analysis and Statistics:

RNA-seq analysis was performed using CLC Genomics Workbench 9.0 (Qiagen ®, Valencia, CA, USA). Quality checks of RNA sequencing reads included statistics on the number of reads per tissue sample, base quality score, read length, GC content, and most frequent 15-mers. Reads were mapped to the most recent feline annotated genome (Felis catus 8.0, NCBI release 103) from NCBI[111,131]. Transcript per million (TPM) was used to quantify transcripts, and data were included with a TPM> 2. To maximize the likelihood of detecting all CYP in the genome, orthologs of human, ferret and feline CYP annotations were identified via ENSEMBL Biomart, a data mining tool allowing for comparison between the annotated genome of organisms. An extensive literature search was also done to ensure that all known feline CYP were accounted. *CYP2B6* was not present in the annotated feline genome, and the sequence information was found in GenBank (ncbi.gov, KU198409.1) and included in the genome[31]. Each gene was checked in Ensembl and NCBI, and if there was not a particular feline description, the orthologue was used as a name (Table 5).

Primer design and quantitative real-time PCR:

Quantitative real-time PCR (qPCR) was compared to the RNA-seq expression pattern of *CYP2B6*, *CYP2D6*, *CYP3A131* and *CYP3A132* in liver (n=4), duodenum (n=4) and lung (n=4). These CYPs were selected due to their described importance in xenobiotic metabolism and their previous verification and publication of primers. Specific primer pairs (IDT®, Coralville, IO, USA) were selected for the four CYP and two housekeeping genes (*GAPDH*, *RPS7*) based on previously published qPCR sequences. The sequences were blasted to the assembled feline transcriptome to verify the target sequence, and gel electrophoresis was completed to verify that

only one band was present for each (Table 6). Reverse transcription (Invitrogen iScript, BioRad, Hercules, CA, USA) was performed at three sites of xenobiotic absorption and metabolism. Quantification of cDNA (NanoDrop 8000, ThermoScientific, Wilmington, DE, USA) was done before qPCR (CFX384 Touch™ Real-Time PCR Detection System, BioRad, Hercules, CA, USA) utilizing SYBR green detection (SsoAdvanced Universal SYBR Green Supermix, BioRad, Hercules, CA, USA). Amplification protocol was: 95˚C for 30 seconds, 40 cycles at 95˚C to denature and 59˚C for 10 seconds to anneal. Melt curve analysis was performed with a temperature range of 55-95˚C, with 0.5˚C increment increase every 5 seconds. Samples were run in triplicate. Relative quantification was done utilizing *RPL7* to standardize all the samples. Samples were normalized via comparison to *GADPH*. Relative expression of qPCR was compared to TPM for the selected genes, and Pearson correlation coefficient utilized to determine the strength of the overall expression pattern between qPCR and RNA-seq.

Results

The number of paired reads/sample averaged 46.4 million (M) with liver having the lowest tissue total (144M) and kidney having the largest (248M). Greater than 90% of reads mapped to the reference genome for all tissues, with an average of 95.6%, and 80% mapped uniquely. The genome annotations accounted for greater than 85% of mapped reads (i.e., less than 15% reads mapping to intergenic regions) for most samples, with an exception for kidney (17.5% mapped to intergenic regions) and neural tissue such as spinal cord (16.1%) and brain (up to 21%). A total of 47 CYP were identified across 20 tissues (Supplemental Table 3). The numbers of biological replicates varied between the samples, ranging from 6 for kidney, brain, and liver to only 1 for the spinal cord, testes, uterus, heart, muscle, pancreas, salivary gland, thymus and bone marrow. The highest CYP isoform transcript expression was in liver (n=5), with 33 individual CYP identified, and the lowest was in pancreas (n=1) with only 3 CYP isoforms transcripts identified (Figure 1). The spinal cord contained the highest number of isoforms involved in sterol synthesis. The liver contained the highest number of xenobiotic isoforms. The tissues with the highest number of eicosanoid isoforms were liver, cartilage, skin, lung, kidney, and duodenum. Vitamin synthesis was highest in cartilage and fetal tissue. The liver contained the highest number of unknown function CYP isoforms. Summation of the CYP TPM shows that liver has the greatest count, with the majority designated for sterol and xenobiotics. The pancreas and muscle had the lowest CYP TPM count (Figure 7).

The five highest expressed CYP in the liver are *CYP2E1/2>2A13>3A132>2D6>3A131* (Figure 8). Comparison between qPCR and RNA-seq indicates an inverse correlation (r=-0.35), with a reversal in the expression pattern between *CYP3A131* and *3A132*. In the duodenum, *CYP3A131* expression was the highest, followed by *CYP2C41>4B1>2J2>2B6* (Figure 9). A strong correlation between qPCR and RNA-seq was present (r=0.96). *CYP2B6* expression in the lung is estimated to be 43% of the CYP content, with *CYP4B1>2S1>1A1>2F5*, making up the remaining four highest expressed CYP mRNA transcripts. qPCR and RNA-seq correlation was strong (r=0.88) (Figure 10). The blood only expressed a total of 6 CYP isoforms, with *CYP4F2* expression the highest, followed by *CYP2J2>4V2>4B1>51A1>4F22* (Figure 11). The kidney had a variety of CYP transcripts *CYP4A6>4F3>4F2>4A11>4A24* (Figure 12).

Discussion

This study is the first to characterize global CYP expression in the domestic feline, providing insight into different tissue CYP transcript profiles at multiple sites in the body. This study was able to combine whole transcriptome sequencing from multiple sources to increase the number of reported feline CYP isoforms from seven to forty-seven. A major CYP xenobiotic family, CYP2C, was also identified and described for the first time.

All of the recognized major drug-metabolizing CYP families (CYP1A, 2A, 2B, 2C, 2D, and 3A) were identified in at least one tissue. Previous studies on *CYP2B6* expression found negligible transcript and protein expression in the liver, but transcript and protein expression were predominant in the lung and detectable in the small intestine[31]. RNA-seq found negligible transcript expression in the liver and blood, with the highest expression in the lung followed by kidney and duodenum. Drugs requiring CYP2B6 for metabolism can be expected to have slower metabolism in the feline compared to the canine due to the lack of CYP2B6 in the liver. Reported CYP2B6 substrates include drugs such as methadone[132], cyclophosphamide[23], propofol, diazepam, midazolam, ketamine, S-medetomidine, R-medetomidine, warfarin, and phenytoin[71]. Additionally, the annotation for CYP2B6 has not been well described, preventing the reporting of an accurate location on the chromosome. This gene requires further manual curation to improve the feline annotation.

The CYP3A family consists of CYP3A131 and 3A132, with previous reports of *CYP3A131* mRNA transcript expression in small intestine and liver, and limited *CYP3A132* expression only in liver[34]. RNA-Seq results indicate *CYP3A131* expression was present in all

five tissues examined, with the majority of expression in liver and duodenum. In contrast to reported results, *CYP3A132* expression was higher in the liver than *CYP3A131* transcript expression and was present in the remaining four tissues, but to a lesser extent than *CYP3A131*[133]. The impact of different isoforms on drug metabolism in cats has not been established, but different human and canine isoforms have different drug metabolism for the CYP3A family[13]; whether this is also true in feline CYP3A needs to be explored further. The CYP3A family is a highly significant xenobiotic-metabolizing family in both humans and canines due to the described large enzyme pocket allowing a variety of substrates to be metabolized[134].

Two isoforms of CYP2E have been reported in the literature, but only one isoform was identified. Reported CYP2E1 transcript and protein expression include liver, kidney, lung, stomach, gastric gland, pyloric gland, small intestine, and pancreas. In contrast, CYP2E2 was reported to be expressed in liver and mononuclear cells and was not expressed in all cats tested[32]. In ENSEMBL, the isoform is denoted as *CYP2E1*, but in NCBI the same gene is denoted as *CYP2E2*. This lack of accurate annotation prevented proper identification of two separate isoform mRNA transcripts if any were present.

This is the first report of *CYP2C21* and *CYP2C41* in the domestic cat. Detection of these two isoforms was based on the automated ENSEMBL annotation prediction algorithm[111]. Therefore, the individual genes have not been completely sequenced and protein content verified, key components necessary to determine the impact on drug metabolism. However, two CYP2C isoforms were detected, compared to the canine CYP2C family where only a small percentage of canines are reported to express both isoforms[13,100]. Substrates reported to be metabolized by CYP2C in humans include celecoxib, omeprazole, phenytoin, tolbutamide, warfarin, diazepam, lansoprazole, and voriconazole. However, humans have four CYP2C isoforms compared to the two detected in felines, and inferences regarding substrate metabolism should be made with caution.

CYP families important for the regulation of inflammation, steroid and vitamin D synthesis, and vascular resistance were prominent in blood and kidney. Biological replicates are essential to improve the accuracy of any prediction, and, therefore, no inferences regarding CYP transcript quantity can be made when there are only a few biological replicates present. There are conflicting reports in the literature regarding the minimum number of biological replicates

necessary, which is based on the type and the purpose of the analysis such as detecting physiological gene expression vs. differential gene expression based on site or disease state. Acknowledging the limited number of samples, the authors elected to place a TPM cut off and compare the qPCR expression in three tissues with previously described qPCR primers. The correlation between relative qPCR expression and RNA-seq expression was strong in duodenum and lung, but there was an inverse relationship in the liver. Possible causes for this inverse correlation includes poor RNA quality, poor qPCR primers, the reported decrease in RNA transcriptome reads compared to the duodenum, or an inability to accurately discern between the CYP3A isoforms.

In conclusion, this is the first global overview of CYP expression in the domestic cat and characterization of CYP expression across a variety of tissues. Studies have shown that the same CYP isoform in different species have variable enzyme kinetics, leading to sub-therapeutic concentrations or toxicity[135]. Additional research into protein quantification and CYP phenotyping will improve the prediction of drug metabolism and decrease the risk of drug-drug interactions.

Acknowledgement: The authors would like to thank Sarah Corum for her technical expertise.
Conflict of interest: The authors do not have any conflict of interest to declare.

Table 5: Identified feline CYP transcripts.

Major Substrate Class	CYP	Chromosome	Start	End	Orientation
Sterol	11A1	B3	33,884,713	33,890,907	FOR
	11B1	F2	81,281,255	81,286,329	FOR
	17A1	D2	63,216,584	63,222,490	REV
	19A1	B3	54,906,326	54,947,654	FOR
	1B1	A3	111,590,785	111,598,266	FOR
	21A2	B2	33,608,201	33,611,240	FOR
	27A1	C1	202,613,034	202,646,735	FOR
	39A1	B2	47,072,745	47,166,176	REV
	46A1	B3	143,222,893	143,247,887	FOR
	51A1	A2	95,975,363	95,996,122	REV
	7A1	F2	9,788,052	9,795,659	REV
	7B1	F2	14,916,910	14,946,537	REV
	8B1	C2	147,429,680	147,431,176	FOR
Xenobiotic	1A1	B3	33,532,067	33,538,470	FOR
	2E2	D2	89,795,938	89,805,869	FOR
	1A2	B3	33,511,989	33,516,370	REV
	2A13	E2	13,310,454	13,316,470	FOR
	2B6	E2	N/A	N/A	MIXED
	2C21	D2	56,761,925	56,790,799	REV
	2C41	D2	56,712,214	56,744,603	FOR
	2D6	B4	137,345,256	137,350,033	REV
	3A131	E3	6,626,641	6,683,350	FOR
	3A132	E3	6,694,663	6,725,095	FOR
Fatty Acid	2J2	C1	47,926,199	47,955,713	REV
	2U1	B1	115,269,943	115,296,613	REV
	4A11	C1	36,255,542	36,278,828	REV
	4B1	C1	36,232,392	36,252,137	FOR
	4F22	A2	11,269,913	11,289,014	FOR
	4V2	B1	15,431,171	15,447,509	FOR
Eicosanoid	4F2	A2	11,312,522	11,362,773	FOR
	4F3	Scaffold JH412587.1	3,637	5,089	REV

Vitamin	2R1	D1	73,109,307	73,127,990	REV
	24A1	A3	8,241,386	8,257,342	FOR
	26A1	D2	55,420,138	55,423,535	FOR
	26B1	A3	90,970,286	90,989,464	REV
	26C1	D2	55,407,595	55,415,342	FOR
	27B1	B4	8,647,0520	86,474,390	REV
	27C1	C1	111,893,493	111,907,924	FOR
Unknown	20A1	C1	188,951,053	189,028,297	FOR
	2F2	E2	13,375,181	13,380,124	FOR
	2F5	E2	13,362,803	13,373,637	FOR
	2G1	E2	13,286,505	13,296,300	FOR
	2S1	E2	13,122,830	13,132,919	REV
	2W1	E3	702,921	708,017	FOR
	4A24	D3	53,493,840	53,494,483	FOR
	4A6	B2	5,035,434	5,035,997	FOR
	4X1	C1	36,365,627	36,403,147	FOR

In addition to the chromosome location, the strand direction is noted if an orthologue was used. N/A indicates that the location could not be determined.

Table 6: qPCR primers. All primer pairs selected have been previously used.

Gene	Forward	Reverse
2D6[125]	GTCCTAGGTACCTGGTGTGC	GTTCTCATCATTGAAGCTGC
2B6[31]	CTTTCCAGGTACACACAGGC	CTGTGACGTGAGGGTACTTG
3A131[124]	GAGATTGATGCAACTTTCCC	GCAAGTTTCATGTTCATGAC
3A132[124]	GAGATTGATGCAACTTTCCC	AAGGAGAAGTTCTGCAGCAC
RPS7[136]	CTCTGGTCATTGAGCACATCC	TCAATGTGGCAGGGAGAGC
GAPDH[136]	AGTATGATTCCACCCACGGCA	GATCTCGCTCCTGGAAGATGGT

Supplemental Table 3: TPM of individual CYP transcript expression in multiple tissues.

	Liver (n=5)	Kidney (n=6)	Duodenum (n=4)	Lung (n=5)	Skin (n=3)	Cartilage (n=2)	Spinal cord (n=1)	Brain (n=6)	Fetus (n=4)	Blood (n=4)
11A1	-----	-----	-----	-----	-----	-----	9.63	2.1 (1.99)	13.05 (7.78)	-----
11B1	-----	-----	-----	-----	-----	-----	5.18	-----	-----	-----
17A1	-----	-----	-----	1.65 (3.31)	-----	-----	2.87	-----	-----	-----
19A1	-----	-----	-----	-----	-----	-----	-----	-----	-----	-----
1A1	1355.02 (140.98)	3.5 (2.79)	3.63 (2.47)	65.8 (77.46)	130.74 (84.93)	276.72 (258.94)	-----	-----	-----	-----
1A2	1430.04 (126.58)	-----	-----	-----	-----	-----	-----	-----	-----	-----
1B1	-----	5.45 (1.37)	-----	10.6 (7.15)	12.63 (3.63)	21.45 (5.61)	-----	-----	5.5 (3.71)	-----
20A1	39.42 (2.81)	8.42 (1.13)	2.84 (0.67)	9.02 (2.61)	8.18 (3.17)	12.44 (9.63)	15.61	9.11 (1.08)	11.26 (4.57)	-----
21A2	2.52 (0.19)	-----	-----	-----	-----	-----	6.14	-----	-----	-----
24A1	-----	51.61 (43.56)	-----	-----	-----	-----	-----	-----	-----	-----
26A1	25.46 (3.37)	-----	-----	-----	-----	5.96 (5.83)	2.12	3.19 (3.65)	2.34 (1.65)	-----
26B1	10.45 (1.6)	2.92 (2.82)	2.23 (1.23)	15.72 (6.5)	73.57 (7.18)	57.44 (5.67)	7.15	13.54 (8.08)	28.58 (5.05)	-----
26C1	-----	-----	-----	-----	-----	-----	-----	-----	-----	-----
27A1	1431.37 (76.12)	136.69 (36.57)	19.63 (9.4)	9.29 (2.25)	20.06 (2.79)	39.28 (7.65)	41.75	23.99 (15.36)	12.42 (7.18)	-----
27B1	-----	7.55 (3.41)	-----	-----	2.34 (0.81)	-----	-----	-----	-----	-----
27C1	-----	-----	-----	-----	27.23 (13.95)	38.75 (8.76)	-----	4.91 (2.75)	21.98 (10.94)	-----
2A13	25466.26 (1175.52)	-----	-----	4.19 (4.9)	129.82 (22.19)	54.08 (50.35)	-----	-----	-----	-----
2B11	-----	-----	100.53 (44.6)	594.88 (153.31)	486.92 (32.73)	274.84 (252.45)	-----	11.78 (13.91)	-----	-----
2C21	141.24 (11.1)	-----	3.74 (1.05)	5.16 (4.18)	12.87 (2.7)	4.06 (1.83)	-----	-----	-----	-----
2C41	1427.59 (91.35)	-----	535.51 (189.29)	-----	-----	2.11 (1.05)	2.16	-----	11.83 (6.58)	-----
2D6	6940.11 (318.75)	-----	2.18 (0.49)	-----	2.64 (1.98)	4.14 (3.03)	22.14	7.19 (6.34)	19.24 (8.71)	-----
2E2	29290.34 (1556.4)	12.8 (8.74)	-----	-----	-----	-----	-----	-----	-----	-----
2F2	26.26 (2.31)	-----	-----	3.41 (1.84)	6.94 (2.3)	2.61 (0.38)	-----	-----	-----	-----
2F5	37.39 (10.57)	-----	-----	51.44 (44.71)	45.47 (12.36)	10.54 (9.72)	-----	-----	-----	-----
2G1	-----	-----	-----	-----	-----	-----	-----	-----	-----	-----
2J2	95.52 (6.3)	-----	135.69 (50.62)	15.17 (2.09)	53.66 (16.19)	46.72 (41.52)	207.89	33.14 (4.54)	5.21 (1.74)	11.09 (5.46)

	Liver (n=5)	Kidney (n=6)	Duodenum (n=4)	Lung (n=5)	Skin (n=3)	Cartilage (n=2)	Spinal cord (n=1)	Brain (n=6)	Fetus (n=4)	Blood (n=4)
2R1	15.59 (0.91)	-----	3.37 (0.44)	3.27 (1.56)	-----	2.95 (2.46)	3.08	-----	2.75 (0.53)	-----
2S1	-----	-----	13.92 (3.86)	69.69 (21.04)	24.42 (0.66)	16.4 (15.17)	10.2	3.09 (2.63)	10.58 (14.5)	-----
2U1	152.28 (17.24)	2.65 (0.56)	-----	6.42 (1.91)	4.39 (0.57)	4.56 (0.87)	11.38	8.09 (2.5)	4.4 (2.11)	-----
2W1	-----	-----	-----	-----	8.05 (1.61)	-----	-----	-----	3.79 (3.03)	-----
39A1	159.21 (10.45)	132.91 (26.1)	2.87 (1.26)	49.87 (9.71)	3.63 (0.65)	19.69 (18.12)	27.61	15.13 (19.17)	3.98 (1.3)	-----
3A131	3569.06 (517.34)	-----	1397.55 (543.21)	3.38 (0.87)	39.78 (6.01)	59.67 (54.57)	2.71	2.1 (0.77)	2.47 (2.14)	-----
3A132	14704.12 (679.33)	-----	8.61 (6.15)	-----	2.17(0.56)	-----	-----	-----	-----	-----
46A1	-----	6.36 (2.28)	-----	-----	-----	2.35 (1.73)	46.15	173.66 (97.12)	-----	-----
4A11	554.36 (98.58)	568.47 (119.1)	2.46 (1.27)	-----	-----	-----	-----	-----	-----	-----
4A24	145.52 (37.08)	236.04 (52.19)	2.64 (1.22)	-----	-----	-----	-----	-----	-----	-----
4A6	158.33 (39.47)	1348.08 (444.11)	-----	-----	-----	-----	-----	-----	-----	-----
4B1	17.91 (1)	11.91 (1.47)	281.84 (119.61)	312.01 (145.23)	10.17 (2.3)	9.73 (0.44)	11.31	6.45 (1.99)	6.05	5.07 (2.05)
4F2	460.52 (22.95)	586.75 (116.64)	25.43 (18.91)	8.84 (3.18)	14.13 (14.23)	4.72 (0.64)	-----	-----	-----	64.42 (26.97)
4F22	6.5 (1.36)	-----	-----	-----	76.59 (33.64)	84.87 (83.3)	-----	-----	2.61	2.08 (1.24)
4F3	1711.95 (88.2)	1039.73 (218.93)	89.74 (66.09)	14.28 (3.56)	61.21 (52.91)	17.73 (0.82)	2.31	1.15	-----	-----
4V2	1594.95 (84.55)	8.65 (3.39)	2.97 (1.81)	32.05 (2.96)	11.8 (1.17)	13.67 (10.09)	12.12	11.67	4.66	6.06 (3.19)
4X1	66.99 (13.27)	5.31 (1.69)	-----	29.58 (8.74)	-----	2 (0.86)	17.92	7.83	-----	-----
51A1	423.78 (24.87)	16.67 (5.66)	14.99 (5.88)	28.86 (7.02)	83.36 (29.18)	29.91 (6.71)	491.76	122.53	81.05	4.43 (1.58)
7A1	358.71 (37.74)	-----	-----	-----	-----	-----	-----	-----	-----	-----
7B1	92.11 (8.58)	7.69 (1.92)	-----	18.96 (6.8)	4 (0.46)	4.85 (3.5)	10.58	11.68	9.85	-----
8B1	1728.09 (149.88)	12.75 (6.81)	5.05 (0.97)	3.17 (1.48)	12.37 (8.33)	7.34 (2.85)	-----	-----	-----	-----

	Testes (n=1)	Uterus (n=1)	Heart (n=1)	Muscle (n=1)	Pancreas (n=1)	Retina (n=2)	Salivary gland (n=1)	Spleen (n=2)	Thymus (n=1)	Bone marrow (n=1)
11A1	502.92	-----	-----	-----	-----	3.69 (1.46)	-----	12.67 (1.97)	3.72	28.5
11B1	-----	-----	-----	-----	-----	-----	-----	-----	-----	-----
17A1	3122.83	-----	-----	-----	-----	-----	-----	11.01 (10.86)	-----	-----
19A1	5.05	-----	-----	-----	-----	-----	-----	-----	4.4	-----
1A1	-----	-----	64.38	5.32	2.91	-----	-----	-----	-----	-----
1A2	-----	-----	-----	-----	-----	-----	-----	-----	-----	-----
1B1	10.79	58	25.46	-----	-----	5.7 (2.35)	9.07	75.86 (3.02)	29.1	-----
20A1	6.93	7.49	5.1	-----	-----	9.89 (1.31)	8.42	5.04 (2.8)	9.92	3.19
21A2	125.28	-----	-----	-----	-----	-----	2.8	6.39 (3.48)	-----	3.25
24A1	-----	-----	-----	-----	-----	28.61 (27.93)	-----	-----	-----	-----
26A1	-----	-----	-----	-----	-----	16.94 (13.63)	-----	-----	-----	-----
26B1	16.86	21.56	4.44	-----	-----	5.25	3.92	2.59 (1.48)	100.13	-----
26C1	-----	-----	-----	-----	-----	-----	-----	-----	-----	-----
27A1	9.06	66.8	9.82	15.05	-----	23.07 (0.43)	6.66	20.86 (1.38)	18.89	2.2
27B1	-----	-----	-----	-----	-----	-----	-----	-----	-----	-----
27C1	-----	13.65	-----	-----	-----	-----	-----	6.27 (1.14)	3.37	2.24
2A13	-----	-----	-----	-----	-----	-----	-----	-----	-----	-----
2B11	-----	-----	-----	-----	-----	-----	-----	19.75 (6.88)	-----	-----
2C21	-----	8.19	5.21	-----	-----	-----	-----	3.47 (1.4)	2.29	-----
2C41	-----	5.61	-----	-----	-----	-----	4.92	-----	8.33	2.13
2D6	33.18	21.21	-----	-----	-----	11.58 (1.73)	-----	5.2 (0.68)	-----	-----
2E2	-----	2.33	-----	-----	-----	-----	-----	3.61 (0.37)	-----	-----
2F2	-----	-----	-----	-----	-----	-----	3.32	-----	-----	-----
2F5	47.98	-----	-----	-----	-----	-----	-----	-----	-----	-----
2G1	-----	-----	-----	-----	-----	-----	-----	-----	-----	-----
2J2	-----	3.66	-----	-----	2.7	9.25 (1.11)	15.79	23.09 (9.52)	5.04	-----
2R1	6.03	2.81	6.32	-----	-----	-----	3.7	2 (0.67)	3.37	2.05
2S1	-----	2.68	-----	-----	-----	9.17 (5.07)	-----	5 (0.83)	-----	2.5

	Testes (n=1)	Uterus (n=1)	Heart (n=1)	Muscle (n=1)	Pancreas (n=1)	Retina (n=2)	Salivary gland (n=1)	Spleen (n=2)	Thymus (n=1)	Bone marrow (n=1)
2U1	6.65	7.34	9.52	-----	-----	13.4 (1.36)	8.94	2.35 (1.77)	689.91	-----
2W1	-----	-----	-----	-----	-----	-----	-----	-----	-----	-----
39A1	5.44	47.88	-----	-----	-----	16.35 (3.9)	-----	4.58 (1.04)	-----	-----
3A131	6.66	4.63	-----	-----	-----	6.75 (3.7)	9.9	5.33 (2.94)	5.21	-----
3A132	-----	2.04	-----	-----	-----	2.11 (0.49)	-----	-----	-----	-----
46A1	-----	2.48	-----	-----	-----	14.6 (6.06)	-----	-----	-----	-----
4A11	-----	-----	-----	-----	-----	-----	-----	-----	-----	-----
4A24	4.42	-----	-----	-----	-----	2.32 (1.48)	-----	-----	-----	-----
4A6	3.36	-----	-----	-----	-----	-----	-----	-----	-----	-----
4B1	139.09	8.82	7.73	5.72	-----	13.55 (0.59)	3.41	5.09 (1.97)	7.99	10.39
4F2	-----	-----	-----	-----	-----	-----	-----	-----	-----	42.97
4F22	3.75	-----	-----	-----	-----	-----	8.23	2.68 (1.36)	-----	-----
4F3	5.72	9.15	2.01	-----	-----	7.5 (0.46)	2.83	2.35 (1.7)	-----	-----
4V2	4.07	31.35	48.6	-----	-----	7.6 (1.94)	24.15	15.88 (9.12)	99.8	6.03
4X1	-----	-----	-----	-----	-----	10.81 (2.9)	-----	-----	-----	-----
51A1	414.77	14.86	40.08	11.18	3.2	75.66 (23.75)	23.5	17.8 (4.05)	22.24	8.48
7A1	-----	-----	-----	-----	-----	-----	-----	-----	-----	-----
7B1	-----	3.15	2.3	-----	-----	8.69 (2.48)	-----	-----	-----	-----
8B1	-----	4.66	-----	-----	-----	-----	3.14	2.97 (0.6)	-----	-----

The table includes a combination of the 99 Lives data as well as experimentally obtained data (liver (n=4); kidney (n=4); blood (n=4); duodenum (n=4); lung (n=4)).

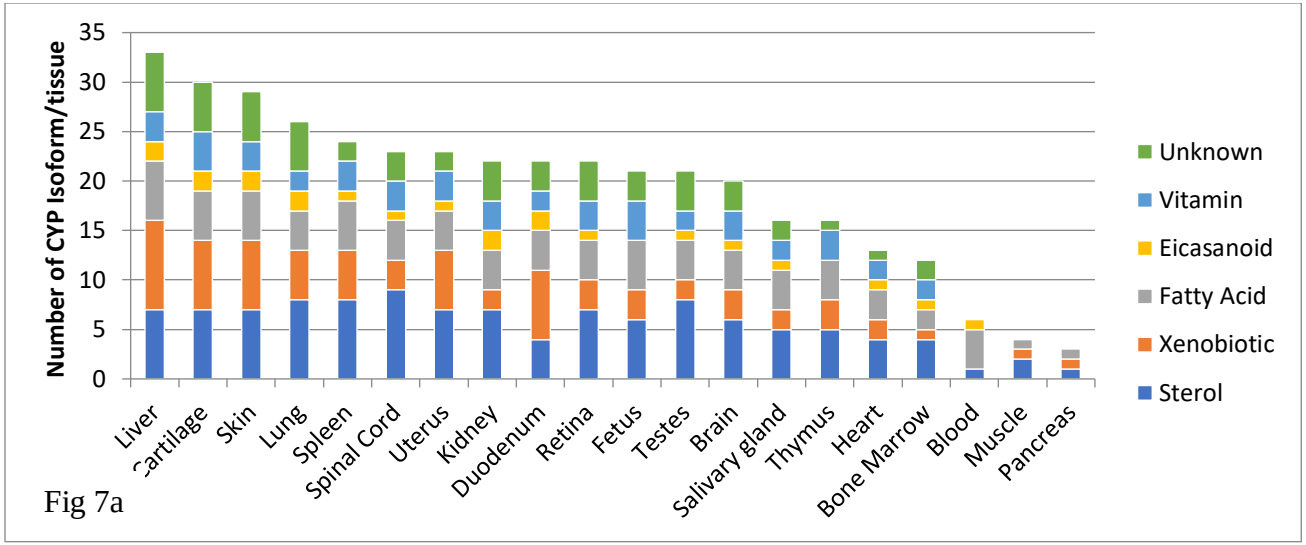

Fig 7a

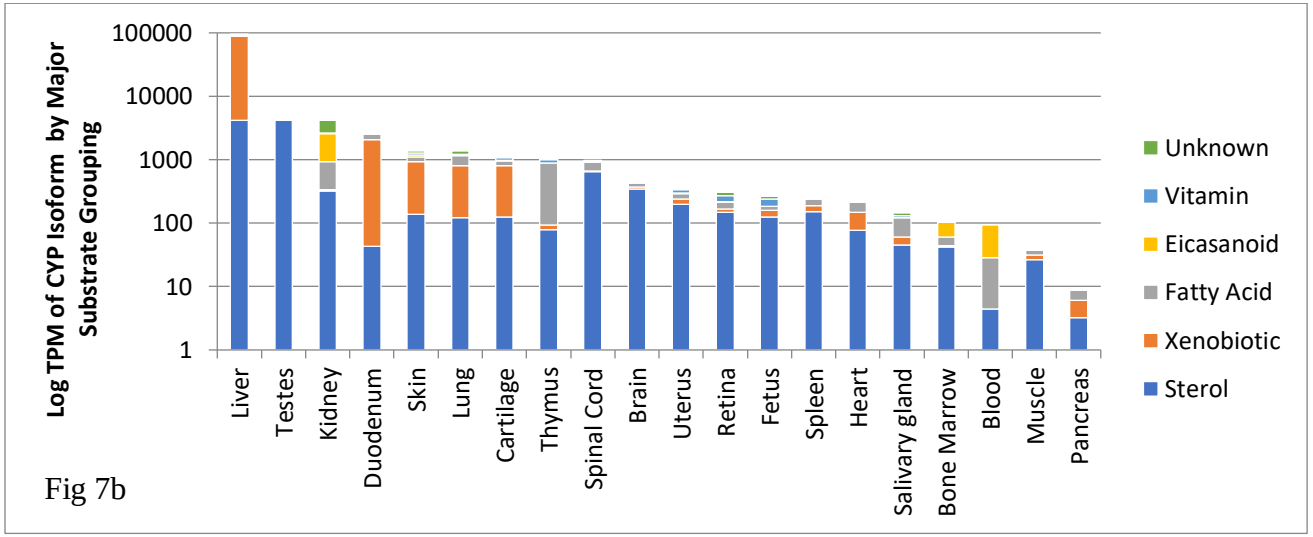

Fig 7b

Figure 7: CYP TPM expression in different tissues

Figure 7a: CYP Isoform expressed within a tissue by major human substrate category. Figure 7b: Sum of the average TPM expression per tissue by major human substrate category.

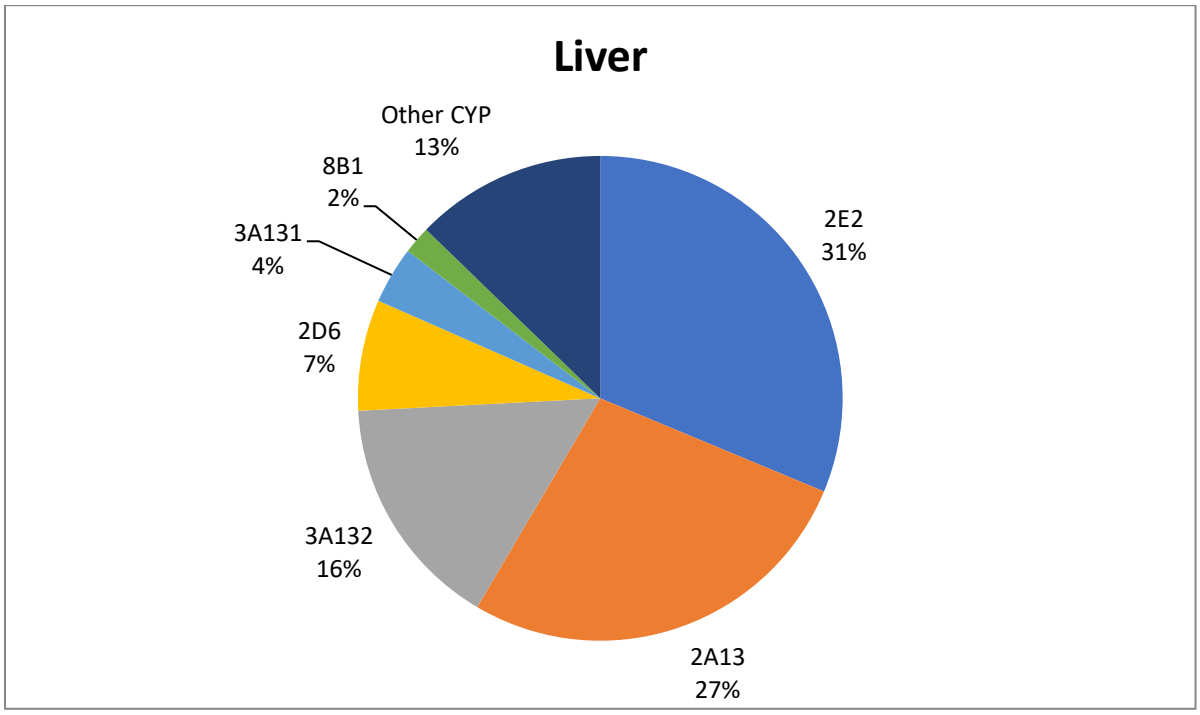

Figure 8: RNA-seq expression of CYP in liver.

Other CYP includes: *CYP4F3*, *4V2*,*27A1*, *1A2*, *2C41*, *1A1*, *4A11*, *4F2*, *51A1*, *7A1*,*39A1*, *4A6*, *2U1*, *4A24*, *2C21*, *2J2*, *7B1*, *4X1*, *20A1*, *2F5*, *2F2*, *26A1*, *4B1*, *2R1*, *26B1*, *4F22*, and *21A2*.

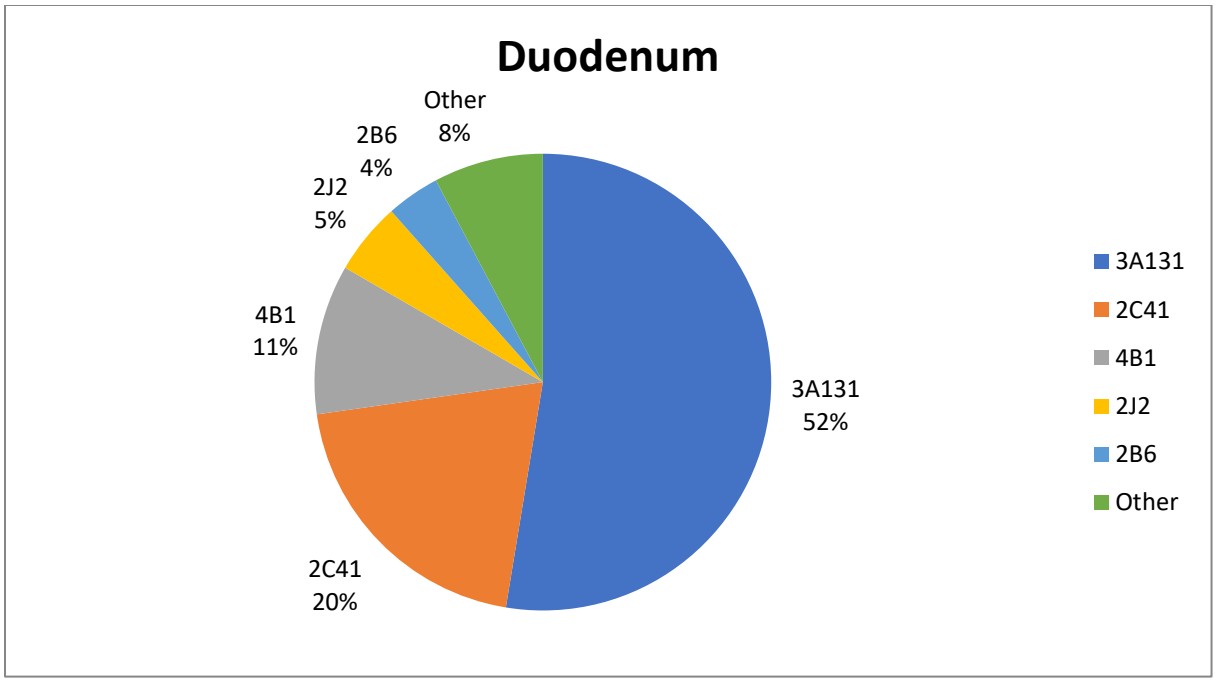

Figure 9: RNA-seq expression in duodenum.

Other CYP includes: *CYP4F3, 4F2, 27A1, 51A1, 2S1, 3A132, 8B1, 2C21, 1A1, 2R1, 4V2, 39A1, 20A1, 4A24, 4A11, 26B1* and *2D6*.

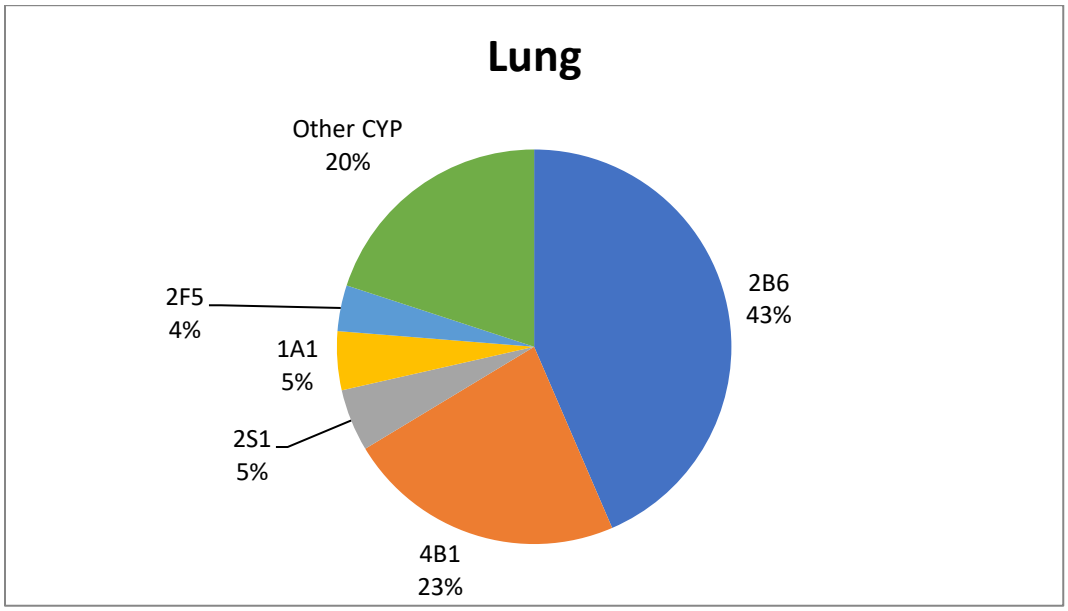

Figure 10: Expression pattern of RNA-seq data in lung.

Other CYP includes: *CYP39A1*, *4V2*, *4X1*, *51A1*, *7B1*, *26B1*, *2J2*, *4F3*, *1B1*, *27A1*, *20A1*, *4F2*, *2U1*, *2C21*, *2A13*, *2F2*,*3A131*, *2R1*, *8B1*, and *17A1*.

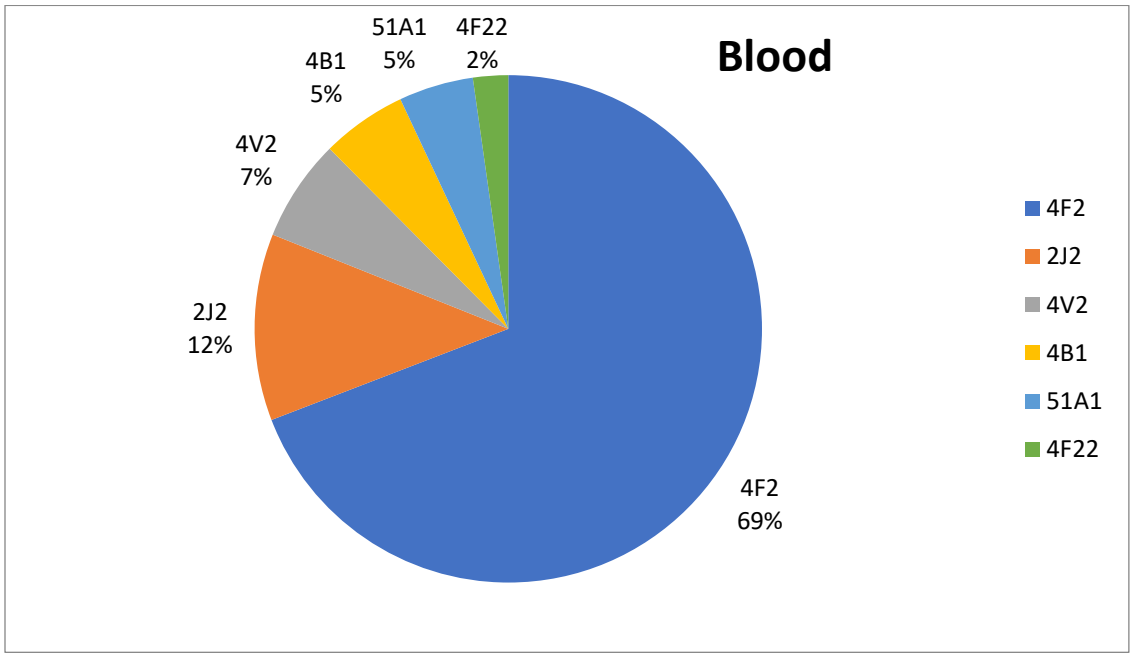

Figure 11: Expression pattern of RNA-seq CYP transcripts in blood.

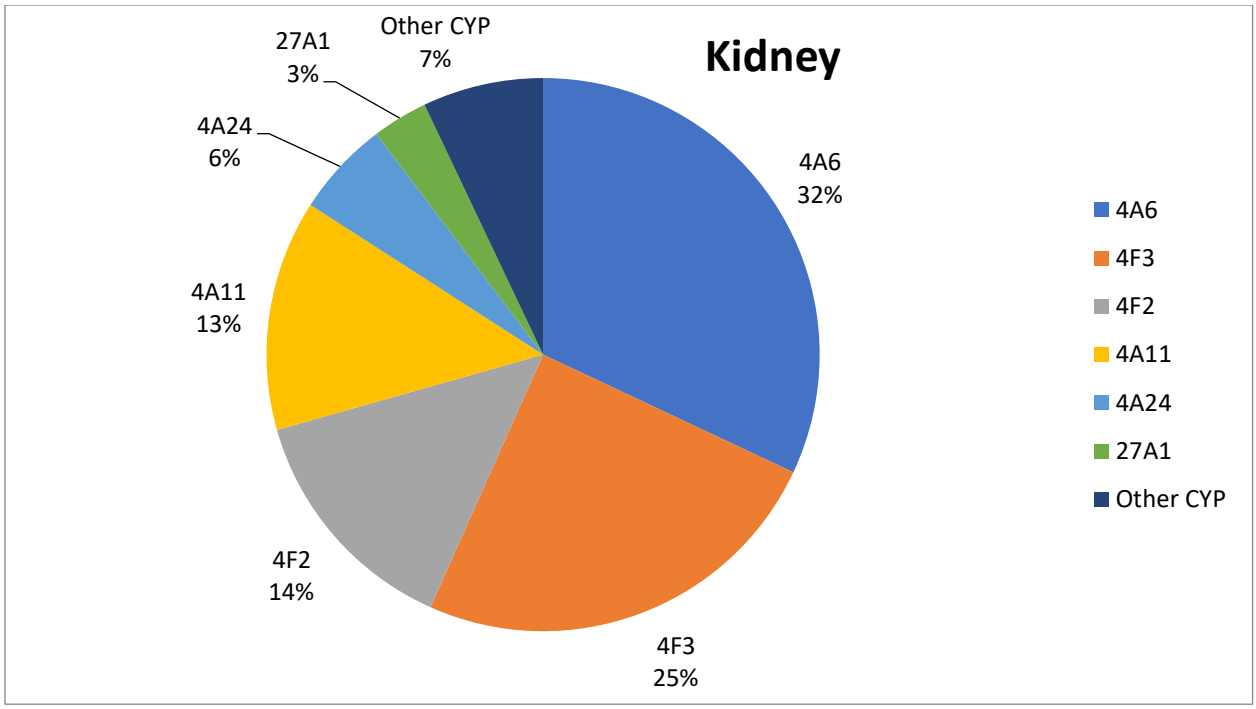

Figure 12: Expression pattern of RNA-seq data in kidney.

Other CYP includes: *CYP39A1*, *24A1*, *51A1*, *2E2*, *8B1*, *4B1*, *4V2*, *20A1*, *7B1*, *27B1*, *46A1*, *1B1*, *4X1*, *1A1*, *26B1*, and *2U1*.

Chapter 4: Comparison of Predicted Intrinsic Hepatic Clearance of 30 Pharmaceuticals in Canine and Feline Liver Microsomes.[5]

Abstract

Known cytochrome P450 (CYP) substrates in humans are used in veterinary medicine, with limited knowledge of the similarity or variation in CYP metabolism. Comparison of canine and feline CYP metabolism via liver microsomes report that human CYP probes and inhibitors have differing rates of intrinsic clearance (CL_{int}). The purpose of this study was to utilize a high-throughput liver microsome substrate depletion assay combined with microsomal and plasma protein binding to compare the predicted hepatic clearance (CL_{hep}) of thirty therapeutic agents used off-label in canines and felines, using both the well-stirred and parallel tube models. In canine liver microsomes, 3/30 substrates did not have quantifiable CL_{int}, while midazolam and amitriptyline CL_{int} were too rapid for accurate determination. A CL_{hep} was calculated for 29/30 substrates in feline microsomes. Overall, canine CL_{hep} was faster compared to feline, with fold differences ranging from 2-20 fold. A comparison between the well-stirred and parallel tube model indicates that the parallel tube model reports a slighter higher CL_{hep} in both species. The differences in CYP metabolism between canine and feline highlight the need for additional research into CYP expression and specificity.

Keyword: microsome, cytochrome P450, canine, feline, predicted hepatic clearance, intrinsic clearance, well-stirred, parallel tube

---

[5] Visser, M., Zaya, M., Locuson, C., Boothe, D., & Merritt, D., (2018) Comparison of Predicted Intrinsic Hepatic Clearance of 30 Pharmaceuticals in Canine and Feline Liver Microsomes *Xenobiotica* (in press).

Introduction

Cytochrome P450 (CYP) is a superfamily of enzymes pivotal in the metabolism of approximately 90% of pharmaceuticals[137] and a wide variety of xenobiotic compounds. These enzymes metabolize drugs to produce both active and inactive metabolites which can be cleared via renal or hepatic clearance processes, or further metabolized. CYP families recognized to be pivotal for drug metabolism include CYP1A, 2A, 2B, 2C, 2D, 2E, and 3A[115]. The importance of CYP in drug metabolism has led to the development of *in vitro* systems including hepatocytes, liver microsomes, or recombinant CYP to assess enzyme kinetics. Microsomal substrate depletion is used as an initial high-throughput screen to determine the intrinsic clearance (CL_{int}) and the predicted hepatic clearance (CL_{hep}) in early drug discovery[138]. Liver microsomes are made by serial centrifugation to isolate the membrane-bound enzymes of the endoplasmic reticulum. Multiple proteins are present in the microsomes, and different reactions studied by the addition of specific cofactors[139].

Using the metabolic stability assay, studies have evaluated traditional human CYP probes and inhibitors in canine liver microsomes to understand how CYP substrate specificity and expression levels differ between the two species. Current probes used for evaluating canine CYP isoform-specific metabolism include phenacetin, tizanidine and 7-ethoxyresorufin for CYP1A1,1A2 [140], diazepam and temazepam for CYP2B11, diclofenac 4′-hydroxylation for CYP2C21/41, bufuralol 1′-hydroxylation for CYP2D6, and diazepam C3-hydroxylation and midazolam for CYP3A12 [119,141]. Compared to the canine, knowledge regarding feline CYP metabolism is limited. Notable differences, based on a combination of genetic and protein expression studies, include a lack of CYP2B6 protein in the feline liver [31], the presence of two CYP2E isoforms [32], and variation in the *CYP3A131* and *CYP3A132* transcript expression in the feline liver compared to extrahepatic locations. *In vitro* studies have reported low activity toward prototypical probes such as 3-Cyano-7-ethoxycoumarin (CYP1A), 7-methoxy-4-trifluoromethylcoumarin (CYP2E), and 7-Benzyloxy-4-(trifluoromethyl)-coumarin (CYP3A) in feline microsomes. With the use of conventional human CYP probe substrates, the activity of the feline hepatic CYP families were found to be significantly different from both canine and human CYP families [126]. Limited feline microsomal studies report variation in the activity of CYP2D and 3A between male and female feline microsomes and negligible hydroxylation of the CYP2C substrate tolbutamide, suggesting limited CYP2C activity in the liver of either gender [67].

The Food and Drug Administration (FDA) acknowledges the importance of human CYP variation in metabolism. For a pharmaceutical with more than 30% metabolism by CYP, the FDA requires the use of *in vitro* assays such as the microsome stability assay, CYP phenotyping and *in vivo* pharmacokinetics. Human drugs are also used in dogs and cats off-label without knowledge regarding the impact that CYP variation can have on the rate of drug clearance in either species. This challenge can lead to dosing extrapolations between the species, placing patients at risk for overdosing or sub-therapeutic concentrations. The purpose of this study is to compare the CL_{hep} between canine and feline liver microsomes of 30 therapeutic compounds reported to be substrates of a variety of human and canine CYP and frequently used in combination therapy in veterinary medicine.

Method

Chemicals and Materials

Selected substrates (Table 7) were chosen based on reported CYP activity in humans or canines, compounds within the same drug class (e.g. benzodiazepines), or reported to have significantly different *in vivo* clearance between canine and feline. Alprazolam, amitriptyline, carvedilol, clarithromycin, clomipramine, cyclosporin, desipramine, diazepam, enrofloxacin, fluvoxamine, loperamide, maropitant, metoclopramide, midazolam, mirtazapine, omeprazole, ondansetron, phenacetin, pimobendan, praziquantel, quinidine, testosterone, toceranib, and vincristine were purchased from Sigma-Aldrich (St. Louis, MO). Additional substrates purchased were grapiprant (MedChemExpress, Princeton, NJ), cyclophosphamide (MP Biomedicals, Solon, OH), vincristine and metronidazole (Alfa Aesar, Ward Hill, MA), and fluoxetine (Toronto Research Chemicals Inc, North York, ON, Canada).

Custom made, mixed gender, healthy adult, sexually mature (n=8) feline liver microsomes (20 mg/ml), and commercial, mixed gender, healthy adult, sexually mature (n=8) canine (beagle) liver microsomes (20 mg/ml) were purchased from Sekisui XenoTech, LLC (Kansas City, KS). The custom made feline liver microsomes were harvested from domestic feline livers (Liberty Research, Waverly, NY) and made by XenoTech. Neither species received any medications prior to the liver being harvested, nor was physiological protein content

assumed. Ultra-performance liquid chromatography grade solvents were purchased from Fisher Scientific (Pittsburg, PA).

Initial Screening

All liquid handling and incubations were completed via the Hamilton Workstation (Franklin, MA). Substrate depletion was accomplished using the methodology previously described [139], with differences as noted. Aliquots from stock solutions were diluted 1:1000 to 10 µM in 0.1 M KPO_4 buffer (pH 7.4). The high-throughput microsomal stability assay was performed in a 384-well format. Microsome mixture containing canine or feline microsomes and a regeneration system consisting of D-(L)-isocitrate trisodium salt (Sigma-Aldrich, St. Louis, MO), porcine isocitrate dehydrogenase type IV glycerol solution (Sigma-Aldrich, St. Louis, MO) and 0.1 M phosphate buffer were aliquoted into wells, equilibrated in a heated plate (38.4˚C) for 10 minutes, and then 5 µl of 10 mM NADP (Sigma-Aldrich, St. Louis, MO) was added. The final concentrations in each well consisted of 0.5 mg/ml microsomal protein, 1 µM of the drug, and 1 uM of NADP. At time points 0, 5, 10, 20, 30 and 60 minutes, the reaction was quenched with 100 µL of acetonitrile containing 100 ng/ml of internal standard (CP-424391) [142]. Controls included no drug and no regeneration system. The plate was centrifuged for 30 minutes at 2,000g. Experiments were repeated in duplicate.

Ultra-performance liquid chromatography (LC) and tandem mass spectrometry/mass spectrometry (MS/MS) were utilized for the detection of compounds. LC was accomplished via a Perkin Elmer Series 2000 micro-pump system (Waltham, MA) and LEAP Technologies HTC PAL Autosampler (Canboro, NC). 10 µL of the supernatant was injected into a C18 2.5X50 column (Phenomex, Torrance, CA) with a mobile phase composed of 0.1% formic acid in water (A) and acetonitrile (B) at a flow rate of 0.7 ml/min for a complete run time of 2 minutes. The initial mobile phase gradient started at A: B 90:10 then changed to 10:90 for 1 minute before switching back to 90:10 for the last 20 seconds of the run. Multiple reaction monitoring (MRM) was optimized for each compound before detection and quantification (Supplemental Table 4). MS/MS was completed via Applied Biosystem MDS/Sciex API 4000 triple quadrupole mass spectrometer (Foster City, CA) in positive ion mode.

Microsomal and Plasma Protein Binding via Equilibrium Dialysis

Microsomal nonspecific binding [143] and plasma protein binding were completed for each compound in quadruplicate via equilibrium dialysis (Single-Use RED Plate, Thermo-Scientific, Rockford, IL). Drug (1 µM) was combined with canine and feline microsomes; conditions were similar to the microsome stability assay (1 mM MgCl, 100 mM KOH buffer). All liquid handling and incubations were completed via the Hamilton Workstation (Franklin, MA). Briefly, 200 uL of 0.5 mg/ml microsomes spiked with 1 µM of the compound was placed in a dialysis chamber and 350 uL of K_2PO_4 added to the buffer chamber. The plate was incubated for 4 hours at 37 ˚C and 5% CO_2 (Cytomat, ThermoFisher Scientific). Incubated microsomes (15 µL) were mixed with control buffer (45 µL), and incubated buffer (45 µL) were mixed with control microsomes (15 µL). Spiked control microsomes (15 µL) were mixed with control buffer (45 µL) to determine the percent recovery from the incubation. Samples were quenched in acetonitrile with 100 ng/ml IS (120 µL). Plates were centrifuged for 30 min at 2,000g, and the supernatant transferred to a fresh 96-well plate. Samples were analyzed via the previously described high-throughput LC/MS/MS method. Canine and feline plasma protein binding was assessed with the described method, with beagle canine (BioreclamationIVT, Baltimore, MD; BGLPLEDTA3; Lot: BGL:91638) and domestic shorthair feline plasma (BioreclamationIVT, Baltimore, MD; CATPLEDTA3; Lot: CAT2417) utilized instead of microsomes and phosphate-buffered saline (Gibco, Grand Island, US) instead of phosphate buffer.

Calculations

The half-life ($t_{1/2}$) and CL_{int} were calculated if the substrate depletion was >20% by 30 minutes. Data were plotted as a percent based on time point zero. A minimum of 3 time points was used for all regression analyses, and a regression criterion of R^2 >0.9 implemented. The percent of substrate was calculated based on substrate peak area/IS peak area for all time points using T=0 as 100% as previously described [57]. Non-linear regression fitting to an exponential function produced the rate constant (k) for the parent compound (Eqn 3).

Equation 3

$$\%\ substrate\ remaining = Ax \times e^{-kt}$$

$$t_{1/2} = -\frac{\ln(2)}{k}$$

Where *Ax* represents the back extrapolated starting substrate concentration in the incubation media. CL_{int} can be estimated by using the rate of parent loss [57] (Eqn 4).

Equation 4

$$CL_{\text{int}}\left(\frac{\text{mL}}{\text{min}}/\text{kg}\right) = \frac{0.693}{t_{1/2}} \times \frac{ml\ incubation}{mg\ microsomal\ protein} \times \frac{mg\ microsomal\ protein}{g\ liver\ weight} \times \frac{g\ liver\ weight}{kg\ bodyweight}$$

Where the 0.5 mg/ml is the mg microsomal protein/ml incubation for both species, 55 mg microsomal protein/gram liver weight was used for canine [144] and 48 mg/g for feline [145]. The liver weights used were 29 g/kg for canine and 30 g/kg for feline [146].

Protein binding calculations for both microsomal and plasma protein binding were based on recovery (Eqn 5).

Equation 5

$$Recovery = \frac{Rp_e + Rb_e}{Rp_i}$$

The response of plasma before dialysis (Rp_i), the response of plasma following dialysis (Rp_e), and response of buffer following dialysis (Rb_e). The bound (F_b) and unbound fractions (F_u) of substrate were calculated (Eqn 6)

Equation 6

$$F_b = \frac{Rp_e - Rb_e}{(Rp_e - Rb_e) + Rb_e}$$

$$F_u = 1 - F_b$$

For the CL_{hep} with correction of microsomal and plasma protein binding, the equation integrated hepatic blood flow based on the well-stirred model (Eqn 7) and the parallel tube model for comparison (Eqn 8) [57].

Equation 7

$$CL_{hep} = \frac{Q_h \times F_{u,pl}(\frac{CL_{int}}{F_{u,mic}})}{Q_h + F_{u,pl}(\frac{CL_{int}}{F_{u,mic}})}$$

Equation 8

$$CL_{hep} = Q_h \times (1 - e\left(\frac{- F_{u,pl} \times CL_{int}}{Q_h \times F_{u,mic}}\right))$$

Where hepatic blood flow (Q_h) for the dog was 35 mL/min/kg and feline was 40 mL/min/kg [146], microsomal binding ($F_{u,mic}$) and plasma protein binding ($F_{u,pl}$) were calculated based on protein binding experiments. While it is recognized red blood cell partitioning can create a disparity between plasma and blood clearance, the blood:plasma ratio has not been reported for many of the substrates in canine or feline blood.

Statistical Analysis

Statistical analysis was completed via GraphPad Prism 7 (La Jolla, CA). The mean and standard deviation (SD) for CL_{int}, $F_{u,mic,}$ and $F_{u,pl}$ were calculated for each species and each drug. The mean CL_{int} was used to calculate the CL_{hep} in each species for each drug (Eqn 5 & 6). A linear regression was used to compare canine and feline $F_{u,mic}$, $F_{u,pl}$, CL_{int}, and CL_{hep}, in addition to a comparison between the well-stirred ($CL_{hep,ws}$) and parallel tube ($CL_{hep,pt}$) models within each species. The root mean square error (RMSE) was calculated for all parameters to describe the extent of the difference between canine and feline $F_{u,mic,}$ and $F_{u,pl}$, CL_{int}, and CL_{hep} (Eqn 7).

Equation 9

$$RMSE = \sqrt{\frac{1}{n}}\Sigma(\text{predicted} - \text{observed})^2$$

Where the predicted values were dog and the observed was cat, or respectively $CL_{hep,ws}$ and $CL_{hep,pt}$. The closer the RMSE is to zero, the closer the points lie along the line of unity.

Results

A total of 30 compounds were screened in canine (Table 8) and feline (Table 9) mixed gender liver microsomes. There was no quantifiable substrate depletion for enrofloxacin, fluvoxamine, and metronidazole in the canine. In contrast, minimal substrate depletion was present for the three substrates in feline microsomes. In the canine, amitriptyline and midazolam clearance was extremely rapid, and an accurate CL_{hep} could not be calculated. The same challenge arose with midazolam in the feline. The fold change in CL_{int} between canine and feline ranged from a two-fold change in alprazolam favoring feline CL_{int} to an almost ten-fold greater diazepam CL_{int} in canine compared to feline. Once the microsomal and plasma protein binding were incorporated to calculate the CL_{hep}, the fold change increased with diazepam and grapriprant having an almost 20-fold greater CL_{hep} in canine compared to feline, regardless of the model used (Table 4), with only maropitant clearance being faster in the feline compared to the canine in the well-stirred model.

A line of unity was produced for all parameters to determine the correlation between canine and feline and the two models. An RMSE < 1 was reported for both $F_{u,mic}$ (0.21) and $F_{u,p}$ (0.33) (Figure 13), and both sets of data lie along the line of regression and have minimal variation. The RMSE was largest for CL_{int} (RMSE= 128.33) (Figure 14), and improved once $F_{u,mic}$ and $F_{u,p}$ were incorporated for both species ($CL_{hep,ws}$ RMSE=12.42; $CL_{hep,pt}$ RMSE=15.37) (Figure 15). The RMSE indicates a correlation exists between the species for $F_{u,mic}$ (RMSE=0.21) and $F_{u,p}$ (RMSE=0.33). When comparing the two models within a species (Figure 16), there is a strong correlation (r^2>0.95) for both models, however, the RMSE for both the $CL_{hep,ws}$ and $CL_{hep,pt}$ are greater than 1, indicating that there is deviation from the line of unity.

Discussion

This study highlights the difference between canine and feline CL_{int} and CL_{hep}. On average, canine CL_{hep} values are higher than feline CL_{hep}. Reasons for the differences include different enzymatic efficiencies between canine and feline CYP isoforms and lack of particular

isoforms, such as CYP2B6 in the feline liver [31]. Quantification of CYP liver content has not been performed in the feline, but estimates for canine liver CYP isoform reports CYP3A12 as the most abundant, followed by CYP2C21, CYP2D15, and equal abundance of CYP1A2, CYP2B11, and CYP2E1 [147]. This study reports the overall differences between feline and canine CYP metabolism, but studies focusing on metabolite formation and CYP phenotyping will be necessary to calculate enzyme efficiency and determine individual isoform contribution [148].

Individual substrate phenotyping is necessary to identify whether the same CYP isoforms in canine and feline metabolize substrates at the same rate as humans. In the canine, CYP1A2 is polymorphic, with a premature stop codon C1117C>T. This SNP was reported to be present in more than 10% of the study population, and a homozygous CC allele frequency of 37% in dogs has been reported, with genotyping reporting a statistically significant different frequency of CYP1A2 CC wildtype genotype between boxers and pure bred dogs [78,149]. Another polymorphism reported in canines is the lack of CYP2C41 in the majority of dogs, with only 11% of tested dogs expressing *CYP2C41* [91]. This finding was further confirmed in a study, where 6/11 beagles had *CYP2C41* mRNA transcripts [13]. No polymorphisms have been reported in the feline. Due to polymorphisms in humans, physiological protein content in human liver microsomes have been reported to vary by 11-129 fold in addition to significant variation in the intrinsic activity of isoforms within the liver microsomes [150].

Age can also impact CYP function, with neonatal CYP function increasing as a puppy ages, reaching full function by 5-8 weeks after birth [151]; *in vivo* studies also report an increase in the rate of theophylline clearance as dogs age [152]. During disease states including liver disease, inflammation and infection, CYP transcripts are downregulated, resulting in a decrease in the enzyme activity in humans [153],[154]. While disease is anticipated to impact CYP function in the canine and feline, no reports regarding the impact are currently available. Research is required to examine the impact of age (neonatal and geriatric) and disease and to identify polymorphisms in both canines and felines that influence CL_{hep}.

The $CL_{hep,ws}$ underpredicted compared to the reported *in vivo* clearance, a recognized problem with the use of this model in the metabolic stability assay [57]. In addition, it is difficult to compare the CL_{hep} to the reported *in vivo* clearance due to the impact of bioavailability on drugs administered via an extravenous route. The prediction improves with drugs considered to be high extraction (E), defined as an E>0.7. Drugs classified as high extraction in humans include

midazolam, carvedilol [155], fluoxetine [156], praziquantel [157], quinidine [158], sildenafil [159], and verapamil. The $CL_{hep,ws}$ model is one of the most frequently used models, and assumes that the substrate is instantly and homogenously distributed through the liver water, the unbound drug concentration in the plasma is identical to unbound drug concentrations in the liver water, there is no active transport involved, and that CYP is the main route for metabolism. In contrast, the $CL_{hep,pt}$ model assumes that the liver consists of parallel tubes with enzymes evenly distributed in each section, and the concentration of the drug decreases along the direction of blood flow in the sinusoids [160]. Both models assume that mixing occurs between the hepatic portal and arterial blood prior to drug partition in the sinusoids, only unbound drug traverses the cellular membranes, the rate of distribution is perfusion-limited without the influence of transporters, and the rate of drug elimination is dependent on the concentration of unbound drug at the enzyme location [161]. The well-stirred model is the most frequently cited model, and is used in physiologically-based pharmacokinetic modeling (PBPK). However, this model is reported to predict lower CL_{hep} compared to the parallel tube model, as observed in this study (Figure 3). The $CL_{hep,pt}$ predictions were higher compared to the well-stirred model, but the fold difference between the species remained similar (Table 10). Additional research and pharmacokinetic studies in both species are necessary to determine the best model for integration with PBPK for each species [162].

The use of either model relies on several assumptions including the lack of active transporters and that only CYP pathways function in the metabolism of the substrate. In addition to the CYP enzymatic differences previously reported, the influence of other metabolic pathways can vary significantly between the species. For example, diazepam is metabolized by CYP, but also UGT, a less predominant pathway in the feline. Therefore, the pharmacokinetics and the risk of toxicity are dramatically different in this species [163]. In contrast, the canine is a reported non-acetylator, reducing this species' ability to metabolize aromatic amines [164]. Both models also rely on the use of specific hepatic blood flow measurements in order to calculate CL_{hep}. References for canine [165] and feline hepatic blood flow [166] [146] are sparse and utilized different techniques, which may have been refuted in later research. The authors referenced multiple articles [146,165-167] and selected a blood flow reference that appears most consistent across references: 35 mL/min/kg for dog and 40 mL/min/kg for cat [146]. This range, combined with the difference in reported microsome content per gram of liver may account for the interspecies CL_{hep} differences.

Plasma protein binding can have a significant impact on the rate of drug clearance. Changes in disease state or competitive binding can alter the free plasma drug concentration, the only component available for metabolism and clearance [168]. For drugs with a low E, the total clearance is proportional to $F_{u,pl}$, but is independent of total clearance in high E drugs [169]. This study was able to document the $F_{u,pl}$ for 30 substrates and report that RMSE between the two species is <1, indicating that the points are concentrated around the line of unity. Differences in the $F_{u,pl}$ and $F_{u,mic}$ could also be due to experimental measurement errors in drugs with a low unbound fraction. A comparison between dog, rat and human reports up to a five-fold difference in $F_{u,pl}$, necessitating the use of species specific $F_{u,pl}$ and $F_{u,mic}$ [170].

In the canine, CL_{hep} for midazolam and amitriptyline could not be calculated due to rapid substrate depletion. To achieve first order linear kinetics required for the initial calculation, the depletion assay would have to be optimized by diluting the microsome concentration. This study did not evaluate gender differences, previously reported in a comparison between female and male domestic feline microsomes [67]. Substrates which did not have any clearance may still act as an inhibitor towards a particular CYP and could influence pharmacokinetics with the use of polypharmacy.

This study underlines the need for *in vivo* pharmacokinetic studies for human drugs used off-label in dogs and cats since the CL_{hep} for most drugs differs between the two species. The need for feline pharmacokinetics is arguably greater because the current literature is sparse. Due to the lower CL_{hep} in felines, prolonged dosing intervals compared to canine may be necessary. It is suggested that characterizing species differences in drug metabolizing enzymes using *in vitro* methods will also be beneficial, since it can be used to identify drugs expected to show species-specific elimination rates.

Acknowledgements: The authors would like to thank Julie White and Jacqueline Kilmer for their technical advice and assistance.

Declaration of Interest:

The authors do not have any conflict of interest to declare.

Table 7: Compound description

Compound ID	MW (g/mol)	logP	pKa / charge type near neutral pH	Human CYP
Alprazolam	308.769	2.1	2.4 / neutral	2C9, 2C19, 3A4 [171]
Amitriptyline	277.411	5	9.76 / base	2C19,2D6>2C9,1A2>3A4 [172]
Carvedilol	406.482	4.2	8.77 / base	2D6>2C9>1A2,2C9, 2E1,3A4 [173]
Clarithromycin	747.964	3.2	8.99 / base	inhibitor
Clomipramine	314.857	5.2	8.98 / base	1A2,3A4,2C19,2D6 [174]
Cyclophosphamide	261.083	0.6	9.91 / acid	CYP2A6, 2B6, 2C19, 2C9, 3A4, 3A5 [175]
Cyclosporin	1202.635	7.5	N/A / neutral	3A [176]
Desipramine	266.388	4.9	10.4 / base	2D6 [177]
Diazepam	284.743	3	3.4 / neutral	2C19, 3A [178]
Enrofloxacin	359.401	-0.2	5.88-6.06 [179] / zwitterion	N/A
Fluoxetine	309.332	4	9.8 / base	Inhibitor [180]
Fluvoxamine	318.34	2.6	8.86 / base	Inhibitor [180]
Grapiprant	491.61	4.6	4.33 / acid	N/A
Loperamide	477.045	5	9.41 / base	2B6, 2C8, 2D6, 3A4 [181]
Maropitant	468.685	7	9.99* / base	N/A
Metoclopramide	299.799	2.6	9.27 / base	2D6 [182]
Metronidazole	171.156	0	2.38 / neutral	Inhibitor [180]
Midazolam	325.771	2.5	5.5 / neutral	3A4, 3A5 [183]
Mirtazapine	265.36	3.3	8.1* / base	1A2, 2C8, 2C9,2D6, 3A4 [184]
Omeprazole	345.417	2.2	1.2 / neutral	2C19 [185]
Ondansetron	293.37	2.3	7.34 / base	1A2, 2D6, 3A [186]
Phenacetin	179.219	1.6	1.42 * / neutral	1A1, 1A2 [187]
Pimobendan	334.379	2.08	N/A / neutral	1A2>3A4 [188]
Praziquantel	312.413	2.66	N/A / neutral	1A2, 2C19, 3A4 [189]
Quinidine	324.424	2.9	8.56 / base	inhibitor

Sildenafil	474.58	1.5	5.99 / base	3A4> 2C9, 2C19> 2D6 [190]
Testosterone	288.431	3.3	N/A / neutral	2C19, 2C9, 3A4 [191] [192]
Toceranib	396.466	1.8	11.7* / base	N/A
Verapamil	454.611	3.8	8.92 / base	3A4, 3A5, 2C8, 2E1 [193]
Vincristine	824.972	2.8	7.4 / base	3A4, 3A5 [194]

Compound information including molecular weight (MW), logP, pKa, and CYP isoforms in humans. Unless otherwise noted, MW, logP and pKa information was collected from PubChem (https://pubchem.ncbi.nlm.nih.gov/). * Data were collected from ChEMBL (https://www.ebi.ac.uk/chembl/).

Table 8: Canine mean and standard deviation (SD) of the half-life ($t_{1/2}$), intrinsic clearance (CL_{int}), microsomal non-specific binding ($F_{u,mic}$) and plasma ($F_{u,pl}$) fraction unbound and calculated hepatic clearance using the well-stirred ($CL_{hep,ws}$) and parallel tube ($CL_{hep,pt}$) models.

Drug	$t_{1/2}$ (min) Average (SD)	$\boldsymbol{CL_{int}}$ (ml/min/kg) Average (SD)	$\boldsymbol{F_{u,mic}}$ Average (SD)	$\boldsymbol{F_{u,pl}}$ Average (SD)	$\boldsymbol{CL_{hep,ws}}$ (ml/min/kg)	$\boldsymbol{CL_{hep,pt}}$ (ml/min/kg)	Published *in vivo* clearance (ml/min/kg)
Alprazolam	104.780 (7.344)	21.202 (1.486)	0.70 (0.05)	0.69 (0.07)	13.038	15.670	
Amitriptyline	<3	>602 (0)	0.23 (0.03)	0.12 (0.01)	N/A	N/A	207[195]
Carvedilol	7.659 (0.038)	288.659 (1.416)	0.22 (0)	0.09 (0.01)	27.306	33.994	11,600 [196]
Clarithromycin	47.903 (0.378)	46.152 (0.364)	0.30 (0.02)	0.36 (0.03)	21.361	27.691	4.3[197]¥
Clomipramine	4.825 (0)	458.126 (0.364)	0.23 (0.02)	0.07 (0.01)	28.018	34.367	23.33[198]
Cyclophosphamide	37.644 (0.645)	58.743 (1.006)	0.86 (0.02)	0.82 (0.18)	21.538	27.934	709[199]
Cyclosporine	11.638 (0)	189.947 (0)	0.02 (0)	0.01 (0)	27.721	34.224	7.0 ± 3.6[200]
Desipramine	9.907 (0.929)	225.129 (21.108)	0.16 (0.02)	0.18 (0.02)	30.648	34.969	
Diazepam	4.883 (0)	452.735 (0)	0.58 (0.11)	0.64 (0.07)	32.732	35.000	3229 [201]
Enrofloxacin	>120	<11.5	0.49 (0.11)	0.60 (0.08)	N/A	N/A	2.71±16.2[202]
Fluoxetine	97.552 (22.448)	23.929 (5.506)	0.05 (0)	0.08 (0.01)	18.606	23.750	
Fluvoxamine	>120	<11.5	0.17 (0.02)	0.99 (0.17)	N/A	N/A	
Grapiprant	60.907 (1.588)	36.320 (0.947)	0.59 (0.04)	0.63 (0.1)	18.410	34.921	7.4 [203] ¥
Loperamide	14.414 (0.045)	153.370 (0.478)	0.28 (0.01)	0.17 (15.61)	25.500	35.000	
Maropitant	82.679 (12.764)	27.391 (4.229)	0.05 (0.01)	0.01 (0)	5.763	34.646	16.1 [204] ¥
Metoclopramide	32.56 (0.51)	67.912 (1.064)	0.73 (0.05)	0.70 (0.04)	22.695	29.465	
Metronidazole	>120	<11.5	0.76 (0.01)	0.54 (0.04)	N/A	N/A	
Midazolam	< 3	>602 (0)	0.31 (0.08)	0.50 (0.08)	N/A	N/A	
Mirtazapine	17.58 (0.089)	125.753 (0.639)	0.70 (0.04)	0.46 (0.05)	24.508	31.615	19.83 [205] ¥
Omeprazole	86.712 (14.557)	26.234 (4.404)	0.46 (0.02)	0.70 (0.08)	18.632	23.788	10.5 [206] ¥

Drug	$t_{1/2}$ (min) Average (SD)	CL_{int} (ml/min/kg) Average (SD)	$F_{u,mic}$ Average (SD)	$F_{u,pl}$ Average (SD)	$CL_{hep,ws}$ (ml/min/kg)	$CL_{hep,pt}$ (ml/min/kg)	Published *in vivo* clearance (ml/min/kg)
Ondansetron	37.709 (1.897)	58.774 (2.957)	0.65 (0.02)	0.59 (0.07)	21.119	27.356	
Phenacetin	23.973(0.925)	92.354 (3.562)	0.39 (0.05)	0.88 (0.02)	29.990	34.912	
Pimobendan	71.662 (1.356)	30.860 (0.584)	0.30 (0.04)	0.20 (0.03)	12.820	15.364	392 [207]
Praziquantel	20.759 (0.154)	106.5 (0.792)	0.95 (0.02)	0.65 (0.05)	23.696	30.697	
Quinidine	52.778 (0.68)	41.893 (0.539)	0.29 (0.02)	0.38 (0.08)	21.322	27.487	
Sildenafil	47.087 (0.024)	156.933 (0.262)	0.14 (0.12)	0.37 (0.09)	32.241	35.000	12 [208]
Testosterone	21.722 (0.552)	101.835 (2.589)	0.57 (0.01)	0.73 (0.03) ¤	27.614	34.982	
Toceranib	21.829 (1.792)	101.959 (8.370)	0.14 (0.01)	0.11 (0.01) ¤	24.539	34.982	24.1 [209]
Verapamil	8.697 (3.318)	447.961 (44.960)	0.31 (0.01)	0.31 (0.02) ¤	32.624	35.000	
Vincristine	38.444 (0.953)	57.539 (1.426)	0.27 (0.02)	0.23 (0.02)	20.463	26.435	24 [210]

¥ *in vivo* clearance is based on oral dosing.

Table 9: Feline mean and standard deviation (S.D) of the half-life ($t_{1/2}$), intrinsic clearance (CL_{int}), microsomal non-specific binding ($F_{u,mic}$) and plasma ($F_{u,pl}$) fraction unbound and calculated hepatic clearance using the well-stirred ($CL_{hep,ws}$) and parallel tube ($CL_{hep,pt}$) models.

	$t_{1/2}$ (min) Average (SD)	$\boldsymbol{CL_{int}}$ (mL/min/kg) Average (SD)	$\boldsymbol{F_{u,mic}}$ Average (SD)	$\boldsymbol{F_{u,pl}}$ Average (SD)	$\boldsymbol{CL_{hep,ws}}$ (ml/min/kg)	$\boldsymbol{CL_{hep,pt}}$ (ml/min/kg)	Published *in vivo* clearance (ml/min/kg)
Alprazolam	51.815 (1.891)	38.569 (1.407)	0.69 (0.07)	0.39 (0.06)	14.159	16.874	
Amitriptyline	6.443 (0.263)	310.297 (12.647)	0.12 (0.01)	0.03 (0)	26.292	34.124	
Carvedilol	3.63 (0.129)	550.492 (19.579)	0.09 (0.01)	0.01 (0.01)	23.904	30.941	5.83 [211] ¥
Clarithromycin	109.283 (10.717)	18.44 (1.808)	0.36 (0.03)	0.05 (0)	2.430	2.506	
Clomipramine	20.346 (0)	98.142 (0)	0.07 (0.01)	0.01 (0)	10.237	11.642	6.55 [212]
Cyclophosphamide	34.869 (0)	57.238 (0)	0.82 (0.18)	0.91 (0.03)	24.506	31.774	
Cyclosporine	20.429 (0)	97.69 5(0)	0.01 (0)	0.01 (0)	25.875	33.595	3.3 [213]
Desipramine	10.748 (0.243)	185.786 (4.202)	0.18 (0.02)	0.06 (0)	24.463	31.715	
Diazepam	49.461 (0)	40.352 (0)	0.64 (0.07)	0.04 (0)	2.359	2.429	4.72±2.45 [214]
Enrofloxacin	83.685 (0)	23.8549(0)	0.60 (0.08)	0.78 (0.06)	17.450	21.550	
Fluoxetine	100.856 (2.305)	19.799 (0.453)	0.08 (0.01)	0.44 (0.02)	28.803	36.946	
Fluvoxamine	49.888 (2.127)	41.250 (0.054)	0.99 (0.17)	0.14 (0.01)	5.100	5.438	
Grapiprant	52.504 (0.392)	38.015 (0.284)	0.63 (0.01)	0.03 (0)	1.740	1.778	
Loperamide	19.496 (0.338)	102.401 (1.777)	0.17 (0.01)	0.04 (0.02)	15.055	18.125	
Maropitant	24.616 (0.474)	81.109 (1.563)	0.01 (0)	0.01 (0)	25.659	33.316	4.6 [215] ¥
Metoclopramide	48.009 (10.914)	43.838 (9.966)	0.70 (0.04)	0.57 (0.02)	18.901	23.669	
Metronidazole	108 (11.95)	18.701 (2.069)	0.54 (0.04)	0.26 (0.03)	7.324	8.032	
Midazolam	<3	>602	0.50 (0.08)	0.02 (0)	N/A	N/A	
Mirtazapine	72.747 (0.123)	27.436 (0.046)	0.46 (0.05)	0.17 (0.01)	8.155	9.037	9.8-18.6 [216] ¥
Omeprazole	36.602 (5.303)	55.697 (8.07)	0.70 (0.08)	0.14 (0.02)	8.677	9.679	

Ondansetron	17.173 (0.532)	116.33 (3.679)	0.59 (0.07)	0.37 (0.02)	25.913	33.644	
Phenacetin	15.502 (0.443)	128.856 (3.679)	0.88 (0.02)	0.75 (0.21)	29.338	37.447	
Pimobendan	37.948 (0.001)	52.594 (0)	0.20 (0.03)	0.03 (0)	6.701	7.292	81.6 [217] ¥
Praziquantel	14.507 (2.089)	140.493 (20.227)	0.65 (0.05)	0.24 (0.02)	22.560	29.028	
Quinidine	29.968 (2.497)	67.064 (5.587)	0.38 (0.08)	0.32 (0.11)	23.475	18.428	
Sildenafil	17.038 (0.720)	117.35 (4.962)	0.37 (0.09)	0.23 (0.13)	28.525	26.422	
Testosterone	10.444 (0.467)	191.474 (8.555)	0.73 (0.03)	0.04 (0)	32.089	33.138	
Toceranib	36.125 (1.036)	55.294 (1.586)	0.11 (0.01)	0.04 (0)	13.247	15.959	
Verapamil	20.899 (0.328)	95.521 (1.498)	0.31 (0.02)	0.03 (0)	7.502	8.246	
Vincristine	42.53 (0.817)	46.945 (0.902)	0.23 (0.02)	0.24 (0.01)	22.092	28.350	

¥ *in vivo* clearance is based on oral dosing.

Table 10: Fold change between canine and feline half-life ($t_{1/2}$), intrinsic microsomal (CL_{int}), and calculated hepatic clearance using the well-stirred ($CL_{hep,ws}$) and parallel tube ($CL_{hep,pt}$) models.

	Canine/Feline Fold Change			
	$t_{1/2}$	CL_{int}	$CL_{hep,ws}$	$CL_{hep,pt}$
Alprazolam	2.02	0.5	0.9	0.9
Amitriptyline	N/A	N/A	N/A	N/A
Carvedilol	2.11	0.5	1.1	1.1
Clarithromycin	0.44	2.5	8.8	11.1
Clomipramine	0.00	4.7	2.7	3.0
Cyclophosphamide	1.08	1.0	0.9	0.9
Cyclosporine	0.57	1.9	1.1	1.0
Desipramine	0.92	1.2	1.3	1.1
Diazepam	0.10	11.2	13.9	14.4
Enrofloxacin	N/A	N/A	N/A	N/A
Fluoxetine	0.97	1.2	0.6	0.6
Fluvoxamine	N/A	N/A	N/A	N/A
Grapiprant	1.16	1.0	17.3	19.6
Loperamide	0.74	1.5	2.2	1.9
Maropitant	3.36	0.3	0.2	1.0
Metoclopramide	0.68	1.5	1.2	1.2
Metronidazole	N/A	N/A	N/A	N/A
Midazolam	N/A	N/A	N/A	N/A
Mirtazapine	0.24	4.6	3.0	3.5
Omeprazole	2.37	0.5	2.1	2.5
Ondansetron	2.20	0.5	0.8	0.8
Phenacetin	1.55	0.7	1.0	0.9
Pimobendan	1.89	0.6	1.9	2.1
Praziquantel	1.43	0.8	1.1	1.1
Quinidine	1.76	0.6	0.9	1.5
Sildenafil	2.76	1.3	1.1	1.3
Testosterone	2.08	0.5	0.9	1.1
Toceranib	0.60	1.8	2.1	2.2
Verapamil	0.42	5.0	4.4	4.2
Vincristine	0.90	1.2	0.9	0.9

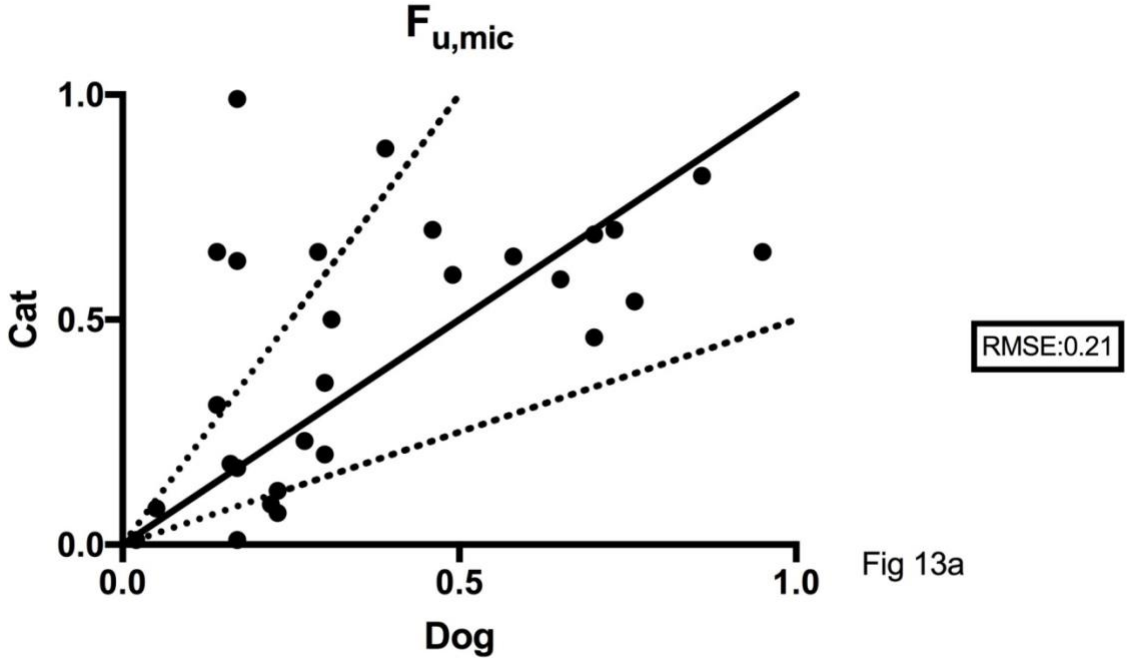

Fig 13a

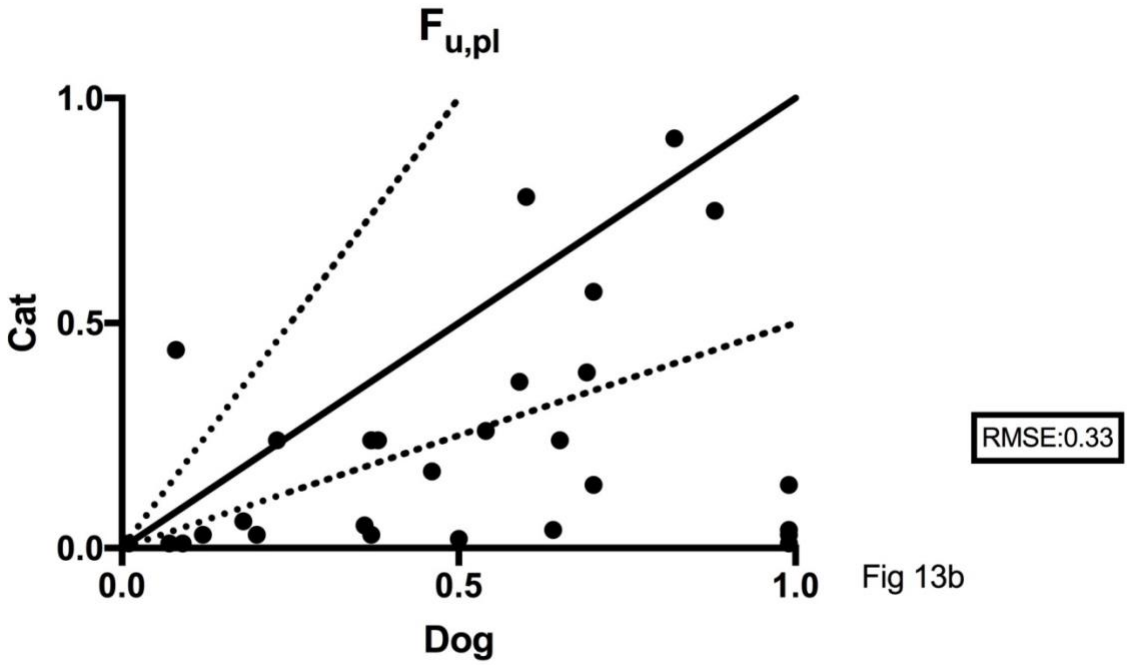

Fig 13b

Figure 13: Comparison of $F_{u,mic}$ (Fig 13a) and $F_{u,pl}$ (Fig 13b) between canine and feline. Solid line is the line of unity, and dashed line indicates two-fold difference from the line of unity.

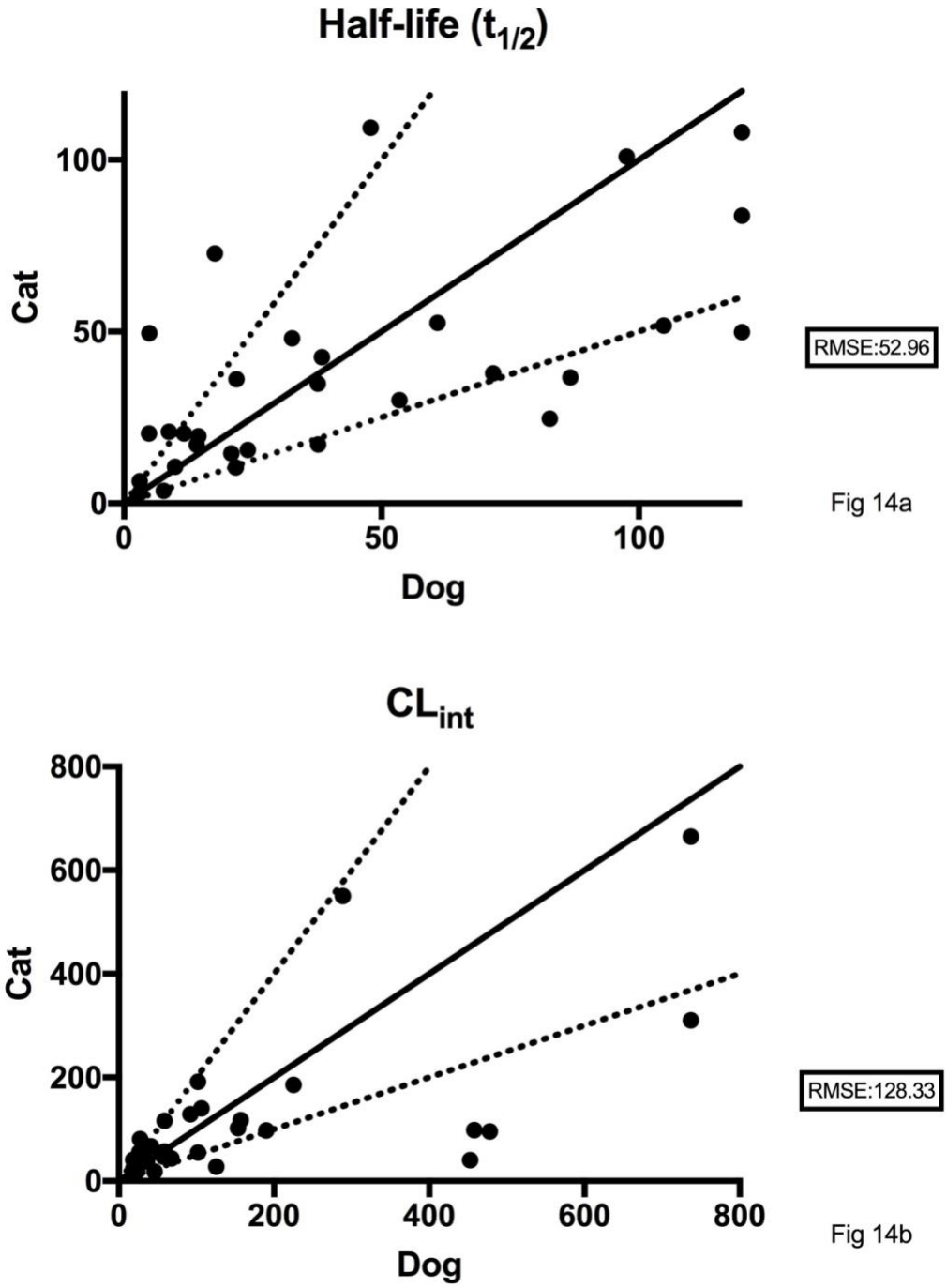

Figure 14: Comparison of microsomal $t_{1/2}$ (Fig 14a) and CL_{int} (Fig 14b). Solid line is the line of unity, and dashed line indicates two-fold difference from the line of unity.

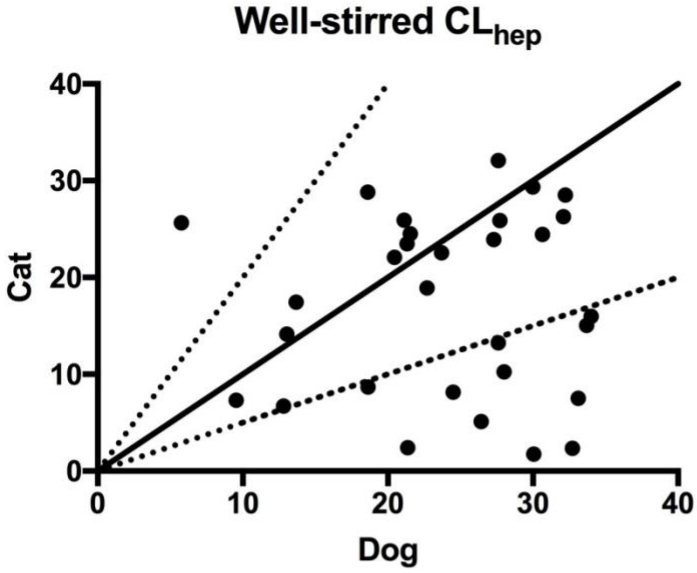

RMSE:12.42

Fig 15a

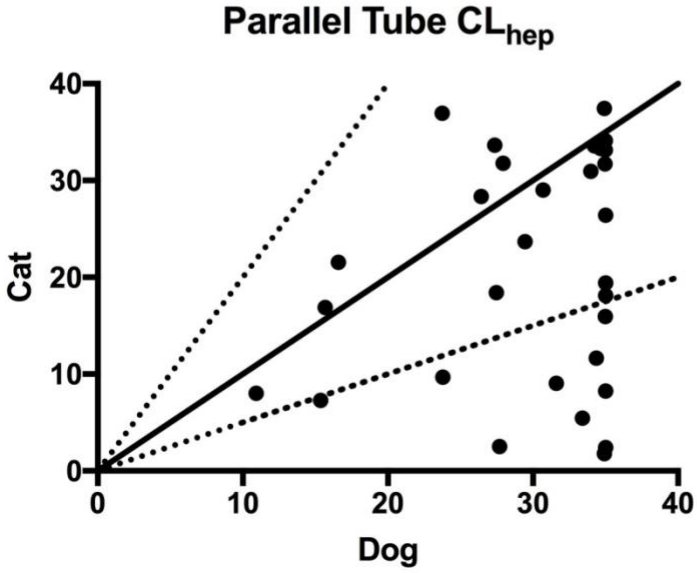

RMSE:15.37

Fig 15b

Figure 15: Interspecies comparison of $CL_{hep,ws}$ (Fig 15a) and $CL_{hep,pt}$ (Fig 15b) models. Solid line is the line of unity, and dashed line indicates two-fold difference from the line of unity.

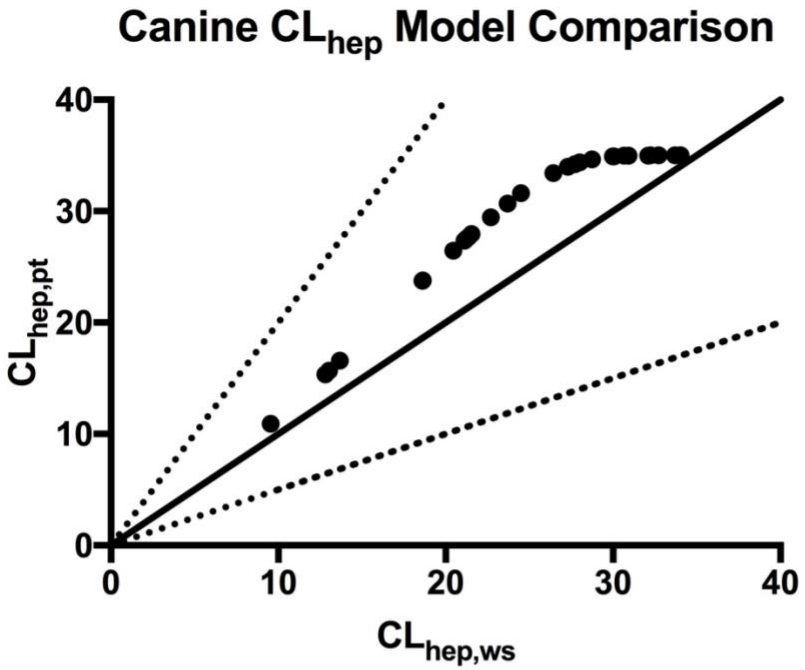

Fig 16a

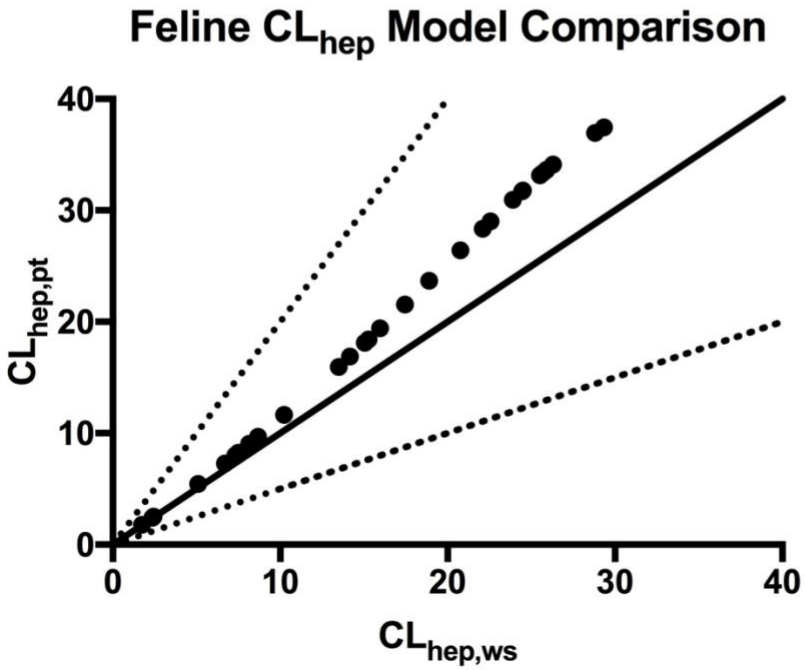

Fig 16b

Figure 16: Intraspecies comparison of the $CL_{hep,ws}$ and $CL_{hep,pt}$ models in canine (Fig 16a) and feline (Fig 16b). Solid line is the line of unity, and dashed line indicates two-fold difference from the line of unity.

Supplemental Table 4: Individual compound multiple reaction monitoring (MRM) profile

Compound ID	Q1 *m/z*	Q3 *m/z*
Alprazolam	310.239	206.063
amitriptyline	278.400	91.100
Carvedilol	407.200	100.200
Clarithromycin	749.500	158.000
Clomipramine	315.108	86.087
Cyclophosphamide	261.005	140.004
Cyclosporin	1202.639	425.168
Desipramine	267.200	72.000
Diazepam	286.140	194.129
Enrofloxacin	360.713	244.982
Fluoxetine	310.096	148.078
Fluvoxamine	319.100	70.960
Grapiprant	492.093	295.088
Loperamide	477.100	266.100
Maropitant	469.327	177.210
Metoclopramide	300.124	227.041
Metronidazole	172.999	153.148
Midazolam	327.091	222.980
Mirtazapine	266.100	195.000
Omeprazole	346.079	198.083
Ondansetron	294.112	170.077
Phenacetin	180.100	110.00
Pimobendan	335.000	206.000
Praziquantel	313.185	203.092
Quinidine	325.583	172.026
Selamectin	770.24	608.198
Sildenafil	475.200	100.100
Testosterone	289.500	109.200
Toceranib	397.200	283.000
Verapamil	454.800	165.100
Vincristine	825.198	765.028
CP-424391*	768.000	486.000

*internal standard

Chapter 5: Cytochrome P450 enzyme reaction phenotyping of clinically relevant drugs using canine recombinant cytochrome P450

Abstract

Reaction phenotyping cytochrome P450 (CYP) metabolic pathways of drugs is helpful in predicting drug-drug interactions and understanding sources of individual differences in pharmacokinetics. For instance, recombinant CYP (rCYP) enzymes are routinely used to screen potential human drug candidates metabolized by polymorphic isozymes to evaluate the risk of variable population pharmacokinetics due to genetic factors. Similar data are unavailable for dogs, few phenotyping studies have been reported, and the clinical impact of polymorphism remains poorly described for most canine CYPs. Utilizing an rCYP metabolic stability assay, 22 drugs used in veterinary medicine were phenotyped using canine rCYP1A1, 1A2, 2B6, 2C21, 2C41, 2D15, 3A12, and 3A26. Three time points were necessary to calculate the rCYP clearance (CL_{rCYP}), and 4/22 substrates required a two- or four-fold rCYP dilution in order to calculate the CL_{rCYP}. The tricyclic antidepressants, amitriptyline and clomipramine, required a two- or four-fold dilution of both rCYP2C41 and rCYP2D15 to achieve the necessary time points. An isoform reported in only 11% of tested beagles, rCYP2C41, was involved in the metabolism of 9/22 substrates. The contribution of rCYP2B11 in canine drug metabolism altered the rCYP metabolism pattern for 8/22 substrates compared to the CYP metabolism pattern reported for humans. This report contributes to our understanding of similarities and differences between humans and canines, and identifies potential probes for canine P450 metabolic pathways.

Keywords: recombinant cytochrome, phenotyping, canine, pharmaceutical

Introduction

Cytochrome P450 (CYP) is a superfamily of enzymes involved in the metabolism of a wide variety of xenobiotic compounds, including an estimated 70-90% of drugs. All CYPs contain a heme prosthetic group that uses molecular oxygen to create reactive oxygen species to oxidize drug substrates, rendering them more water soluble for excretion via biliary or renal pathways. Major human CYP involved in drug metabolism include CYP1A1/2, CYP2B6, CYP2C8/9/19, CYP2D6 and CYP3A4/5. Drugs utilizing the same CYP pathway can result in

drug-drug interactions (DDI), prolonging the elimination half-life and increasing the risk of adverse drug reactions[4,98]. Other drugs such as phenobarbital and rifampin induce CYP expression, resulting in an increase in the rate of drug clearance[28,98].

Using high-throughput sequencing, the canine CYP transcriptome has been described in a variety of tissues[218], highlighting important differences between dogs and humans that could result in differences in drug metabolism. Canines do not have orthologs to every human CYP isoform important for drug metabolism. For example, humans have four CYP2C isoforms, while canines have only two, CYP2C21 and CYP2C41. CYP2C21 has 66% amino acid homology to CYP2C8 and 70-75% amino acid homology to CYP2C18[219]. These differences in amino acid homology could result in substrate affinity variation and different rates of drug metabolism. In addition to amino acid differences, polymorphisms within the canine population can also impact rates of drug clearance. CYP2C41 is present in only 11% of beagles that were tested, and the impact this has on pharmacokinetics continues to be explored[100]. Differences in protein quantities of isoforms between canines and humans have been reported, with CYP3A having the highest protein quantification in both species, but CYP2D15 and CYP2B11 liver protein expression is greater in the dog than human[13].

The presence of a CYP orthologue does not indicate similar substrate specificity, affinity or kinetics[126]. Phenacetin is considered a human CYP1A2 selective substrate but canine *in vivo* pharmacokinetics suggests that it is not selective in this species[220]. The metabolism of tramadol in dogs yields two main metabolites, M1 and M2. The rate of active metabolite M1 formation in the dog is 3.9 fold slower compared to the cat, but 7 fold faster than humans[75]. Use of probe substrates, inhibitors and fluorescent assays commonly utilized in human medicine have reported differences in the enzyme kinetics or inhibitory kinetics when used in both canine and feline microsomes[67,126].

Reaction phenotyping combines multiple techniques to identify the isoforms involved in the metabolism of a specific substrate. Using the cDNA of a particular isoform transfected into a non-metabolizing cell line (baculosome, insect cell), the isoform protein is expressed as a recombinant CYP (rCYP)[221]. This method is also used to study the impact of specific mutations and polymorphisms on the rate of substrate clearance and metabolite formation. A combination of methods has been described including the use of antibody inhibition in liver microsomes to identify substrate affinity, relying on antibody potency and isoform specificity to identify the

correct isoforms[222]. Currently, there are no canine CYP-specific antibodies commercially available, and polyclonal human antibodies are frequently used. Chemical inhibition has also been utilized in reaction phenotyping, but, again, the inhibitor must be isoform-specific. Only a few specific chemical inhibitors have been identified in the canine. Recombinant cytochromes (rCYP) have been used to phenotype individual CYP isoforms, describe enzyme kinetics and identify differences in metabolite formation by CYP isoforms[223]. Using rCYP, a substrate depletion assay can be utilized to rapidly phenotype multiple substrates. The purpose of this study was to phenotype 22 pharmaceuticals identified as human CYP substrate probes using canine rCYP and to compare the CYP profile to the reported human CYP profile such that similarities and differences between the two species might be identified.

Materials and Methods

Chemicals and Materials

Drugs considered for phenotyping included drug families with variation in *in vitro* clearance (benzodiazepines, tricyclic antidepressants), drugs with turnover that are only metabolized by a single isozyme in humans, or drugs with at least a twofold difference in metabolism between canine and feline clearance based on previous research[224]. Drugs with microsomal intrinsic clearance (CL_{int}) >30 µg/ml/min were selected, and further individual cytochrome phenotyping was completed. Recombinant canine cytochromes (1A1, 1A2, 2B11, 2D15, 2C21, 2C41, 3A12, and 3A26) were purchased from Cypex (Dundee, Scotland, UK).

rCYP Substrate Depletion Assay

Each recombinant assay consisted of 50 pmol/ml CYP content, 1µM of NADPH (Sigma) and 1uM of selected drug. A 96-well 2 ml plate was placed in a 37.5C hot water bath and the rCYP allowed to reach equilibrium for 5 minutes, after which NAPDH and drug were added.At removed at 0, 5, 10, 20, 30 and 60 minutes, a 50 µL aliquote was quenched in 100 µL ice cold acetonitrile with internal standard (100 ng/ml CP-424391)[142]. Each assay was completed in quadruplicate, and controls included no drug and no NADPH. Plates were sealed and centrifuged at 2,000g for 30 minutes. Samples with an rCYP clearance (CL_{rCYP}) >4.62 mL/min/pmol were further diluted to 25 pmol/mL and 12.5 pmol/mL to provide an accurate CL_{rCYP}. This dilution was completed to obtain the three points for linear regression.

Ultra-performance liquid chromatography (LC) and mass spectrometry/mass spectrometry (MS/MS) were utilized for the detection of compounds. LC was accomplished via a Perkin Elmer Series 2000 micro-pump system (Waltham, MA) and LEAP Technologies HTC PAL Autosampler (Canboro, NC). 10 uL of the supernatant were injected into a C18 2.5X50 column (Phenomex, Torrance, CA) with a mobile phase composed of 0.1% formic acid in water (A) and acetonitrile (B) at a flow rate of 0.7ml/min for a complete run time of 2 minutes. The initial mobile phase gradient started at A: B 90:10 then changed to 10:90 for 1 minute before switching back to 90:10 for the last 20 seconds of the run. Multiple reaction monitoring (MRM) was optimized for each compound before detection and quantification (Supplemental Table 5). MS/MS was completed via Applied Biosystem DS/Sciex API 4000 triple quadrupole mass spectrometer (Foster City, CA) in positive ion mode.

Calculations

The half-life ($t_{1/2}$) and CL_{rCYP} were calculated if the substrate depletion was >20% by 30 minutes[139]. Data were plotted as a percent remaining based on time point zero. A minimum of 3 time points was used for all regression analyses, and a regression criterion of R^2 >0.9 implemented. The percent of the substrate remaining was calculated based on the substrate peak area/IS peak area for all time points using T=0 as 100% as previously described[57]. Non-linear regression fitting to an exponential function produced the rate constant (*k*) for the parent compound (Eqn 10).

Equation 10

$$\%\ substrate\ remaining = Ax \times e^{-kt}$$

$$t_{1/2} = -\frac{\ln(2)}{k}$$

Where *Ax* represents the back extrapolated substrate concentration in the incubation media. CL_{rCYP} can be estimated to by using the rate of parent loss [57,225] (Eqn 11).

Equation 11

$$\mathrm{CL}_{rCYP} = \frac{0.693}{t_{1/2}} \times \frac{mL\ incubation}{[pmol\ rCYP]}$$

Where the standard concentration of rCYP/mL incubation was 50 pmol/mL, unless the substrate had to be diluted down to 25 pmol/mL or 12.5 pmol/ mL.

Statistical Analysis

Descriptive statistics included the average CL_{rCYP} ± standard deviation (SD) reported for each rCYP. The literature was also scoured for any data regarding human isoforms with reported influence on substrate metabolism for comparison between the two species.

Results

The CL_{rCYP} for a given substrate ranged from no change to a CL_{rCYP} >4.62 mL/min/pmol for a given rCYP (Table 11). Only metoclopramide and alprazolam were metabolized by a single isoform, rCYP2D15 and rCYP3A26 respectively. The CL_{rCYP} in the benzodiazepine family varied widely, with minimal CL_{rCYP} of alprazolam by only rCYP3A26 and rapid CL_{rCYP} for both diazepam and midazolam. A two-fold dilution of rCYP2B11 for diazepam and rCYP3A12 for midazolam was necessary to calculate a CL_{rCYP} . The midazolam CL_{rCYP} profile involved different CYP isoforms and rates of clearance compared to alprazolam and diazepam, with CYP3A12 (requiring a four-fold dilution to 12.5 pmol/mL) followed by rCYP2B11, rCYP2C41, rCYP2D15, and rCYP3A26. The tricyclic antidepressants (TCA), amitriptyline and clomipramine, were metabolized by all rCYP except CYP3A26. The rCYP enzyme CL_{rCYP} pattern was similar between TCA, with both substrates requiring a two-fold decrease in the rCYP2C41 concentration (clomipramine and amitriptyline) and a four-fold decrease for rCYP2D15 concentration (clomipramine) to achieve three time points for calculations. A two-fold decrease in enzyme concentration of rCYP2B11 for desipramine was necessary to calculate a CL_{rCYP} .

Summation of the individual rCYP CL_{rCYP} shows that amitriptyline and clomipramine have the highest rate of CL_{rCYP}, followed by carvedilol, midazolam, desipramine, diazepam, and mirtazapine. The slowest rate of CL_{rCYP} included alprazolam and metoclopramide, along with phenacetin, cleared by rCYP1A2 and rCYP2C21, and vincristine, cleared by rCYP2B11 and rCYP3A12 (Figure 17).

Comparison between the reported human CYP isoforms involved in metabolism compared to the canine rCYP isoforms showed a wide variety of results. Clarithromycin is

reported to be an inhibitor in humans, but was a substrate for canine rCYP3A12, rCYP3A26 and rCYP1A1 (Table 12). In the canine, rCYP2B11 was involved in more CL_{rCYP} compared to the reports of human CYP involvement in the CL_{rCYP} of amitriptyline, clomipramine, desipramine, diazepam, loperamide, midazolam, mirtazapine, testosterone, and vincristine.

Discussion

This study emphasizes the differences in CYP metabolism across a wide variety of pharmaceuticals reported to be human CYP substrates or inhibitors. Five substrates required further rCYP dilution to calculate the substrate depletion $t_{1/2}$ and CL_{rCYP}. The majority of substrates were metabolized by a variety of rCYP, with only alprazolam and metoclopramide targeted by a single rCYP, but with minimal clearance. Pimobendan and phenacetin were cleared by two isoforms, with pimobendan only cleared by the rCYP1A isoforms and phenacetin cleared by rCYP1A2 and rCYP2C21. The clearance of phenacetin in this study by rCYP2C21 contradicts previous reports measuring the phenacetin metabolite 4-acetamidophenol, which reports clearance by rCYP1A1 and rCYP2D15 but not rCYP2C21[60]. Differences in experimental conditions between the experimental results and published reports include differences in the phenacetin drug concentration, which may result in an inhibitory effect at high concentrations or non-specific binding at low concentrations[60].

Three benzodiazepines were tested, each showing remarkable differences in individual rCYP clearance. While alprazolam was minimally cleared by rCYP3A26, midazolam and diazepam were extensively cleared by two different isoforms, rCYP3A12 and 3CYP2B11, respectively. These differences are likely due to variation in the chemical structure of the three drugs, and the same pattern is reflected in humans[171,178,183]. These three benzodiazepines are utilized for different treatments; midazolam and diazepam are used as pre-anesthetic sedatives are the treatment of active seizures. Midazolam cannot be orally administered due to low bioavailability, while alprazolam can be administered orally to aid in the management of behavioral problems.

Vincristine is a vinca alkaloid used for the treatment of variety of canine neoplasias. Reaction phenotyping indicates that the substrate is depleted by both CYP2B11 and CYP3A12, a contrast to previous vinblastine reaction phenotyping which reports metabolism by only CYP3A12[226]. Both vinca alkaloids are derived from the periwinkle plant (*Vinca rosea*), but have differences in efficacy, safety, and pharmacokinetics. Both drugs are transported by P-

glycoprotein, with vincristine reported to be more likely to produce neurotoxicity compared to vinblastine, hypothesized to be due to the slower clearance compared to vinblastine. This describes how small changes in the chemical structure can result in difference enzyme affinities but maintain clinical safety and efficacy[227].

Substrates reported to be cleared by rCYP2C41 include amitriptyline, carvedilol, clomipramine, cyclosporine, diazepam, midazolam, mirtazapine, sildenafil, testosterone, toceranib, and verapamil. Previous research has shown that CYP2C41 enzyme efficiency is lower than CYP2C21, and, overall, these results are consistent with the current study, with the exception of amitriptyline, clomipramine and cyclosporine[13,59,228]. Additional *in vivo* research is necessary to determine the pharmacokinetic and clinical impact of the presence of CYP2C41 on the metabolism of amitriptyline and clomipramine. These two drugs may be able to serve as markers to identify CYP2C41 within the canine population or require altered dosing if given to canines with the enzyme. In humans, the CYP2C family consists of four isozymes that account for the metabolism of 20% of drugs and are polymorphic. Whether canine CYP2C has this extensive involvement in drug metabolism remains unknown[229].

A wide variety of drugs used for a number of different diseases were phenotyped in this study. Disease states that utilize one or more of these drugs includes cardiac disease (carvedilol, pimobendan, sildenafil), neoplasia (toceranib, vincristine), immune-mediated (cyclosporine), seizures (diazepam, midazolam), infectious (clarithromycin, metronidazole, praziquantel), and behavioral (alprazolam, amitriptyline, clomipramine). In addition, drugs used to treat symptoms common in a variety of diseases were also phenotyped including anti-nausea medications (omeprazole, ondansetron), appetite stimulant medications (mirtazapine), and anti-diarrheal medications (loperamide). The chance of DDI interactions increases with concomitant use of these drugs, and additional *in vitro* and *in vivo* studies are necessary to improve dosing efficacy and safety.

This study described a rapid early screening of phenotype CYP isoforms involved in the metabolism of a given substrate. Using the metabolic stability assay provides a predicted CYP clearance, but does not take into account the variation in CYP isoform quantity nor enzyme efficiency[230]. Individual rCYP phenotyping provides a method to calculate the rate of clearance by an isoform. In the cases of alprazolam and metoclopramide, the results are straightforward, because only one isoform is involved in the metabolism of the compounds. However, when

multiple isoforms are involved, additional studies are required to determine the relative contribution of each isoform to the *in vivo* metabolism. This can be completed using specific antibodies (currently not commercially available) or combining the intrinsic clearance with the relative abundance of each isoform in the liver[222]. Quantification of CYP content in canine liver and intestine via LC/MS/MS has been reported for CYP1A2, CYP2B11, CYP2C21, CYP2D15, CYP2E1, CYP3A12 and CYP3A26. CYP3A12 was found to be the most abundant in the liver, followed by decreasing quantity of CYP2B11, CYP2D15, CYP2E1, CYP2C21, and CYP3A26. In the intestine, only CYP3A12 and CYP2B11 were quantifiable[70]. Additional research into specific canine CYP antibodies and CYP quantification is required to calculate the relative contribution of these CYP to the metabolism of substrates targeted by multiple isoforms.

Table 11: Reaction phenotyping of substrates

mL/min/pmol	CYP1A1	CYP1A2	CYP2B11	CYP2C21	CYP2C41	CYP2D15	CYP3A12	CYP3A26
Alprazolam	---	---	---	---	---	---	---	0.118 (0.003)
Amitriptyline	0.788 (0.047)	0.310 (0.028)	0.706 (0.099)	2.039 (0.383)	7.27*(0.57)	7.63* (0.67)	0.184 (0.066)	---
Carvedilol	2.000 (0.339)	1.263 (0.408)	---	0.527 (0.188)	0.301 (0.010)	2.675 (0.364)	0.603 (0.042)	0.280 (0.014)
Clarithromycin	---	0.124 (0.002)	0.140 (0.018)	---	---	---	0.563 (0.049)	0.223 (0.082)
Clomipramine	0.328 (0.034)	0.380 (0.045)	0.392 (0.035)	2.571 (0.764)	9.31# (0.43)	10.97# (0.95)	0.198 (0.033)	---
Cyclosporine	---	---	---	---	0.180 (0.039)	0.193 (0.047)	1.259 (0.241)	---
Desipramine	---	---	0.182 (0.037)	0.182 (0.304)	---	6.42* (0.75)	---	---
Diazepam	---	---	5.12* (0.30)	1.111 (0.131)	0.133 (0.007)	---	0.388 (0.06)	---
Loperamide	---	---	0.132 (0.014)	---	---	---	1.755 (0.16)	0.493 (0.159)
Metoclopramide	---	---	---	---	---	0.248 (0.079)	---	---
Midazolam	---	---	2.364 (0.335)	---	0.156 (0.068)	0.200 (0.101)	3.05* (0.65)	0.141 (0.043)
Mirtazapine	---	---	2.195 (0.121)	2.637 (0.344)	0.195 (0.014)	0.649 (0.060)	0.165 (0.027)	0.493 (0.159)
Omeprazole	0.129 (0.008)	---	---	---	---	---	0.550 (0.099)	0.481 (0.194)
Ondansetron	---	---	---	0.350 (0.042)	---	0.875 (0.153)	0.203 (0.019)	---
Phenacetin	---	0.283 (0.031)	---	0.164 (0.006)	---	---	---	---
Pimobendan	3.796 (0.564)	0.207 (0.019)	---	---	---	---	---	---
Praziqunatel	---	0.219 (0.103)	---	0.841 (0.090)	---	---	0.875 (0.133)	---
Sildenafil	---	0.165 (0.026)	---	---	0.243 (0.123)	0.423 (0.161)	3.393 (0.105)	---
Testosterone	---	---	0.782 (0.039)	4.163 (0.087)	0.317 (0.176)	0.152 (0.025)	0.243 (0.04)	---
Toceranib	0.196 (0.035)	---	---	---	0.237 (0.082)	0.884 (0.182)	---	0.172 (0.002)
Verapamil	---	---	---	---	0.244 (0.030)	1.079 (0.505)	3.544 (0.641)	0.157 (0.01)
Vincristine	---	---	0.318 (0.038)	---	---	---	0.146 (0.01)	---

Average(SD); --- indicates that there was no Cl_{int} calculated for that isoform due to lack of substrate depletion.* Dilution to 25 pmol/mL, # dilution to 12.5 pmol/mL.

Table 12: Human vs Canine Reaction Phenotyping

Drug	Human Cytochrome	Canine Cytochrome
Alprazolam	2C9, 2C19, 3A4[171]	3A26
Amitriptyline	2C19,2D6>2C9,1A2>3A4[172]	2C41,2D15>>2C21>>1A1>2B11 >1A2>3A12
Carvedilol	2D6>2C9>1A2,2C9, 2E1,3A4[173]	2D15>1A1>1A2>>3A12>2C21>3 A26
Clarithromycin	inhibitor	3A12>3A26>1A1
Clomipramine	1A2,3A4,2C19,2D6[174]	2C41,2D15>>2C21>>1A1,1A2,2 B11
Cyclosporine A	3A[176]	3A12>>2D15,2C41
Desipramine	2D6[177]	2D15>>2B11,2C21
Diazepam	2C19, 3A[178]	2B11>>2C21>>3A12>2C41
Loperamide	2B6, 2C8, 2D6, 3A4[181]	3A12>>3A26>2B11
Metoclopramide	2D6[182]	2D15
Midazolam	3A4, 3A5[183]	3A12>>2B11>>2D15,3A26
Mirtazapine	1A2, 2C8, 2C9,2D6, 3A4[184]	2B11,2C21>>2D15>3A26>3A12, 2C41
Omeprazole	2C19[185]	3A12>3A26>1A1
Ondansetron	1A2, 2D6, 3A[186]	2D15>2C21>3A12
Phenacetin	1A1, 1A2[187]	1A2>2C21
Pimobendan	1A2>3A4[188]	1A1>>1A2
Praziquantel	1A2, 2C19, 3A4[189]	3A12,2C21>1A2
Sildenafil	3A4> 2C9, 2C19> 2D6[190]	3A12>>2D15>2C41>1A2
Testosterone	2C19, 2C9, 3A4[191 192]	2C21>> 2B11>2C41>3A12>2D15
Toceranib	N/A	2D15>2C41>1A1, 3A26
Verapamil	3A4, 3A5, 2C8, 2E1[193]	3A12>>2D15>2C41>3A26
Vincristine	3A4, 3A5[194]	2B11>3A12

Comparison between the reported human CYP involved in the metabolism of substrates compared to the quantified canine CYP substrate depletion. >> indicates that the Cl_{int} for the isoform has a greater than 2-fold difference in clearance compared to the next isoform.

Supplemental Table 5: Individual compound multiple reaction monitoring (MRM) profile

Compound ID	Q1 *m/z*	Q3 *m/z*
Alprazolam	310.239	206.063
Amitriptyline	278.400	91.100
Carvedilol	407.200	100.200
Clarithromycin	749.500	158.000
Clomipramine	315.108	86.087
Cyclosporine	1202.639	425.168
Desipramine	267.200	72.000
Diazepam	286.140	194.129
Loperamide	477.100	266.100
Metoclopramide	300.124	227.041
Midazolam	327.091	222.980
Mirtazapine	266.100	195.000
Omeprazole	346.079	198.083
Ondansetron	294.112	170.077
Phenacetin	180.100	110.000
Pimobendan	335.000	206.000
Praziquantel	313.185	203.092
Sildenafil	475.200	100.100
Testosterone	289.500	109.200
Toceranib	397.200	283.000
Verapamil	454.800	165.100
Vincristine	825.198	765.028
CP-424391*	768	486

*Internal standard

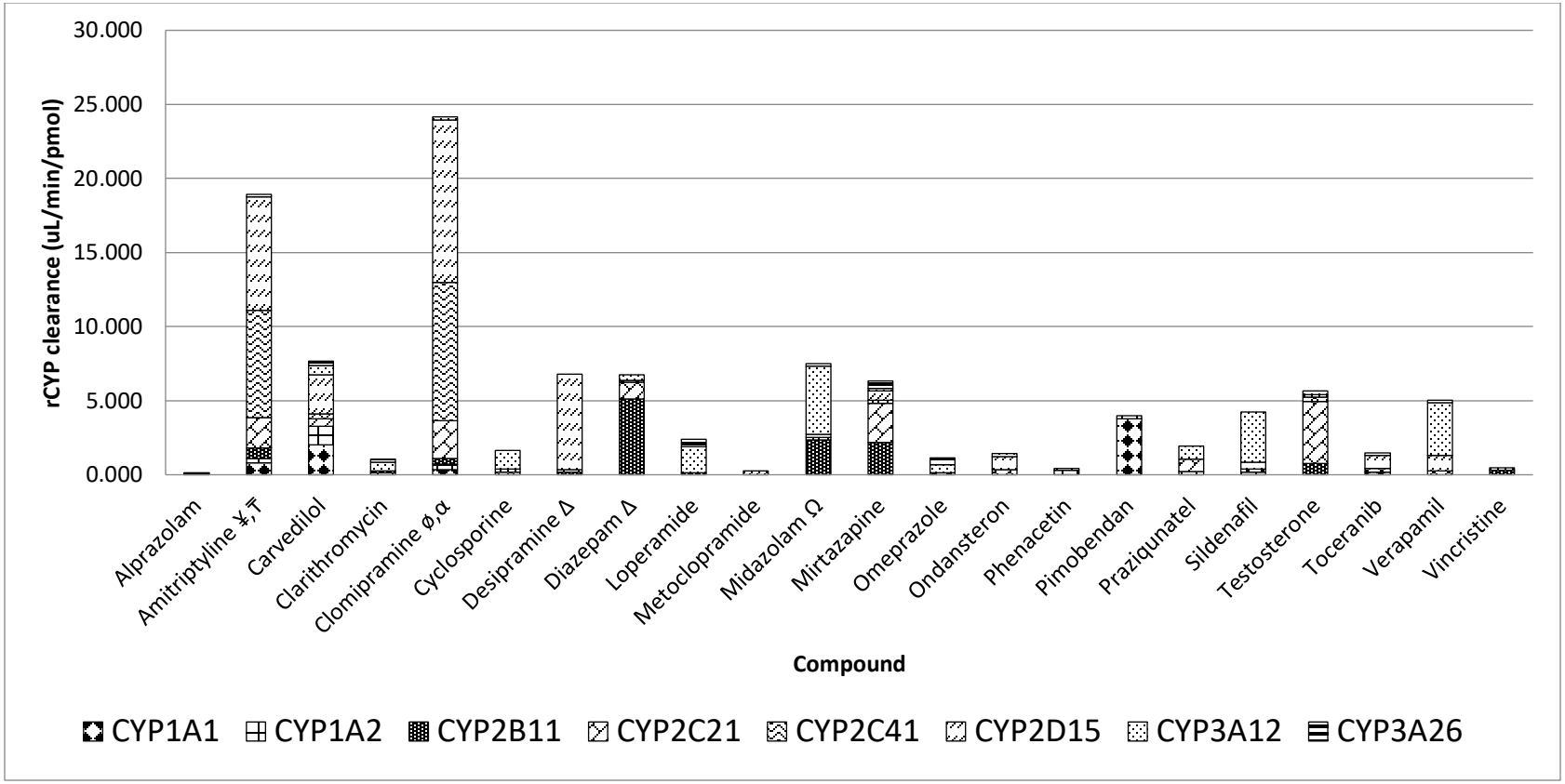

Figure 17: Summation of clearance by the individual rCYP for each compound.

¥ indicates rCYP2C41 dilution to 25 pmol; Ω indicates rCYP3A12 dilution to 25 pmol; Δ indicates rCYP2B11 dilution to 25 pmol; ₸ indicates rCYP2D15 dilution to 25 pmol; α indicates rCYP2D15 dilution to 12.5 pmol; ø indicates rCYp2C41 dilution to 12.5 pmol.

Chapter 6: Summary and Future Directions

Summary

This body of research utilized two difference approaches to describe expression and metabolic differences between the canine and feline CYP profile. A comparison between the canine and feline transcriptome at three sites important for drug metabolism (lung, liver and duodenum) identified differences that can have a significant influence on the pharmacokinetics between and within species. The makeup of the liver transcriptome "pie" is distinct between the two species, with *CYP2E2* estimated to make up 31% of the feline liver transcriptome compared to 54% of *CYP2E1* in the canine liver. In the canine liver, *CYP2C21, 2A13, 3A26, 2D15* and *2B11* are the highest expressed, compared to *CYP2A13, 3A132, 2D6* and *3A131* in the feline liver. In the duodenum of these two species, *CYP3A12* (dog) and *CYP3A132* (cat) are the highest expressed isoforms. The two species diverge at the second highest expressed, with *CYP2B11* the highest in the dog, while *CYP2C41* is the highest expressed in the feline and *CYP2B6* is the fifth highest expressed. LC/MS/MS of canine intestine report that CYP2B11 and CYP3A12 were quantifiable in the proximal intestine[70,147]. There are no reports of feline CYP intestinal quantification for comparison. Two *CYP2C* isoforms were identified in the feline transcriptome. The isoforms were identified by the canine annotations *CYP2C21* and *CYP2C41*, since the canine CYP annotations were used for the initial identification of feline CYP. The liver CYP transcriptome variation is also reflected in a comparison of the rate of substrate depletion. Of the 30 substrates evaluated, the intrinsic microsomal clearance (CL_{int}) varied from 2-10 fold. The microsomal protein binding and plasma protein binding were added to calculate the predicted hepatic clearance using both the well-stirred ($CL_{hep,ws}$) and parallel-tube models ($CL_{hep,pt}$). Canine liver microsomes had a faster rate of clearance overall, ranging from 2-20 fold. Using recombinant CYP (rCYP) phenotyping, the isoforms involved in the metabolism of 22 substrates were described. Within the benzodiazepine family, the isoform affinity varied, with alprazolam barely metabolized by CYP3A26, diazepam primarily metabolized by CYP2B11 and midazolam metabolism relying on CYP3A12. These differences are reflected in the liver microsomes, with a lack of CYP2B6 in the feline resulting in an almost 10-fold difference in CL_{hep}. A comparison between the isoforms in humans and canines indicates that CYP2B11 is utilized more frequently in the canine compared to human. In addition, the CYP2C41 isoform has an extensive

involvement in the metabolism of the tricyclic antidepressants, amitriptyline and clomipramine. This isoform is present in a minority of dogs and requires further studies. The use of metabolite studies combined with liver microsome studies is necessary to determine the contribution of individual isoforms to the overall clearance, and will improve drug-drug interaction predictions and the design of safer, effective dosing intervals. The differences reported in the canine rCYP profile indicates that caution should be used when applying human CYP profiles to both cat and dog, and the need for species-specific studies.

Future Research Directions

Further exploration of feline CYP protein expression and function

The sequencing of feline CYP2C isoforms and protein expression and quantification are necessary to complete the xenobiotic feline CYP profile. If both CYP2C isoforms are present in the liver and intestine, CYP2C substrates may be metabolized faster compared to the canine. A feline CYP "pie" is necessary for the feline, extending beyond the liver to include intestine and lung to determine differences between the two species. In addition, the development of feline rCYP to compare to the canine rCYP substrate depletion profile will advance our understanding of the differences in substrate affinity between the species.

Identifying the frequency and implication of cytochrome P450 variants in the canine and feline populations.

Polymorphisms can have a significant effect on the rate of drug metabolism. The impact that these mutations will have on affected dogs requires further study, since the impact of these SNP has only been studied in a limited number of breeds. Polymorphisms have also been reported in CYP2D15, CYP2E1 and CYP3A12. The *in vivo* effect of these polymorphisms remains unknown[13], and no CYP polymorphisms have been reported in the feline. In order to address these additional questions, the selection of *in vivo* probes, genome sequencing and the development of rCYP with the SNP can be used.

References

1. Paine SW, Menochet K, Denton R, et al. Prediction of human renal clearance from preclinical species for a diverse set of drugs that exhibit both active secretion and net re-absorption. Drug Metab Disposition 2011:dmd. 110.037267.

2. Kebamo S, Tesema S, Geleta B. The Role of Biotransformation in Drug Discovery and Developement. J Drug Metab Toxicol 2015;6:196-209.

3. Baier F, Copp JN, Tokuriki N. Evolution of Enzyme Superfamilies: Comprehensive Exploration of Sequence-Function Relationships. Biochemistry 2016;55:6375-6388.

4. Guengerich FP, Waterman MR, Egli M. Recent structural insights into cytochrome P450 function. Trends Pharmacol Sci 2016;37:625-640.

5. Nelson DR. Cytochrome P450 and the individuality of species. Arch Biochem Biophys 1999;369:1-10.

6. Nelson DR. Cytochrome P450 Nomenclature, 2004. In: Cytochrome P450 protocolsSpringer; 2006:1-10.

7. Guengerich FP. Intersection of the Roles of Cytochrome P450 Enzymes with Xenobiotic and Endogenous Substrates: Relevance to Toxicity and Drug Interactions. Chem Res Toxicol 2017;30:2-12.

8. Drug Development and Drug Interactions: Table of Substrates, Inhibitors and Inducers. In: U.S Food and Drug Administration.

9. Prueksaritanont T, Chu X, Gibson C, et al. Drug-drug interaction studies: regulatory guidance and an industry perspective. AAPS J 2013;15:629-645.

10. Patricelli AJ, Hardie RJ, McAnulty JE. Cyclosporine and ketoconazole for the treatment of perianal fistulas in dogs. J Am Vet Med Assoc 2002;220:1009-1016.

11. Dahlinger J, Gregory C, Bea J. Effect of ketoconazole on cyclosporine dose in healthy dogs. Vet Surg 1998;27:64-68.

12. Orito K, Saito M, Fukunaga K, et al. Pharmacokinetics of zonisamide and drug interaction with phenobarbital in dogs. J Vet Pharmacol Ther 2008;31:259-264.

13. Court MH. Canine Cytochrome P450 (CYP) Pharmacogenetics. Vet Clin North Am Small Anim Pract 2013;43:1027-1038.

14. Zanger UM, Schwab M. Cytochrome P450 enzymes in drug metabolism: Regulation of gene expression, enzyme activities, and impact of genetic variation. Pharmacology and Therapeutics 2013;138:103-141.

15. Nelson DR. The cytochrome p450 homepage. Hum Genomics 2009;4:59-65.

16. Mac Munn CA. Researches on Myohaematin nad the Histohaematins. Phil Tans R Soc 1886;177:267-298.

17. Hartree EF. Obituary Notice: David Keilin (1887-1963). Biochem J 1963;89:1-5.

18. Brodie BB, Axelrod J, Cooper JR, et al. Detoxication of drugs and other foreign compounds by liver microsomes. Science 1955;121:603-604.

19. Omura T, Sato R. The Carbon Monoxide-Binding Pigment of Liver Microsomes. I. Evidence for Its Hemoprotein Nature. J Biol Chem 1964;239:2370-2378.

20. Omura T, Sato R. The Carbon Monoxide-Binding Pigment of Liver Microsomes. Ii. Solubilization, Purification, and Properties. J Biol Chem 1964;239:2379-2385.

21. Meunier B, de Visser SP, Shaik S. Mechanism of Oxidation Reactions Catalyzed by Cytochrome P450 Enzymes Chem Rev 2007;104:3947-3980.

22. Dempsey DA, St Helen G, Jacob P, 3rd, et al. Genetic and pharmacokinetic determinants of response to transdermal nicotine in white, black, and Asian nonsmokers. Clin Pharmacol Ther 2013;94:687-694.

23. Bachanova V, Shanley R, Malik F, et al. Cytochrome P450 2B6*5 Increases Relapse after Cyclophosphamide-Containing Conditioning and Autologous Transplantation for Lymphoma. Biol Blood Marrow Transplant 2015;21:944-948.

24. Ingelman-Sundberg M, Sim SC, Gomez A, et al. Influence of Cytochrome P450 Polymorphisms on Drug Therapies: Pharmacogenetic, Pharmacoepigenetic and Clinical Aspects. Pharmacology & Therapeutics 2007;116:496-526.

25. Zhou Y, Ingelman-Sundberg M, Lauschke VM. Worldwide Distribution of Cytochrome P450Alleles: A Meta-analysis of Population-scaleSequencing Projects. Clin Pharmacol Ther 2017;102:688-700.

26. Reis-Pardal J, Rodrigues A, Rodrigues E, et al. Comparing cytochrome P450 pharmacogenetic information available on United States drug labels and European Union Summaries of Product Characteristics. Pharmacogenomics J 2017;17:488-493.

27. Martinez MN, Antonovic L, Court M, et al. Challenges in Exploring the Cytochrome P450 System as a Source of Variation in Canine Drug Pharmacokinetics. Drug Metab Rev 2013;45:218-230.

28. Nilsen BM, Berg K, Goksoyr A. Induction of cytochrome P450 1A (CYP1A) in fish. A biomarker for environmental pollution. Methods Mol Biol 1998;107:423-438.

29. Kennedy SW, Jones SP, Elliott JE. Sensitivity of bald eagle (Haliaeetus leucocephalus) hepatocyte cultures to induction of cytochrome P4501A by 2,3,7,8-tetrachlorodibenzo-p-dioxin. Exotoxicology 2003;12:163-170.

30. Mary VS, Valdehita A, Navas JM, et al. Effects of aflatoxin B_1, fumonisin B_1 and their mixture on the aryl hydrocarbon receptor and cytochrome P450 1A induction. Food Chem Toxicol 2015;75:104-111.

31. Okamatsu G, Komatsu T, Ono Y, et al. Characterization of feline cytochrome P450 2B6. Xenobiotica 2017;47:93-102.

32. Tanaka N, Shinkyo R, Sakaki T, et al. Cytochrome P450 2E polymorphism in feline liver. Biochim Biophys Acta 2005;1726:194-205.

33. Roussel F, Duignan DB, Lawton MP, et al. Expression and characterization of canine cytochrome P450 2D15. Arch Biochem Biophys 1998;357:27-36.

34. Honda K, Komatsu T, Koyama F, et al. Expression of two novel cytochrome P450 3A131 and 3A132 in liver and small intestine of domestic cats. J Vet Med Sci 2011;73:1489-1492.

35. Okamatsu G, Komatsu T, Kubota A, et al. Identification and functional characterization of novel feline cytochrome P450 2A. Xenobiotica 2015;45:503-510.

36. Komatsu T, Honda K, Kubota A, et al. Molecular cloning and expression of cytochrome P450 2D6 in the livers of domestic cats. J Vet Med Sci 2010;72:1633-1636.

37. Hubbard T, Barker D, Birney E, et al. The Ensembl genome database project. Nucleic Acids Res 2002;30:38-41.

38. Pruitt KD, Tatusova T, Maglott DR. NCBI Reference Sequence (RefSeq): a curated non-redundant sequence database of genomes, transcripts and proteins. Nucleic Acids Res 2005;33:D501-504.

39. NCBI. Eukaryotic Genome Annotation at NCBI. In: 2016.

40. Simao FA, Waterhouse RM, Ioannidis P, et al. BUSCO: assessing genome assembly and annotation completeness with single-copy orthologs. Bioinformatics 2015;31:3210-3212.

41. Aken BL, Ayling S, Barrell D, et al. The Ensembl gene annotation system. Database (Oxford) 2016;2016.

42. Jensen RA. Orthologs and paralogs- we need to get it right. Genome Biol 2001;2.

43. Koonin EV. Orthologs, paralogs, and evolutionary genomics. Annu Rev Genet 2005;39:309-338.

44. Mardis ER. Next-generation DNA sequencing methods. Annu Rev Genomics Hum Genet 2008;9:387-402.

45. Ansorge WJ. Next-generation DNA sequencing techniques. N Biotechnol 2009;25:195-203.

46. Koboldt DC, Steinberg KM, Larson DE, et al. The next-generation sequencing revolution and its impact on genomics. Cell 2013;155:27-38.

47. Reuter JA, Spacek DV, Snyder MP. High-throughput sequencing technologies. Mol Cell 2015;58:586-597.

48. Ozsolak F, Milos PM. RNA sequencing: advances, challenges and opportunities. Nat Rev Genet 2011;12:87-98.

49. Tenmizu D, Endo Y, Noguchi K, et al. Identification of the novel canine CYP1A2 1117 C > T SNP causing protein deletion. Xenobiotica 2004;34:835-846.

50. Atherton M, Braceland M, Harvie J, et al. Characterisation of the normal canine serum proteome using a novel electrophoretic technique combined with mass spectrometry. The Veterinary Journal 2013;196:315-319.

51. Brandt LE, Ehrhart EJ, Scherman H, et al. Characterization of the canine urinary proteome. Vet Clin Pathol 2014;43:193-205.

52. Lacerda CM, Disatian S, Orton EC. Differential protein expression between normal, early-stage, and late-stage myxomatous mitral valves from dogs. PROTEOMICS-Clinical Applications 2009;3:1422-1429.

53. Klopfleisch R, Klose P, Weise C, et al. Proteome of metastatic canine mammary carcinomas: similarities to and differences from human breast cancer. J Proteome Res 2010;9:6380-6391.

54. Ferlizza E, Campos A, Neagu A, et al. The effect of chronic kidney disease on the urine proteome in the domestic cat (Felis catus). Vet J 2015;204:73-81.

55. Jia L, Liu X. The conduct of drug metabolism studies considered good practice (II): in vitro experiments. Curr Drug Metab 2007;8:822-829.

56. Asha S, Vidyavathi M. Role of human liver microsomes in in vitro metabolism of drugs-a review. Appl Biochem Biotechnol 2010;160:1699-1722.

57. Obach RS. Prediction of human clearance of twenty-nine drugs from hepatic microsomal intrinsic clearance data: An examination of in vitro half-life approach and nonspecific binding to microsomes. Drug Metab Dispos 1999;27:1350-1359.

58. Brandon EF, Raap CD, Meijerman I, et al. An update on in vitro test methods in human hepatic drug biotransformation research: pros and cons. Toxicol Appl Pharmacol 2003;189:233-246.

59. Shou M, Norcross R, Sandig G, et al. Substrate specificity and kinetic properties of seven heterologously expressed dog cytochromes p450. Drug Metab Dispos 2003;31:1161-1169.

60. Locuson CW, Ethell BT, Voice M, et al. Evaluation of Escherichia coli membrane preparations of canine CYP1A1, 2B11, 2C21, 2C41, 2D15, 3A12, and 3A26 with coexpressed canine cytochrome P450 reductase. Drug Metab Dispos 2009;37:457-461.

61. Okamatsu G, Kawakami K, Komatsu T, et al. Functional expression and comparative characterization of four feline P450 cytochromes using fluorescent substrates. Xenobiotica 2017;47:951-961.

62. Baratta MT, Zaya MJ, White JA, et al. Canine CYP2B11 Metabolizes and is Inhibited by Anesthetics Agents Often Co-Administered in Dogs. J Vet Pharmacol Ther 2009;33:50-55.

63. Aidasani D, Zaya MJ, Malpas PB, et al. In Vitro Drug-Drug Interaction Screens for Canine Veterinary Medicine: Evaluation of Cytochrome P450 Reversible Inhibition. Drug Metabalism and Disposition 2008;36:1512-1518.

64. Ryu JY, Song IS, Sunwoo YE, et al. Development of the "Inje cocktail" for High-throughput Evaluation of Five Human Cytochrome P450 Isoforms In Vivo. Clin Pharmacol Ther 2007;82:531-540.

65. Sakai C, Iwano S, Yamazaki Y, et al. Species Difference in the Pharmacokinetic Parameters of Cytochrome P450 Probe Substrates between Experimental Animals, such as Mice, Rats, Dogs, Monkeys, and Microminopigs, and Humans J Drug Metab Toxicol 2014;5.

66. Nishimuta H, Nakagawa T, Nomura N, et al. Species Differences in Hepatic and Intestinal Metabolic Activities for 43 Human Cytochrome P450 Substrates between Humans and Rats or Dogs. Xenobiotica 2013;43:948-955.

67. Shah SS, Sanda S, Regmi NL, et al. Characterization of cytochrome P450-mediated drug metabolism in cats. J Vet Pharmacol Ther 2007;30:422-428.

68. Chauret N, Gauthier A, Martin J, et al. In Vitro Comparison of Cytochrome P450-Mediated metabolic Acivtities in Human, Dog, Cat, and Horse. Drug Metab Disp 1997;25:1130-1136.

69. van Beusekom CD, Schipper L, Fink-Gremmels J. Cutochrome P45-mediated Hepatic Metabolism of New Fluorescent Substrates in Cats and Dogs. J Vet Pharmacol Therap 2010;33:519-527.

70. Heikkinen AT, Friedlein A, Lamerz J, et al. Mass spectrometry-based quantification of CYP enzymes to establish in vitro/in vivo scaling factors for intestinal and hepatic metabolism in beagle dog. Pharm Res 2012;29:1832-1842.

71. Martinez MN, Antonovic L, Court M, et al. Challenges in exploring the cytochrome P450 system as a source of variation in canine drug pharmacokinetics. Drug Metab Rev 2013;45:218-230.

72. Regmi NL, Abd El-Aty AM, Kubota R, et al. Effect of Ofloxacin on Theophylline Pharmacokinetics at Clinical Dosage in Dogs. J Vet Pharmacol Ther 2006;29:403-408.

73. Regmi NL, Abd El-Aty AM, Kuroha M, et al. Inhibitory Effect of Several Fluoroquinolones on Hepatic Microsomal Cytochrome P450 1A Activities in Dogs. J Vet Pharmacol Ther 2005;28:553-557.

74. Tanaka N, Miyasho T, Shinkyo R, et al. cDNA cloning and characterization of feline CYP1A1 and CY1A2. Life Sci 2006;26:2463-2473.

75. Perez TE, Mealey KL, Grubb TL, et al. Tramadol Metabolism to O-Desmethyl Tramadol (M1) and N-Desmethyl Tramadol (M2) by Dog Liver Microsomes: Species Comparison and Identification of Responsible Canine Cytochrome P450s. Drug Metab Disposition 2016;44:1963-1972.

76. Mills BM, Zaya MJ, Walters RR, et al. Current cytochrome P450 phenotyping methods applied to metabolic drug-drug interaction prediction in dogs. Drug Metab Dispos 2010;38:396-404.

77. Mise M, Yadera S, Matsuda M, et al. Polymorphic expression of CYP1A2 leading to interindividual variability in metabolism of a novel benzodiazepine receptor partial inverse agonist in dogs. Drug Metab Dispos 2004;32:240-245.

78. Scherr MC, Lourenco GJ, Albuquerque DM, et al. Polymorphism of cytochrome P450 A2 (CYP1A2) in pure and mixed breed dogs. J Vet Pharmacol Ther 2011;34:184-186.

79. Aretz JS, Geyer J. Detection of the CYP1A2 1117C>T Polymorphism in 14 Dog Breeds. J Vet Pharmacol Ther 2010;34:98-100.

80. Mise M, Hashizume T, Komuro S. Characterization of Susbtrate Specificity of Dog CYP1A2 Using CYP1A2-Deficient and Wild-Type Dog Liver Microsomes. Drug Metab Dispos 2008;36:1903-1908.

81. Locuson CW, Williams P, Adcock JM, et al. Evaluation of Tizanidine as a Marker of Canine CYP1A2 Activity. J Vet Pharmacol Ther 2016;39:122-130.

82. Intorre L, Mengozzi G, Maccheroni M, et al. Enrofloxacin-theophylline interaction: influence of enrofloxacin on theophylline steady-state pharmacokinetics in the beagle dog. J Vet Pharmacol Ther 1995;18:352-356.

83. Hirt R, Teinfalt M, Dederichs D, et al. The effect of orally administered marbofloxacin on the pharmacokinetics of theophylline. Transbound Emerg Dis 2003;50:246-250.

84. Papich MG. Drugs that Affect the Respiratory System. In: Riviere JE, Papich MG, eds. Veterinary Pharmacology and Therapeutics, 9th ed. Ames, Iowa: Wiley-Blackwell:1295-1311.

85. Heikkinen AT, Friedlein A, Lamerz J, et al. Mass Spectrometry-Based Quantification of CYP Enzymes to Establish In Vitro/In Vivo Scaling Factors for Intestinal and Hepatic Metabolism in Beagle Dogs Pharm Res 2012;29:183-1842.

86. Zoran DL, Ridesel DH, Dyer DC. Pharmacokinetics of Propofol in Mixed-bree Dogs and Greyhounds. Am J Vet Res 1993;54:755-760.

87. Hay Kraus BL, Greenblatt DJ, Venkatakrishnan K, et al. Evidence for propofol hydroxylation by cytochrome P4502B11 in canine liver microsomes: breed and gender differences. Xenobiotica 2000;30:575-588.

88. Zonca A, Ravasio G, Gallo M, et al. Pharmacokinetics of ketamine and propofol combination administered as ketofol via continuous infusion in cats. J Vet Pharmacol Ther 2012;35:580-587.

89. Graham RA, Tyler LO, Krol WL, et al. Temporal kinetics and concentration-response relationships for induction of CYP1A, CYP2B, and CYP3A in primary cultures of beagle dog hepatocytes. J Biochem Mol Toxicol 2006;20:69-78.

90. van Beusekom CD, van den Heuvel JJ, Koenderink JB, et al. Feline hepatic biotransformation of diazepam: Differences between cats and dogs. Res Vet Sci 2015;103:119-125.

91. Blaisdell J, Goldstein JA, Bai SA. Isolation of a New Canine Cytochrome P450 cDNA from the Cytochrome P450 2C Subfamily (CYP2C41) and Evidence for Polymorphic Differences in its Expression. Drug Metab Dispos 1998;26:278-283.

92. Tasaki T, Nakamura A, Itoh S, et al. Expression and Characterization of Dog CYP2D15 Using Baculovirus Expression System. The Journal of Biochemistry 1998;123:162-168.

93. Pedersen RS, Damkier P, Brosen K. Tramadol as a new probe for cytochrome P450 2D6 phenotyping: a population study. Clin Pharmacol Ther 2005;77:458-467.

94. Komatsu T, Honda K, Kubota A, et al. Molecular Cloning and Expression of Cytochrome P450 2D6 in the Livers of Domestic Cats. J Vet Med Sci 2010;72:1633-1636.

95. Zanger UM, Raimundo S, Eichelbaum M. Cytochrome P450 2D6: overview and update on pharmacology, genetics, biochemistry. Naunyn-Schmiedeberg's Arch Pharmacol 2004;369:23-37.

96. Mealy KL, Jabbes M, Spencer E, et al. Differential Expression of CYP3A12 and CYP3A26 mRNAs in Canine Liver and Intestine. Xenobiotica 2008;38:1305-1312.

97. Fraser DJ, Feyereisen R, Harlow GR, et al. Isolation, heterologous expression and functional characterization of a novel cytochrome P450 3A enzyme from a canine liver cDNA library. J Pharmacol Exp Ther 1997;283:1425-1432.

98. Zanger UM, Schwab M. Cytochrome P450 enzymes in drug metabolism: regulation of gene expression, enzyme activities, and impact of genetic variation. Pharmacol Ther 2013;138:103-141.

99. Danielson PB. The cytochrome P450 superfamily: biochemistry, evolution and drug metabolism in humans. Curr Drug Metab 2002;3:561-597.

100. Blaisdell J, Goldstein JA, Bai SA. Isolation of a new canine cytochrome P450 CDNA from the cytochrome P450 2C subfamily (CYP2C41) and evidence for polymorphic differences in its expression. Drug Metab Dispos 1998;26:278-283.

101. Trepanier LA. Cytochrome P450 and its role in veterinary drug interactions. Vet Clin North Am Small Anim Pract 2006;36:975-985, v.

102. Chen G, Wang C, Shi T. Overview of available methods for diverse RNA-Seq data analyses. Sci China Life Sci 2011;54:1121-1128.

103. Marguerat S, Bahler J. RNA-seq: from technology to biology. Cell Mol Life Sci 2010;67:569-579.

104. Consortium SM-I. A comprehensive assessment of RNA-seq accuracy, reproducibility and information content by the Sequencing Quality Control Consortium. Nat Biotechnol 2014;32:903-914.

105. Stefaniuk M, Ropka-Molik K, Piórkowska K, et al. Analysis of polymorphisms in the equine MSTN gene in Polish populations of horse breeds. Livestock Science 2016;187:151-157.

106. Wickramasinghe S, Rincon G, Islas-Trejo A, et al. Transcriptional profiling of bovine milk using RNA sequencing. BMC Genomics 2012;13:45.

107. Rojas CAA, Ansell BR, Hall RS, et al. Transcriptional analysis identifies key genes involved in metabolism, fibrosis/tissue repair and the immune response against Fasciola hepatica in sheep liver. Parasites & vectors 2015;8:124.

108. Mooney M, Bond J, Monks N, et al. Comparative RNA-Seq and microarray analysis of gene expression changes in B-cell lymphomas of Canis familiaris. PLoS One 2013;8:e61088.

109. Paulson SK, Engel L, Reitz B, et al. Evidence for polymorphism in the canine metabolism of the cyclooxygenase 2 inhibitor, celecoxib. Drug Metab Dispos 1999;27:1133-1142.

110. Ashurst JL, Collins JE. Gene annotation: prediction and testing. Annu Rev Genomics Hum Genet 2003;4:69-88.

111. Curwen V, Eyras E, Andrews TD, et al. The Ensembl automatic gene annotation system. Genome research 2004;14:942-950.

112. Mortazavi A, Williams BA, McCue K, et al. Mapping and quantifying mammalian transcriptomes by RNA-Seq. Nat Methods 2008;5:621-628.

113. Fleming I. Cytochrome p450 and vascular homeostasis. Circ Res 2001;89:753-762.

114. Pikuleva IA. Cytochrome P450s and cholesterol homeostasis. Pharmacol Ther 2006;112:761-773.

115. Sikka R, Magauran B, Ulrich A, et al. Bench to bedside: Pharmacogenomics, adverse drug interactions, and the cytochrome P450 system. Acad Emerg Med 2005;12:1227-1235.

116. Haller S, Schuler F, Lazic SE, et al. Expression profiles of metabolic enzymes and drug transporters in the liver and along the intestine of beagle dogs. Drug Metab Dispos 2012;40:1603-1610.

117. Gaedigk A, Simon S, Pearce R, et al. The CYP2D6 activity score: translating genotype information into a qualitative measure of phenotype. Clin Pharmacol Ther 2008;83:234-242.

118. Schwanhausser B, Busse D, Li N, et al. Global quantification of mammalian gene expression control. Nature 2011;473:337-342.

119. Lu P, Singh SB, Carr BA, et al. Selective inhibition of dog hepatic CYP2B11 and CYP3A12. J Pharmacol Exp Ther 2005;313:518-528.

120. Visser M, Weber K, Rincon G, et al. Use of RNA-seq to determine variation in canine cytochrome P450 mRNA expression between blood, liver, lung, kidney and duodenum in healthy beagles. J Vet Pharmacol Ther 2017:1-8.

121. Bogaards JJ, Bertrand M, Jackson P, et al. Determining the best animal model for human cytochrome P450 activities: a comparison of mouse, rat, rabbit, dog, micropig, monkey and man. Xenobiotica 2000;30:1131-1152.

122. Graham MJ, Bell AR, Crewe HK, et al. mRNA and protein expression of dog liver cytochromes P450 in relation to the metabolism of human CYP2C substrates. Xenobiotica 2003;33:225-237.

123. Lee JY, Lee SY, Lee K, et al. Determination of species-difference in microsomal metabolism of amitriptyline using a predictive MRM-IDA-EPI method. Chem Biol Interact 2015;229:109-118.

124. Honda K, Komatsu T, Koyama F, et al. Expression of two novel cytochrome P450 3A131 and 3A132 in liver and small intestine of domestic cats. Journal of Veterinary Medical Science 2011;73:1489-1492.

125. Komatsu T, Honda K, Kubota A, et al. Molecular cloning and expression of cytochrome P450 2D6 in the livers of domestic cats. Journal of Veterinary Medical Science 2010;72:1633-1636.

126. van Beusekom CD, Schipper L, Fink-Gremmels J. Cytochrome P450-mediated hepatic metabolism of new fluorescent substrates in cats and dogs. J Vet Pharmacol Ther 2010;33:519-527.

127. Ertl R, Klein D. Transcriptional profiling of the host cell response to feline immunodeficiency virus infection. Virology journal 2014;11:52.

128. Hong LZ, Li J, Schmidt-Kuntzel A, et al. Digital gene expression for non-model organisms. Genome Res 2011;21:1905-1915.

129. Xu X, Sun X, Hu XS, et al. Whole Genome Sequencing Identifies a Missense Mutation in HES7 Associated with Short Tails in Asian Domestic Cats. Sci Rep 2016;6:31583.

130. Lyons LA. 99 Lives Cat Whole Genome Sequencing Initiative Update, nearly there! In: Plant and Animal Genome XXIV Conference 2016.

131. Cunningham F, Amode MR, Barrell D, et al. Ensembl 2015. Nucleic Acids Res 2015;43:D662-669.

132. Kharasch ED, Stubbert K. Role of cytochrome P4502B6 in methadone metabolism and clearance. The Journal of Clinical Pharmacology 2013;53:305-313.

133. Okamatsu G, Kawakami K, Komatsu T, et al. Functional expression and comparative characterization of four feline P450 cytochromes using fluorescent substrates. Xenobiotica 2016:1-11.

134. Ekins S, Stresser DM, Williams JA. In vitro and pharmacophore insights into CYP3A enzymes. Trends on Pharmacological Sciences 2003:161-166.

135. Kimble B, Li KM, Valtchev P, et al. In vitro hepatic microsomal metabolism of meloxicam in koalas (Phascolarctos cinereus), brushtail possums (Trichosurus vulpecula), ringtail possums (Pseudocheirus peregrinus), rats (Rattus norvegicus) and dogs (Canis lupus familiaris). Comp Biochem Physiol C Toxicol Pharmacol 2014;161:7-14.

136. Kessler Y, Helfer-Hungerbuehler AK, Cattori V, et al. Quantitative TaqMan® real-time PCR assays for gene expression normalisation in feline tissues. BMC Mol Biol 2009;10:106.

137. Rendic S, Guengerich FP. Survey of Human Oxidoreductasees and Cytochrome P450 Enzymes Involved in the Metabolism of Xenobiotic and Naterual Chemicals. Chem Res Toxicol 2015;8:38-42.

138. Komura H, Kawase A, Iwaki M. Application of substrate depletion assay for early prediction of nonlinear pharmacokinetics in drug discovery: assessment of nonlinearity of metoprolol, timolol, and propranolol. J Pharm Sci 2005;94:2656-2666.

139. Jones HM, Houston JB. Substrate depletion approach for determining in vitro metabolic clearance: time dependencies in hepatocyte and microsomal incubations. Drug Metab Dispos 2004;32:973-982.

140. Locuson C, Williams P, Adcock J, et al. Evaluation of tizanidine as a marker of canine CYP1A2 activity. J Vet Pharmacol Ther 2016;39:122-130.

141. Aidasani D, Zaya MJ, Malpas PB, et al. In vitro drug-drug interaction screens for canine veterinary medicines: evaluation of cytochrome P450 reversible inhibition. Drug Metab Dispos 2008;36:1512-1518.

142. Pan LC, Carpino PA, Lefker BA, et al. Preclinical pharmacology of CP-424,391, an orally active pyrazolinone-piperidine [correction of pyrazolidinone-piperidine] growth hormone secretagogue. Endocrine 2001;14:121-132.

143. Austin RP, Barton P, Cockroft SL, et al. The influence of nonspecific microsomal binding on apparent intrinsic clearance, and its prediction from physicochemical properties. Drug Metab Dispos 2002;30:1497-1503.

144. Smith R, Jones RD, Ballard PG, et al. Determination of microsome and hepatocyte scaling factors for in vitro/in vivo extrapolation in the rat and dog. Xenobiotica 2008;38:1386-1398.

145. Kato R. Possible role of P-450 in the oxidation of drugs in liver microsomes. J Biochem 1966;59:574-583.

146. Greenway CV, Stark RD. Hepatic vascular bed. Physiol Rev 1971;51:23-65.

147. Heikkinen AT, Friedlein A, Matondo M, et al. Quantitative ADME proteomics–CYP and UGT enzymes in the Beagle dog liver and intestine. Pharm Res 2015;32:74-90.

148. Emoto C, Iwasaki K. Approach to Predict the Controbiution of Cytochrome P450 Enzymes to Drug Metablism in the Early Drug-Discovery Stage: The Effect of the Expression of Cytochrome b5 with Recombinant P450 Enzymes. Xenobiotica 2009:986-999.

149. Mise M, Hashizume T, Matsumoto S, et al. Identification of Non-Functional Allelic Variant og CYP1A2 in Dogs. Pharmacogenetics 2004;14:769-773.

150. Zhang HF, Wang HH, Gao N, et al. Physiological Content and Intrinsic Activities of 10 Cytochrome P450 Isoforms in Human Normal Liver Microsomes. J Pharmacol Exp Ther 2016;358:83-93.

151. Tavoloni N. Postnatal changes in hepatic microsomal enzyme activities in the puppy. Biol Neonate 1985;47:305-316.

152. Alberola J, Perez Y, Puigdemont A, et al. Effect of age on theophylline pharmacokinetics in dogs. Am J Vet Res 1993;54:1112-1115.

153. Renton KW. Cytochrome P450 regulation and drug biotransformation during inflammation and infection. Curr Drug Metab 2004;5:235-243.

154. Pichette V, Leblond FA. Drug metabolism in chronic renal failure. Curr Drug Metab 2003;4:91-103.

155. Rasool MF, Khalil F, Laer S. A physiologically based pharmacokinetic drug-disease model to predict carvedilol exposure in adult and paediatric heart failure patients by incorporating pathophysiological changes in hepatic and renal blood flows. Clin Pharmacokinet 2015;54:943-962.

156. Altamura AC, Moro AR, Percudani M. Clinical pharmacokinetics of fluoxetine. Clin Pharmacokinet 1994;26:201-214.

157. Mandour ME, el Turabi H, Homeida MM, et al. Pharmacokinetics of praziquantel in healthy volunteers and patients with schistosomiasis. Trans R Soc Trop Med Hyg 1990;84:389-393.

158. Sugihara N, Furuno K, Kita N, et al. The influence of increased plasma protein binding on the disposition of quinidine in turpentine-treated rats. Biol Pharm Bull 1993;16:63-67.

159. Mehrota N, Gupta M, Kovar A, et al. The Rold of Pharmacokinetics and Pharmacodynamics in Phosphodiesterase-5 Inhibitor Therapy. Int J Impot Res 2007;19:253-267.

160. Chao P, Uss AS, Cheng K. Use of intrinsic clearance for prediction of human hepatic clearance. Expert Opin Drug Metab Toxicol 2010;6:189-198.

161. Pang KS, Rowland M. Hepatic Clearance of Drugs . I. Theoretical Considerations of "Well-Stirred" Models and a "Parallel Tube" Model. Influence of Hepatic Blood Flow, Plasma and Blood Cell Binding, and the Hepatocellular Enzymatic Activity on Hepatic Drug Clearance. J Pharmacokinet Biopharm 1977:625-653.

162. Kuepfer L, Niederalt C, Wendl T, et al. Applied concepts in PBPK modeling: how to build a PBPK/PD model. CPT: pharmacometrics & systems pharmacology 2016;5:516-531.

163. van Beusekom CD, Fink-Gremmels J, Schrickx JA. Comparing the glucuronidation capacity of the feline liver with substrate-specific glucuronidation in dogs. J Vet Pharmacol Ther 2014;37:18-24.

164. Boothe DM. Principles of Drug Therapy, 2 edSaunders; 2012.

165. Boxenbaum H. Interspecies variation in liver weight, hepatic blood flow, and antipyrine intrinsic clearance: extrapolation of data to benzodiazepines and phenytoin. J Pharmacokinet Biopharm 1980;8:165-176.

166. Larson JA. Elimination of Glycerol as a Measure of Hepatic Blood Flow in the Cat. Acta Physiologic 1963:224-234.

167. Richardson PD, Withrington PG. Liver blood flow. I. Intrinsic and nervous control of liver blood flow. Gastroenterology 1981;81:159-173.

168. Ascenzi P, Fanalo G, Fasano M, et al. Clinical Relevance of Drug Binding to Plasma Proteins. J Mol Struct 2014;1077:4-13.

169. Toutain PL, Buosquet-Melou A. Free Drug Fraction vs Free Drug Concentration: A Matter of Frequenct Confusion. J Vet Pharmacol Therap 2002;25:460-463.

170. Colclough N, Ruston L, Wood JM, et al. Species differences in drug plasma protein binding. MedChemComm 2014;5:963-967.

171. Gorski JC, Jones DR, Hamman MA, et al. Biotransformation of alprazolam by members of the human cytochrome P4503A subfamily. Xenobiotica 1999;29:931-944.

172. Venkatakrishnan K, Greenblatt DJ, von Moltke LL, et al. Five distinct human cytochromes mediate amitriptyline N-demethylation in vitro: dominance of CYP 2C19 and 3A4. J Clin Pharmacol 1998;38:112-121.

173. Oldham HG, Clarke SE. In vitro identification of the human cytochrome P450 enzymes involved in the metabolism of R (+)-and S (−)-carvedilol. Drug Metab Disposition 1997;25:970-977.

174. Nielsen KK, Flinois JP, Beaune P, et al. The biotransformation of clomipramine in vitro, identification of the cytochrome P450s responsible for the separate metabolic pathways. J Pharmacol Exp Ther 1996;277:1659-1664.

175. Takada K, Arefayene M, Desta Z, et al. Cytochrome P450 pharmacogenetics as a predictor of toxicity and clinical response to pulse cyclophosphamide in lupus nephritis. Arthritis & Rheumatology 2004;50:2202-2210.

176. Watkins PB. The role of cytochromes P-450 in cyclosporine metabolism. J Am Acad Dermatol 1990;23:1301-1309; discussion 1309-1311.

177. Dahl ML, Iselius L, Alm C, et al. Polymorphic 2-hydroxylation of desipramine. A population and family study. Eur J Clin Pharmacol 1993;44:445-450.

178. Yasumori T, Nagata K, Yang SK, et al. Cytochrome P450 mediated metabolism of diazepam in human and rat: involvement of human CYP2C in N-demethylation in the substrate concentration-dependent manner. Pharmacogenetics 1993;3:291-301.

179. Trouchon T, Lefebvre S. A review of enrofloxacin for veterinary use. Open Journal of Veterinary Medicine 2016;6:40-58.

180. Lynch T, Price A. The effect of cytochrome P450 metabolism on drug response, interactions, and adverse effects. Am Fam Physician 2007;76:391-396.

181. Kim KA, Chung J, Jung DH, et al. Identification of cytochrome P450 isoforms involved in the metabolism of loperamide in human liver microsomes. Eur J Clin Pharmacol 2004;60:575-581.

182. Livezey MR, Briggs ED, Bolles AK, et al. Metoclopramide is metabolized by CYP2D6 and is a reversible inhibitor, but not inactivator, of CYP2D6. Xenobiotica 2014;44:309-319.

183. Wandel C, Böcker R, Böhrer H, et al. Midazolam is metabolized by at least three different cytochrome P450 enzymes. BJA: British Journal of Anaesthesia 1994;73:658-661.

184. Stormer E, von Moltke LL, Shader RI, et al. Metabolism of the antidepressant mirtazapine in vitro: contribution of cytochromes P-450 1A2, 2D6, and 3A4. Drug Metab Dispos 2000;28:1168-1175.

185. Andersson T, Miners JO, Veronese ME, et al. Identification of human liver cytochrome P450 isoforms mediating omeprazole metabolism. Br J Clin Pharmacol 1993;36:521-530.

186. Dixon CM, Colthup PV, Serabjit-Singh CJ, et al. Multiple forms of cytochrome P450 are involved in the metabolism of ondansetron in humans. Drug Metab Dispos 1995;23:1225-1230.

187. Tassaneeyakul W, Birkett DJ, Veronese ME, et al. Specificity of substrate and inhibitor probes for human cytochromes P450 1A1 and 1A2. J Pharmacol Exp Ther 1993;265:401-407.

188. Kuriya S, Ohmori S, Hino M, et al. Identification of cytochrome P-450 isoform(s) responsible for the metabolism of pimobendan in human liver microsomes. Drug Metab Dispos 2000;28:73-78.

189. Li X-Q, Björkman A, Andersson T, et al. Identification of human cytochrome P 450 s that metabolise anti-parasitic drugs and predictions of in vivo drug hepatic clearance from in vitro data. Eur J Clin Pharmacol 2003;59:429-442.

190. Warrington JS, Shader RI, von Moltke LL, et al. In vitro biotransformation of sildenafil (Viagra): identification of human cytochromes and potential drug interactions. Drug Metab Dispos 2000;28:392-397.

191. Yamazaki H, Shimada T. Progesterone and testosterone hydroxylation by cytochromes P450 2C19, 2C9, and 3A4 in human liver microsomes. Arch Biochem Biophys 1997;346:161-169.

192. Wang RW, Newton DJ, Scheri TD, et al. Human Cytochrome P450 3A4-Catalyzed Testosterone 6β-Hydroxylation and ErythromycinN-Demethylation. Drug Metab Disposition 1997;25:502-507.

193. Tracy TS, Korzekwa KR, Gonzalez FJ, et al. Cytochrome P450 isoforms involved in metabolism of the enantiomers of verapamil and norverapamil. Br J Clin Pharmacol 1999;47:545-552.

194. Dennison JB, Kulanthaivel P, Barbuch RJ, et al. Selective metabolism of vincristine in vitro by CYP3A5. Drug Metab Dispos 2006;34:1317-1327.

195. Norkus C, Rankin D, KuKanich B. Pharmacokinetics of intravenous and oral amitriptyline and its active metabolite nortryptyline in Greyhound dogs. In: Vet Anaesth Analg2015:1-10.

196. Arsenault WG, Boothe DM, Gordon SG, et al. Pharmacokinetics of carvedilol after intravenous and oral administration in conscious healthy dogs. Am J Vet Res 2005;66:2172-2176.

197. VilmGnyi E, Küng K, Riond JL, et al. Clarithromycin pharmacokinetics after oral administration with or without fasting in crossbred beagles. J Small Anim Pract 1996;37:535-539.

198. King JN, Maurer MP, Hotz RP, et al. Pharmacokinetics of clomipramine in dogs following single-dose intravenous and oral administration. Am J Vet Res 2000;61:74-79.

199. Warry E, Hansen RJ, Gustafson DL, et al. Pharmacokinetics of cyclophosphamide after oral and intravenous administration to dogs with lymphoma. J Vet Intern Med 2011;25:903-908.

200. D'Mello A, Venkataramanan R, Satake M, et al. Pharmacokinetics of the cyclosporine-ketoconazole interaction in dogs. Res Commun Chem Pathol Pharmacol 1989;64:441-454.

201. Boxenbaum H. Comparative pharmacokinetics of benzodiazepines in dog and man. J Pharmacokinet Biopharm 1982;10:411-426.

202. Kung K, Riond JL, Wanner M. Pharmacokinetics of enrofloxacin and its metabolite ciprofloxacin after intravenous and oral administration of enrofloxacin in dogs. J Vet Pharmacol Ther 1993;16:462-468.

203. Lebkowska-Wieruszewska B, Barsotti G, Lisowski A, et al. Pharmacokinetics and estimated bioavailability of grapiprant, a novel selective prostaglandin E2 receptor antagonist, after oral administration in fasted and fed dogs. N Z Vet J 2017;65:19-23.

204. Benchaoui HA, Cox SR, Schneider RP, et al. The pharmacokinetics of maropitant, a novel neurokinin type-1 receptor antagonist, in dogs. J Vet Pharmacol Ther 2007;30:336-344.

205. Giorgi M, Yun H. Pharmacokinetics of mirtazapine and its main metabolites in Beagle dogs: a pilot study. Vet J 2012;192:239-241.

206. Regardh CG, Gabrielsson M, Hoffman KJ, et al. Pharmacokinetics and metabolism of omeprazole in animals and man--an overview. Scand J Gastroenterol Suppl 1985;108:79-94.

207. Bell ET, Devi JL, Chiu S, et al. The pharmacokinetics of pimobendan enantiomers after oral and intravenous administration of racemate pimobendan formulations in healthy dogs. J Vet Pharmacol Ther 2016;39:54-61.

208. Walker DK, Ackland MJ, James GC, et al. Pharmacokinetics and metabolism of sildenafil in mouse, rat, rabbit, dog and man. Xenobiotica 1999;29:297-310.

209. Yancey M, Merritt D, Lesman S, et al. Pharmacokinetic properties of toceranib phosphate (Palladia™, SU11654), a novel tyrosine kinase inhibitor, in laboratory dogs and dogs with mast cell tumors. J Vet Pharmacol Ther 2010;33:162-171.

210. Silverman JA, Deitcher SR. Marqibo®(vincristine sulfate liposome injection) improves the pharmacokinetics and pharmacodynamics of vincristine. Cancer Chemother Pharmacol 2013;71:555-564.

211. Durtschi AL, Gompf RE, Martin-Jimenez T, et al. Pharmacokinetics and Bioavailability of Carvedilol in Cats. In: ACVIM Forum, Denver, CO 2011.

212. Lainesse C, Frank D, Meucci V, et al. Pharmacokinetics of clomipramine and desmethylclomipramine after single-dose intravenous and oral administrations in cats. J Vet Pharmacol Ther 2006;29:271-278.

213. Mehl ML, Kyles AE, Craigmill AL, et al. Disposition of cyclosporine after intravenous and multi-dose oral administration in cats. J Vet Pharmacol Ther 2003;26:349-354.

214. Cotler S, Gustafson JH, Colburn WA. Pharmacokinetics of diazepam and nordiazepam in the cat. J Pharm Sci 1984;73:348-351.

215. Hickman M, Cox S, Mahabir S, et al. Safety, pharmacokinetics and use of the novel NK-1 receptor antagonist maropitant (CereniaTM) for the prevention of emesis and motion sickness in cats. J Vet Pharmacol Ther 2008;31:220-229.

216. Quimby JM, Gustafson DL, Samber BJ, et al. Studies on the pharmacokinetics and pharmacodynamics of mirtazapine in healthy young cats. J Vet Pharmacol Ther 2011;34:388-396.

217. Hanzlicek AS, Gehring R, Kukanich B, et al. Pharmacokinetics of oral pimobendan in healthy cats. J Vet Cardiol 2012;14:489-496.

218. Visser M, Weber K, Rincon G, et al. Use of RNA-seq to determine variation in canine cytochrome P450 mRNA expression between blood, liver, lung, kidney and duodenum in healthy beagles. J Vet Pharmacol Ther 2017;40:583-590.

219. Pan ST, Xue D, Li ZL, et al. Computational Identification of the Paralogs and Orthologs of Human Cytochrome P450 Superfamily and the Implication in Drug Discovery. Int J Mol Sci 2016;17:1020.

220. Whiterock VJ, Morgan DG, Lentz KA, et al. Phenacetin pharmacokinetics in CYP1A2-deficient beagle dogs. Drug Metab Dispos 2012;40:228-231.

221. Harper TW, Brassil PJ. Reaction phenotyping: current industry efforts to identify enzymes responsible for metabolizing drug candidates. The AAPS journal 2008;10:200-207.

222. Lu AY, Wang RW, Lin JH. Cytochrome P450 in vitro reaction phenotyping: a re-evaluation of approaches used for P450 isoform identification. Drug Metab Disposition 2003;31:345-350.

223. Zhang H, Davis CD, Sinz MW, et al. Cytochrome P450 reaction-phenotyping: an industrial perspective. Expert Opin Drug Metab Toxicol 2007;3:667-687.

224. Visser M, Zaya MJ, Locuson CW, et al. Comparison of Predicted Intrinsic Hepatic Clearance of 30 Pharmaceuticals in Canine and Feline Liver Microsomes. Xenobiotica 2018;in press:1-29.

225. Stringer RA, Strain-Damerell C, Nicklin P, et al. Evaluation of recombinant cytochrome P450 enzymes as an in vitro system for metabolic clearance predictions. Drug Metab Disposition 2009;37:1025-1034.

226. Achanta S, Maxwell L. Reaction phenotyping of vinblastine metabolism in dogs. Vet Comp Oncol 2016;14:161-169.

227. Coppoc GL. Chemotherapy of Neoplastic Diseases. In: Riviere JE, Papich MG, eds. Veterinary Pharmacology and Therapeutics, 9 ed. Ames, IO: Wiley-Blackwell; 2009:1205-1231.

228. Court MH. Canine cytochrome P-450 pharmacogenetics. Vet Clin North Am Small Anim Pract 2013;43:1027-1038.

229. Goldstein JA. Clinical relevance of genetic polymorphisms in the human CYP2C subfamily. Br J Clin Pharmacol 2001;52:349-355.

230. Crespi CL, Miller VP. The use of heterologously expressed drug metabolizing enzymes—state of the art and prospects for the future. Pharmacol Ther 1999;84:121-131.